SHRP-A-399

Low-Temperature Cracking: Binder Validation

D.H. Jung
T.S. Vinson

Department of Civil Engineering
Oregon State University
Corvallis, Oregon 97331

Strategic Highway Research Program
National Research Council
Washington, DC 1994

SHRP-A-399
Contract A-003A
ISBN: 0-309-05806-6
Product No.: 1001

Program Manager: *Edward T. Harrigan*
Project Manager: *Rita B. Leahy*
Program Area Secretary: *Juliet Narisah*

June 1994

key words:
asphalt concrete
asphalt
cold climates
cracking
low-temperature cracking
pavements,
temperature
thermal cracking

Strategic Highway Research Program
National Research Council
2101 Constitution Avenue N.W.
Washington, DC 20418

(202) 334-3774

1500/NAP/694

Acknowledgments

The research described herein was supported by the Strategic Highway Research Program (SHRP). SHRP is a unit of the National Research Council that was authorized by section 128 of the Surface Transportation and Uniform Relocation Assistance Act of 1987.

This project, entitled "Performance Related Testing and Measuring of Asphalt-Aggregate Interactions and Mixtures," was conducted at the Institute of Transportation Studies, University of California at Berkeley, with Carl L. Monismith as Principal Investigator.

The support and encouragement of R. Gary Hicks, Co-principal Investigator of the C.3 Low-Temperature Cracking Subtask, is gratefully acknowledged. In addition, special appreciation is extended to Marco Fellin, who prepared the test samples, Charles Antle of Pennsylvania State University, who provided invaluable guidance for the statistical analyses performed, and Teresa Culver, who typed the report.

Contents

Acknowledgments iii

List of Figures vii

List of Tables xi

Abstract 1

Executive Summary 3

1 Introduction 5

1.1 Background 5
1.2 Objectives 5

2 A-002A Hypothesis 7

3 Experiment Design 11

3.1 Experiment Design 11
3.2 Materials Selected 11
3.3 Sample Preparation 12
3.4 Test Procedures 20

4 TSRST Results for Asphalt-Aggregate Mixture 23

4.1 Fracture Temperature 23
4.2 Fracture Strength 28
4.3 Slope (dS/dT) 28
4.4 Transition Temperature 39
4.5 Summary of Results 45

5 Statistical Analysis of TSRST Results 47

5.1 Data Description 47
5.2 Analysis of Covariance 47

5.2.1 Fracture Temperature Model 49
5.2.2 Fracture Strength Model 50
5.2.3 Slope (dS/dT) Model 52
5.2.4 Transition Temperature Model 56

5.3 Waller-Duncan t-test 60
5.4 Discussion of Results 60

6 Rankings of Asphalts and Aggregates, and Comparison of A-002A and A-003A Results 71

6.1 Rankings of Asphalts and Aggregates 71
6.2 Relationship Between Fracture Temperature and A-002A Low-Temperature Index Test Results 73
6.3 Relationship Between Fracture Temperature and A-002A Asphalt Cement Properties 82
6.4 Significance of Results 89

7 Conclusions and Recommendations 93

7.1 Conclusions 93
7.2 Recommendations 95

8 References 97

Appendix A
Results of TSRST 99

List of Figures

Figure 3.1 Aggregate gradation 15

Figure 3.2 Test specimen locations in the beam sample 19

Figure 3.3 Schematic of TSRST equipment 21

Figure 3.4 Typical results of TSRST 22

Figure 4.1 Mean and range of fracture temperature (RC) 26

Figure 4.2 Mean and range of fracture temperature (RH) 27

Figure 4.3 Mean and range of fracture strength (RC) 32

Figure 4.4 Mean and range of fracture strength (RH) 33

Figure 4.5 Mean and range of slope (RC) 37

Figure 4.6 Mean and range of slope (RH) 38

Figure 4.7 Mean and range of transition temperature (RC) 43

Figure 4.8 Mean and range of transition temperature (RH) 44

Figure 5.1 Comparison of fracture temperature for STOA and LTOA specimens 51

Figure 5.2 Comparison of fracture temperature for RC and RH aggregates 51

Figure 5.3 Comparison of fracture strength for STOA and LTOA specimens 54

Figure 5.4 Comparison of fracture strength for RC and RH aggregates 54

Figure 5.5 Comparison of fracture strength for high and low air voids 55

Figure 5.6 Comparison of slope for STOA and LTOA specimens 58

Figure 5.7 Comparison of slope for RC and RH aggregates 58

Figure 5.8 Comparison of slope for high and low air voids 59

Figure 5.9 Comparison of transition temperature for STOA and LTOA specimens . . . 59

Figure 5.10 Comparison of transition temperature for RC and RH aggregates 61

Figure 5.11 Waller's grouping of asphalts for fracture temperature (RC) 62

Figure 5.12 Waller's grouping of asphalts for fracture temperature (RH) 63

Figure 5.13 Waller's grouping of asphalts for fracture strength (RC) 64

Figure 5.14 Waller's grouping of asphalts for fracture strength (RH) 65

Figure 5.15 Waller's grouping of asphalts for slope (RC) 66

Figure 5.16 Waller's grouping of asphalts for slope (RH) 67

Figure 5.17 Waller's grouping of asphalts for transition temperature (RC) 68

Figure 5.18 Waller's grouping of asphalts for transition temperature (RH) 69

Figure 6.1 Relationship between fracture temperature and limiting stiffness temperature after tank (unaged) 75

Figure 6.2 Relationship between fracture temperature and limiting stiffness temperature after PAV (aged) 76

Figure 6.3 Relationship between fracture temperature and m-value at 0°C after tank (unaged) 77

Figure 6.4 Relationship between fracture temperature and m-value at -10°C after PAV (aged) 78

Figure 6.5 Relationship between fracture temperature and creep stiffness at -10°C after PAV (aged) 79

Figure 6.6 Relationship between fracture temperature and ultimate strain at failure at -26°C after tank (unaged) 80

Figure 6.7 Relationship between fracture temperature and ultimate strain at failure at -10°C after PAV (aged) 81

Figure 6.8 Comparison of fracture temperature (STOA) predicted with A-002A index test results 83

Figure 6.9 Comparison of fracture temperature (LTOA) predicted with A-002A index test results 84

Figure 6.10 Relationship between fracture temperature and penetration at 15°C after tank (unaged) 86

Figure 6.11 Relationship between fracture temperature and penetration at 15°C after TFOT (aged) 87

Figure 6.12 Relationship between fracture temperature and penetration at 15°C after PAV (aged) 88

Figure 6.13 Relationship between fracture temperature and Fraass brittle point after tank (unaged) 90

Figure 6.14 Comparison of fracture temperature (STOA) predicted with A-002A asphalt cement properties 91

Figure 6.15 Comparison of fracture temperature (LTOA) predicted with A-002A asphalt cement properties 92

List of Tables

Table 2.1 Ranking of SHRP tank asphalts for resistance to low-temperature cracking as indicated by A-002A 8

Table 2.2 A portion of the SHRP binder specification 9

Table 3.1 Materials involved in the experiment design 12

Table 3.2 Asphalt properties 13

Table 3.3 Mixing and compaction temperatures 16

Table 3.4 Compaction schedules for RC aggregate 17

Table 3.5 Compaction schedules for RH aggregate 18

Table 3.6 Oven-aging schedule 20

Table 4.1 Fracture temperature for short-term aged specimens 24

Table 4.2 Fracture temperature for long-term aged specimens 25

Table 4.3 Summary statistics for fracture temperature 29

Table 4.4 Fracture strength for short-term aged specimens 30

Table 4.5 Fracture strength for long-term aged specimens 31

Table 4.6 Summary statistics for fracture strength 34

Table 4.7 Slope for short-term aged specimens 35

Table 4.8 Slope for long-term aged specimens 36

Table 4.9 Summary statistics for slope 40

Table 4.10 Transition temperature for short-term aged specimens 41

Table 4.11 Transition temperature for long-term aged specimens 42

Table 4.12 Summary statistics for transition temperatures 46

Table 5.1 Description of variables 48

Table 5.2 Mean square errors for fracture temperature models 50

Table 5.3 Mean square errors for fracture strength models 53

Table 5.4 Mean square errors for slope (dS/dT) models 57

Table 5.5 Mean square errors for transition temperature models 57

Table 6.1 Ranking of asphalts for resistance to low-temperature cracking indicated by A-003A and A-002A 72

Table 6.2 Ranking of aggregates for resistance to low-temperature cracking indicated by A-003A 72

Table 6.3 Summary statistics of linear regression analyses with the A-002A index test results 74

Table 6.4 Summary statistics of linear regression analyses with the A-002A asphalt cement properties 85

Table A.1 Results of TSRST for short-term aged (STOA) mixtures with RC aggregate 99

Table A.2 Results of TSRST for long-term aged (LTOA) mixtures with RC aggregate 101

Table A.3 Results of TSRST for short-term aged (STOA) mixtures with RH aggregate 103

Table A.4 Results of TSRST for long-term aged (LTOA) mixtures with RH aggregate 105

Abstract

The thermal stress restrained specimen test (TSRST) was developed at Oregon State University under the Strategic Highway Research Program (SHRP) A-003A contract as an accelerated laboratory test to evaluate the thermal, or the low-temperature cracking resistance of asphalt concrete mixes. The test system is capable of cooling an asphalt concrete specimen (rectangular or cylinder) at a constant rate, while restraining the specimen from contraction and periodically measuring elapsed time, specimen surface temperature, and tensile load.

TSRSTs were performed on both short-term and long-term aged specimens to (1) relate fundamental properties of asphalt cement and aggregate to the thermal cracking resistance of asphalt concrete mixtures, and (2) validate the A-002A contractor's hypothesis for low-temperature cracking. Statistical analyses were performed on the test results. A ranking of asphalt concrete mixtures based on fracture temperature compared favorably with a ranking given by the A-002A contractor based on fundamental properties of the asphalt cement. Fracture temperature was highly correlated to the A-002A low-temperature index test results.

Executive Summary

The objectives of Task D.2.c were to (1) relate fundamental properties of asphalt cement and aggregate to the thermal cracking resistance of asphalt concrete mixtures, and (2) validate the A-002A contractor's hypothesis for low-temperature cracking.

Thermal stress restrained specimen tests (TSRSTs) were performed on both short- and long-term aged specimens prepared with a combination of fourteen asphalt types and two aggregate types. The TSRST results were expressed in terms of fracture temperature, fracture strength, slope, and transition temperature.

A statistical analysis was performed on the TSRST results using a Statistical Analysis System (SAS) software package. From the analysis of TSRST results, it was observed that asphalt type, aggregate type, degree of aging, and air void content have a substantial influence on the thermal cracking resistance of asphalt concrete mixtures. Fracture temperature and transition temperature were strongly dependent on asphalt type and degree of aging, and less dependent on aggregate type and air void content. Fracture strength and slope were highly dependent on air void content and aggregate type, and less dependent on asphalt type and degree of aging. That is, asphalt type, aggregate type, degree of aging, and air void content were identified as significant factors relating to the low-temperature cracking characteristics of asphalt concrete mixes. Interactions between variables were not significant.

A ranking of asphalt concrete mixtures based on fracture temperature compared favorably with a ranking given by the A-002A contractor based on fundamental properties of the asphalt cement. The favorable comparison validates the A-002A contractor's hypothesis for low-temperature cracking. Fracture temperature was highly correlated to A-002A low-temperature index test results, specifically the temperature at limiting stiffness, the m-value, and the ultimate strain at failure. Fraass brittle point and penetration of asphalt cement at 15°C may also be a good indicator of the low-temperature performance of asphalt concrete mixtures.

1

Introduction

1.1 Background

Several variables may affect the thermal, or low-temperature cracking characteristics of asphalt concrete mixtures. These include asphalt cement type, aggregate type, air void content, degree of aging, and interactions among them. The thermal stress restrained specimen test (TSRST) was developed at Oregon State University under the Strategic Highway Research Program (SHRP) A-003A contract as an accelerated laboratory test to evaluate the effect of these variables on the low-temperature cracking of asphalt concrete.

Concurrent with this work, researchers at Pennsylvania State University under SHRP contract A-002A developed the bending beam rheometer test and the direct tension test to measure fundamental properties of asphalt cement at cold temperatures (Peterson et al. 1992). The bending beam rheometer is used to evaluate the rheological properties of asphalt cement at lower temperatures. The bending beam rheometer test measures the flexural creep stiffness of asphalt cement in the range of temperatures from -40° to 0°C. The direct tension test is used to measure the uniaxial failure properties of asphalt in the temperature range of -30° to 5°C.

1.2 Objectives

The objectives of the research reported herein are to (1) relate the fundamental properties of asphalt cement and aggregate to the low-temperature cracking characteristics of asphalt concrete mixtures, and (2) validate the A-002A contractor's hypothesis for low-temperature cracking. To accomplish these objectives, TSRSTs were performed on both short- and long-term aged specimens prepared with a combination of fourteen asphalt cements and two aggregate types. Statistical analyses were performed on the TSRST results using a Statistical Analysis System (SAS) package, and asphalt mixtures were ranked in terms of their low-temperature cracking susceptibility. The ranking was compared to the ranking based on fundamental properties of asphalt cement provided by the A-002A researchers. The fracture temperature of mixtures was also correlated to the A-002A low-temperature index test results and fundamental properties of both unaged and aged [thin film oven test (TFOT) and pressure aging vessel (PAV)] asphalt cements.

2

A-002A Hypothesis

The performance rankings of asphalt cements for resistance to low-temperature cracking are based on the following parameters provided by A-002A (see Table 2.1):

(1) Limiting stiffness temperature.
(2) m-value.
(3) Ultimate strain at failure.

These parameters are included in the Strategic Highway Research Project (SHRP) binder specification for evaluation of low-temperature thermal cracking of asphalt concrete mixes. A portion of the SHRP binder specification is presented in Table 2.2.

The rankings for resistance to low-temperature cracking were estimated based on the limiting stiffness temperature, the m-value, and the ultimate strain at failure. In the bending beam rheometer test, the limiting stiffness temperature of unaged asphalt cements was estimated based on a stiffness value of 200 MPa at a loading time of 2 hours, while that of aged (pressure aging vessel [PAV]) asphalt cements was estimated based on a stiffness value of 200 MPa at a loading time of 60 seconds.

Likewise in the bending beam rheometer test, the m-value of unaged asphalt cements was estimated at 0°C, while that of aged (PAV) asphalt cements was estimated at -10°C.

And finally, in the direct tension test, the ultimate strain of failure of unaged asphalt cements was estimated at -26°C at a loading time of 2 hours, while that of unaged (PAV) asphalt cements was estimated at -10°C.

To determine individual rankings of asphalt, a score ranging from 1 (best) to 14 (worst) was assigned to each asphalt considered in this study based on the parameter values (i.e., limiting stiffness temperature, m-value, and ultimate strain at failure) of unaged asphalt cements. For the parameters of aged asphalt cements, a score ranging from 1 to 9 (or 10) was assigned to each asphalt, depending on the data available. The overall ranking was determined based on

Table 2.1. Ranking of SHRP tank asphalts for resistance to low-temperature cracking as indicated by A-002A low temperature index test results (Materials Reference Library asphalt properties, 4/29/92, 6/26/92, 10/22/92)

Asphalt Type	Limiting Stiffness Temp. @ S=200 MPa, Unaged (tank) (Ranking)	m-Value @ 0°C, Unaged (tank) (Ranking)	Ultimate Strain at Failure @ -26°C, Unaged (tank) (Ranking)	Limiting Stiffness Temp. @ S=200 MPa, Aged (PAV) (Ranking)	m-Value @ -10°C, Aged (PAV) (Ranking)	Ultimate Strain at Failure @ -10°C, Aged (PAV) (Ranking)	Overall Rank 1 = best
AAA-1	-31 (1)	0.53 (2)	3.1 (1)	-18 (1)	0.41 (1)	10.70 (1)	1
AAB-1	-28 (5)	0.42 (4)	1.7 (5)	-14 (4)	0.34 (6)	7.23 (3)	5
AAC-1	-25 (7)	0.39 (8)	1.5 (8)	-11 (7)	0.30 (8)	4.07 (5)	7
AAD-1	-30 (2)	0.50 (3)	2.5 (3)	-16 (3)	0.38 (4)	10.51 (2)	3
AAF-1	-21 (11)	0.32 (9)	1.2 (10)	-10 (8)			11
AAG-1	-18 (14)	0.28 (14)	0.8 (14)	-7 (10)			14
AAK-1	-27 (6)	0.42 (4)	1.7 (5)	-13 (6)			6
AAL-1	-30 (2)	0.55 (1)	2.8 (2)	-18 (1)	0.41 (1)	3.74 (6)	2
AAM-1	-24 (9)	0.29 (11)	1.5 (8)	-10 (8)	0.29 (10)	5.23 (4)	9
AAV-1	-25 (7)	0.40 (7)	1.2 (10)	-14 (4)	0.39 (3)	2.14 (8)	8
AAW-1	-22 (10)	0.29 (11)	1.6 (7)			0.92 (9)	9
AAX-1	-20 (12)	0.30 (10)	1.1 (13)		0.30 (8)		13
AAZ-1	-20 (12)	0.29 (11)	1.2 (10)		0.34 (6)	2.43 (7)	12
ABC-1	-30 (2)	0.41 (6)	2.2 (4)		0.37 (5)		4

Table 2.2. A portion of the SHRP binder specification

PERFORMANCE GRADE	PG 46-			PG 52-							PG 58-					PG 64-					
	34	40	46	10	16	22	28	34	40	46	16	22	28	34	40	10	16	22	28	34	40
Average 7-day Maximum Pavement Design Temperature, °C[a]	<46			<52							<58					<64					
Minimum Pavement Design Temperature, °C[a]	> −34	> −40	> −46	> −10	> −16	> −22	> −28	> −34	> −40	> −46	> −16	> −22	> −28	> −34	> −40	> −10	> −16	> −22	> −28	> −34	> −40
ORIGINAL BINDER																					
Flash Point Temp, T48: Minimum °C	230																				
Viscosity, ASTM D4402[b]: Maximum, 3 Pa·s, Test Temp, °C	135																				
Dynamic Shear, TP5[c]: G*/sinδ, Minimum, 1.00 kPa Test Temp @ 10 rad/s, °C	46			52							58					64					
ROLLING THIN FILM OVEN (T240) OR THIN FILM OVEN RESIDUE (T179)																					
Mass Loss, Maximum, percent	1.00																				
Dynamic Shear, TP5: G*/sinδ, Minimum, 2.20 kPa Test Temp @ 10 rad/s, °C	46			52							58					64					
PRESSURE AGING VESSEL (PAV) RESIDUE (PP1)																					
PAV Aging Temperature, °C[d]	90			90							100					100					
Dynamic Shear, TP5: G*sinδ, Maximum, 5000 kPa Test Temp @ 10 rad/s, °C	10	7	4	25	22	19	16	13	10	7	25	22	19	16	13	31	28	25	22	19	16
Physical Hardening[e]	Report																				
Creep Stiffness, TP1:[f] S, Maximum, 300 MPa, *m* - value, Minimum, 0.300 Test Temp @ 60s, °C	−24	−30	−36	0	−6	−12	−18	−24	−30	−36	−6	−12	−18	−24	−30	0	−6	−12	−18	−24	−30
Direct Tension, TP3:[f] Failure Strain, Minimum, 1.0% Test Temp @ 1.0 mm/min, °C	−24	−30	−36	0	−6	−12	−18	−24	−30	−36	−6	−12	−18	−24	−30	0	−6	−12	−18	−24	−30

[a] Pavement temperatures may be estimated from air temperatures using an algorithm contained in the SUPERPAVE software program; provided by the specifying agency; or found by following the procedures as outlined in PPX.

[b] This requirement may be waived at the discretion of the specifying agency if the supplier warrants that the asphalt binder can be adequately pumped and mixed at temperatures that meet all applicable safety standards.

[c] For quality control of unmodified asphalt cement production, measurement of the viscosity of the original asphalt cement may be substituted for dynamic shear measurements of G*/sinδ at test temperatures where the asphalt is a Newtonian fluid. Any suitable standard means of viscosity measurement may be used, including capillary or rotational viscometry (AASHTO T201 or T202).

[d] The PAV aging temperature is based on simulated climatic conditions and is one of three temperatures: 90°C, 100°C or 110°C. The PAV aging temperature is 100°C for PG 58- and above, except for paving materials to be used in desert climates, where it is 110°C.

[e] Physical Hardening—TP1 is performed on a set of asphalt beams according to section 13.1, except the conditioning time is extended to 24 hrs ± 10 minutes at 10°C above the minimum performance temperature. The 24-hour stiffness and *m*-value are reported for information purposes only.

[f] If the creep stiffness is below 300 MPa, the direct tension test is not required. If the creep stiffness is between 300 and 600 MPa, the direct tension failure strain requirement can be used in lieu of the creep stiffness requirement. The *m*-value requirement must be satisfied in both cases.

the average of the three individual rankings of unaged asphalt cements, since some parameter values of aged asphalt cements were missing.

The individual rankings for resistance to low-temperature cracking based on a specific parameter value of asphalt cements, together with the overall ranking based on a combination of the parameters, are given in Table 2.1.

3

Experiment Design

The experiment design for this study was developed to relate the fundamental properties of asphalt cement, as determined by the A-002A contractor, to the low-temperature cracking characteristics of asphalt concrete mixtures, measured with the thermal stress restrained specimen test (TSRST). The details of experiment design are discussed in this section. Descriptions of sample/specimen preparation and the TSRST procedure are also given.

3.1 Experiment Design

The experiment design includes fourteen asphalt cements and two aggregate types. Two degrees of aging and two levels of air void content are employed. A 14 × 2 × 2 × 2 × 2 replicated full-factorial design was developed as follows:

Experiment Design Variable	Levels
Asphalt type	14
Aggregate type	2
Degree of aging	2 (short, long)
Air void content	2 (4%, 8%)
Rate of cooling	1 (10°C/hr.)
Replicates	2
Total no. of tests	224

3.2 Materials Selected

The asphalts and aggregates were selected from the Strategic Highway Research Project (SHRP) Materials Reference Library (MRL). The asphalts and aggregates involved in the experiment design are presented in Table 3.1. Fourteen asphalt cements were selected from several crude sources with a wide range of temperature susceptibility characteristics. Mineral aggregates from two sources were used in the experiment. The RC aggregate is an

Table 3.1. Materials involved in the experiment design

Materials	Type
Asphalt	AAA-1*, AAB-1*, AAC-1*, AAD-1,* AAF-1*, AAG-1*, AAK-1* AAL-1, AAM-1*, AAV-1, AAW-1, AAX-1, AAZ-1, ABC-1
Aggregate	RC Limestone / Kansas RH Greywacke / California

* SHRP Core Asphalts

absorptive limestone from Kansas, which has a rough surface texture and an angular shape; the RH aggregate is a silicious greywacke (high SiO_2 content), which has a smooth surface texture and an angular shape. The relevant properties for the asphalt cements evaluated are given in Table 3.2.

3.3 Sample Preparation

The aggregate gradation for the RC and RH aggregates used to prepare the asphalt concrete mixtures is shown in Figure 3.1. The asphalt cement content used with the RC aggregate is 6.25 percent of total weight of aggregate (5.9 percent of total weight of the mixture) and with the RH aggregate is 5.2 percent of total weight of aggregate (4.9 percent of total weight of the mixture).

Both the aggregate and asphalt to be mixed were preheated at a specified mixing temperature, depending on asphalt type. The mixing temperature for each asphalt was selected from a Bitumen Test Data Chart (BTDC) and is presented in Table 3.3. The mixing temperature corresponds to a viscosity of 170 ± 20 centistokes (approximately 160 ± 20 centipoise). After mixing, the loose mixture was subjected to short-term aging in an oven for 4 hours at 135°C. Following short-term oven aging, the mixture was compacted.

Beam samples were prepared using a kneading compactor. The compaction tools, compaction equipment, and mixture were preheated at the compaction temperature. The compaction temperature for each asphalt type was determined from the BTDC and is given in Table 3.3. The compaction temperature corresponds to a viscosity of 280 ± 30 centistokes (approximately 265 ± 30 centipoise).

Two levels of compactive efforts were employed to prepare the beam samples (15.2 × 15.2 × 40.6 cm), depending on the target air void contents. The higher air void content beam was compacted with two lifts, whereas the lower air void content beam was compacted with four lifts. The compaction schedules for RC and RH aggregates are presented in Tables 3.4 and 3.5.

Four test specimens (5.0 × 5.0 × 25.0 cm) were sawed from a large beam sample. Two test specimens were obtained from the top half of the beam sample and two were obtained from the bottom half, as shown in Figure 3.2.

Table 3.2. Asphalt properties

Asphalt Type	AAA-1	AAB-1	AAC-1	AAD-1
Asphalt Grade	150/200	AC-10	AC-8	AR-4000
Penetration @ 15°C (dmm)				
after tank	52	28	27	44
after TFOT	33	20	16	25
after PAV	19	12	10	15
Fraass Brittle Point (°C)	-18	-14	-13	-14
Specification Properties (PTI Rheometer, Bending Beam Rheometer)				
m, (0.1 s) (0°C)	0.53	0.42	0.39	0.50
Temp. @ S(t)=200 MPa,°C	-31	-28	-25	-30
Ultimate Strain, %	3.1	1.7	1.5	2.5

Asphalt Type	AAF-1	AAG-1	AAK-1	AAL-1
Asphalt Grade	AC-20	AR-4000	AC-30	150/200
Penetration @ 15°C (dmm)				
after tank	14	12	23	52
after TFOT	9	9	14	
after PAV	7	4	10	
Fraass Brittle Point (°C)	-4	1	-10	
Specification Properties (PTI Rheometer, Bending Beam Rheometer)				
m, (0.1 s) (0°C)	0.32	0.28	0.42	0.55
Temp. @ S(t)=200 MPa,°C	-21	-18	-27	-30
Ultimate Strain, %	1.2	0.8	1.7	2.8

Continued on page 14

Table 3.2 (continued). Asphalt properties

Asphalt Type	AAM-1	AAV-1	AAW-1	AAX-1
Asphalt Grade	AC-20	AC-5	AC-20	AC-20
Penetration @ 15°C (dmm)		37	18	
after tank	17			
after TFOT	13			
after PAV	9			
Fraass Brittle Point (°C)	-12			
Specification Properties (PTI Rheometer, Bending Beam Rheometer)				
m, (0.1 s) (0°C)	0.29	0.40	0.29	0.30
Temp. @ S(t)=200 MPa,°C	-24	-25	-22	-20
Ultimate Strain, %	1.5	1.2	1.6	1.1

Asphalt Type	AAZ-1	ABC-1
Asphalt Grade	AC-20	AC-20
Penetration @ 15°C (dmm)		
after tank	18	31
after TFOT		
after PAV		
Fraass Brittle Point (°C)		
Specification Properties (PTI Rheometer, Bending Beam Rheometer)		
m, (0.1 s) (0°C)	0.29	0.41
Temp. @ S(t)=200 MPa,°C	-20	-30
Ultimate Strain, %	1.2	2.2

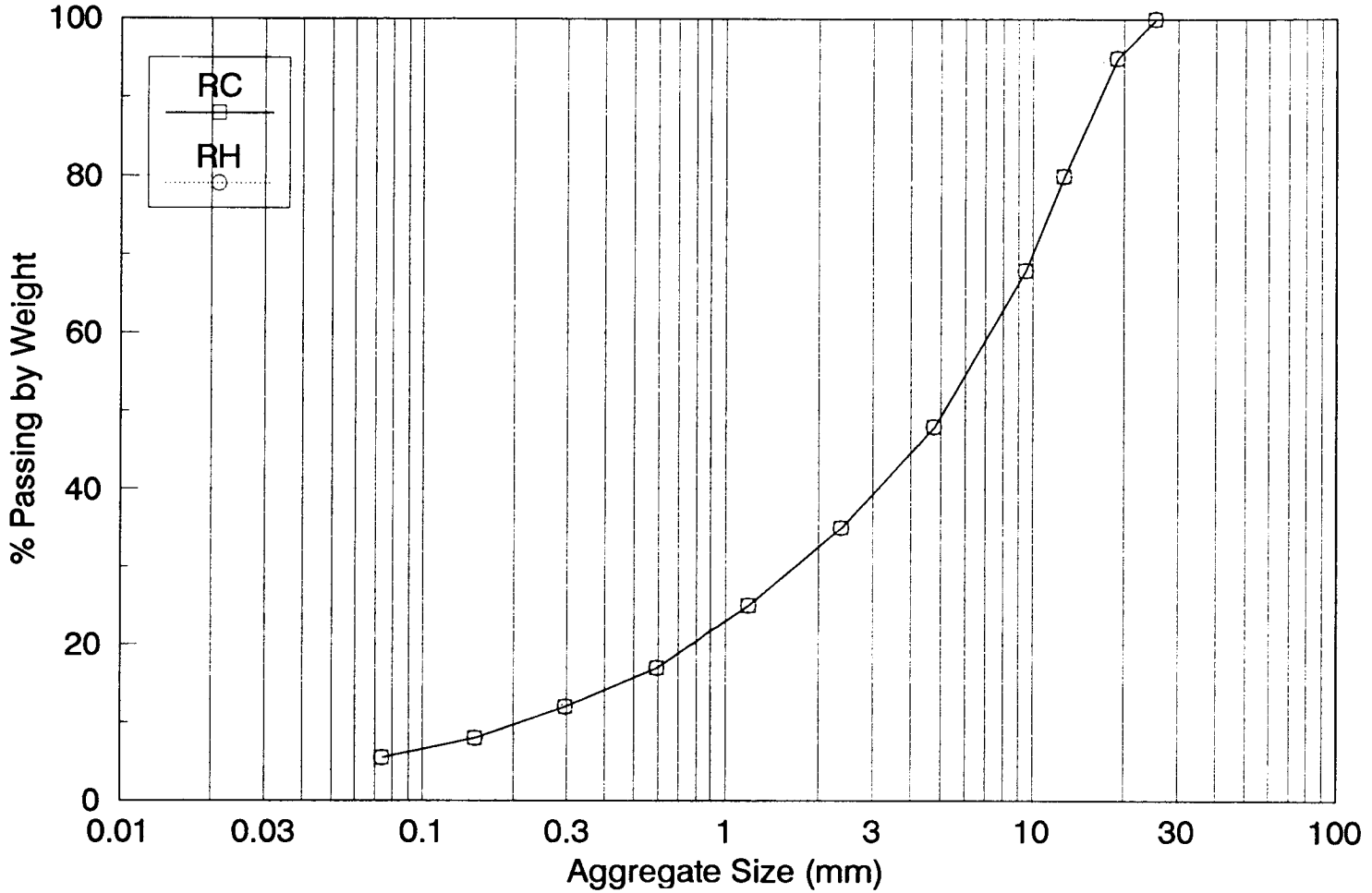

Figure 3.1. Aggregate gradation

Table 3.3. Mixing and compaction temperatures

Asphalt Type	Mixing Temp.,°C	Compaction Temp.,°C
AAA-1	146 ± 2	119 ± 2
AAB-1	146 ± 2	120 ± 2
AAC-1	137 ± 2	112 ± 2
AAD-1	148 ± 2	122 ± 2
AAF-1	148 ± 2	124 ± 2
AAG-1	142 ± 2	119 ± 2
AAK-1	160 ± 2	133 ± 2
AAL-1	143 ± 2	133 ± 2
AAM-1	160 ± 2	133 ± 2
AAV-1	142 ± 2	132 ± 2
AAW-1	151 ± 2	141 ± 2
AAX-1	151 ± 2	141 ± 2
AAZ-1	150 ± 2	140 ± 2
ABC-1	156 ± 2	145 ± 2

Table 3.4. Compaction schedules for RC aggregate

(a) Target Air Void Content = 8%

Lift Number		Stage 1	Stage 2	Stage 3
1	Pressure	75 psi	150 psi	225 psi
	No. of Passes	4	6	8
2	Pressure	75 psi	225 psi	300 psi
	No. of Passes	4	10	16

(b) Target Air Void Content = 4%

Lift Number		Stage 1	Stage 2	Stage 3
1	Pressure	75 psi	125 psi	200 psi
	No. of Passes	2	3	6
2	Pressure	75 psi	150 psi	225 psi
	No. of Passes	2	5	10
3	Pressure	75 psi	175 psi	250 psi
	No. of Passes	2	7	14
4	Pressure	75 psi	225 psi	275 psi
	No. of Passes	2	9	30

1 psi = 6.9 kPa

Table 3.5. Compaction schedules for RH aggregate

(a) Target Air Void Content = 8%

Lift Number		Stage 1	Stage 2	Stage 3
1	Pressure	75 psi	100 psi	175
	No. of Passes	2	3	3
2	Pressure	150 psi	250 psi	300 psi
	No. of Passes	2	5	5

(b) Target Air Void Content = 4%

Lift Number		Stage 1	Stage 2	Stage 3
1	Pressure	75 psi	125 psi	200 psi
	No. of Passes	2	4	6
2	Pressure	75 psi	150 psi	250 psi
	No. of Passes	2	8	12
3	Pressure	75 psi	175 psi	325 psi
	No. of Passes	2	10	18
4	Pressure	75 psi	250 psi	400 psi
	No. of Passes	2	16	26

1 psi = 6.9 kPa

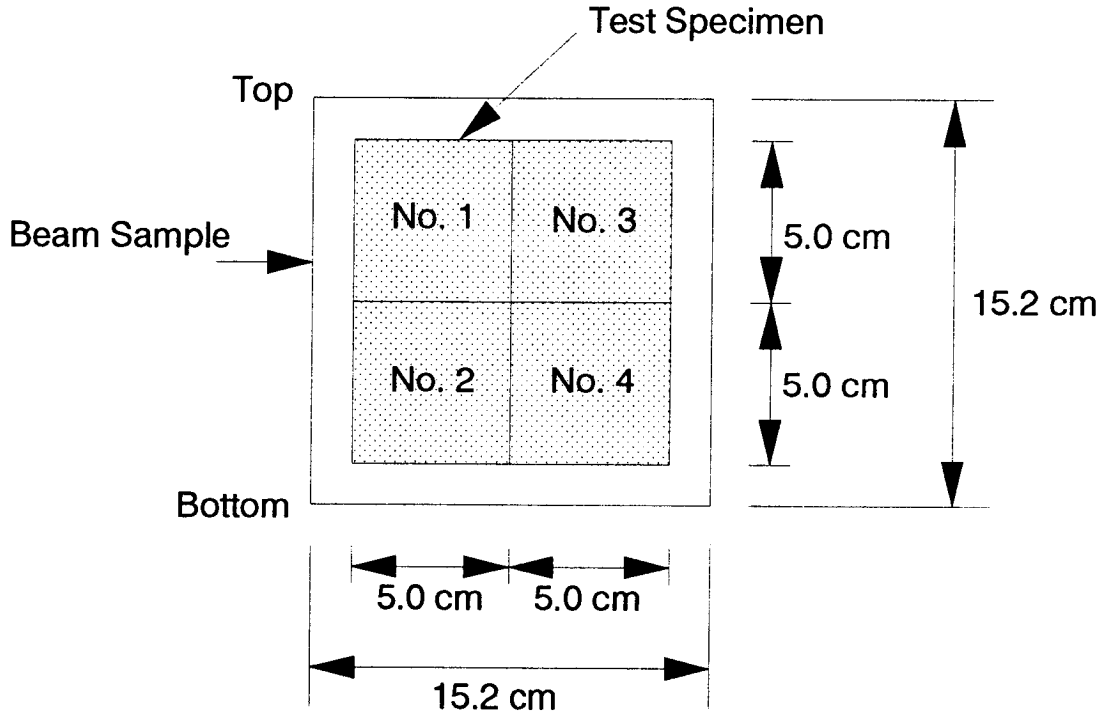

Figure 3.2. Test specimen locations in the beam sample

As indicated above, short-term oven aging (STOA) was performed on the loose mixture prior to compaction; long-term oven aging (LTOA) was performed on test specimen No. 3 and No. 4 after cutting. The aging schedules are given in Table 3.6.

Table 3.6. Oven-aging schedule

Degree of Aging	Condition	Procedure
Short-Term	Loose Mix	4 hours @ 135°C (275°F)
Long-Term	Compacted Specimen	5 days @ 85°C (185°F)

3.4 Test Procedures

The test used to evaluate all mixtures (STOA and LTOA) was the TSRST. The test specimens were aligned with an alignment stand and glued to end platens with an epoxy compound. Two epoxy compounds were used in this study, namely, DC-80 (Thermoset Plastics, Inc.) and Plastic Steel Putty (Devcon). The test specimen was left in the alignment stand for 24 hours (DC-80) or 4 hours (Plastic Steel Putty), depending on the epoxy compound used.

After the epoxy had cured, the test specimen with end platens was cooled to a temperature of 5°C for 1 hour to establish thermal equilibrium prior to testing. Next, the specimen with end platens was set up in the environmental cabinet as shown in Figure 3.3. TSRST was performed at a monotonic cooling rate of 10°C per hour until fracture.

Typical TSRST results are shown in Figure 3.4. The thermally induced stress gradually increases as temperature decreases until the specimen fractures. At the break point, the stress reaches its maximum value, which is referred to as the *fracture strength,* with a corresponding *fracture temperature.* The *slope* of the stress-temperature curve, dS/dT, increases until it reaches a maximum value. At colder temperatures, dS/dT becomes constant and the stress-temperature curve is linear. The *transition temperature* divides the curve into two parts, relaxation and nonrelaxation. As the temperature approaches the transition temperature, the asphalt cement becomes stiffer and the thermally induced stresses are not relaxed beyond this temperature. The slope tends to decrease again when the specimen is close to fracture. This reaction may be due to the stiffness of the asphalt cement or the development of microcracks.

The application of the TSRST results to predict field performance is the subject of ongoing research. It is clear, however, that the colder the TSRST fracture temperature, the greater the mixture resistance to low-temperature cracking. Also, it is reasonable to conclude that mixtures with steeper slope values and warmer transition temperatures would be more susceptible to low-temperature cracking.

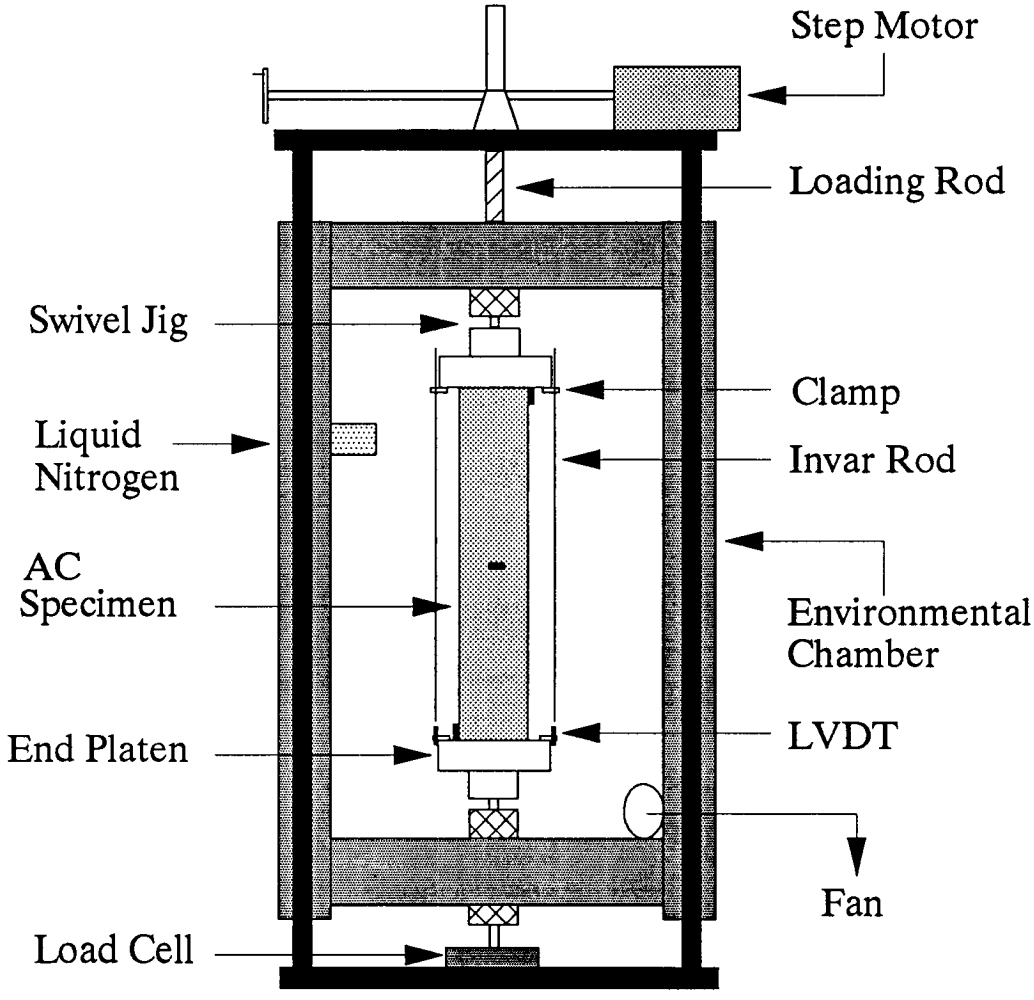

Figure 3.3. Schematic of TSRST equipment

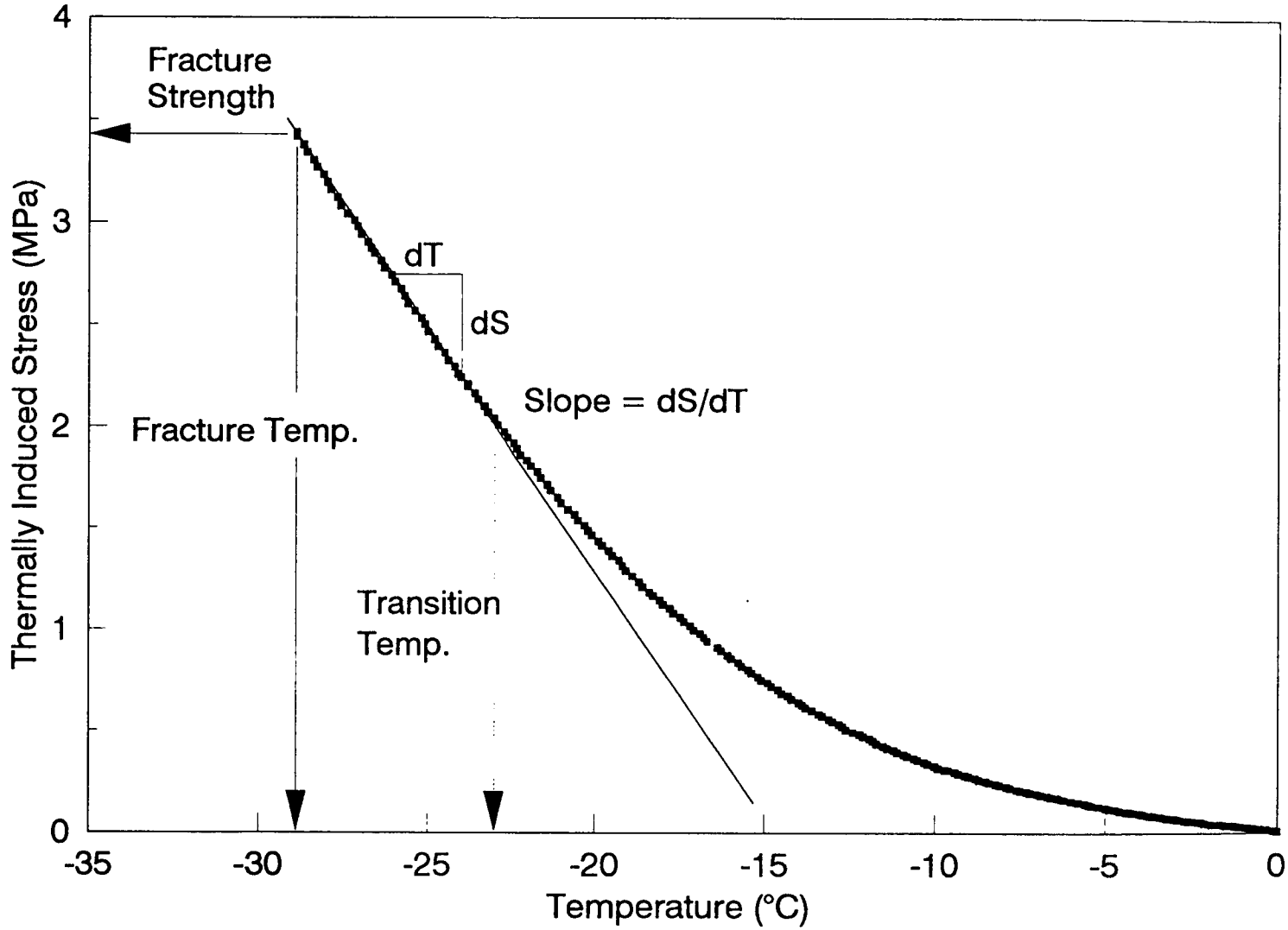

Figure 3.4. Typical results of TSRST

4

TSRST Results for Asphalt-Aggregate Mixture

A total of 201 thermal stress restrained specimen tests (TSRSTs) were conducted to accomplish the project objectives. The results are presented in Appendix A. Mean values and the coefficients of variation of the test results are presented in this section. The repeatability of TSRST was estimated for each property measured, based on the 95 percent limit (American Society for Testing and Materials [ASTM] C 670-90a and E 177-90a). The repeatability was estimated for each asphalt type for which there were three or more observations.

4.1 Fracture Temperature

Fracture temperature is defined as the temperature at which the thermal stress induced in the specimen is maximum. Mean values and the coefficients of variation of fracture temperature for a specific asphalt type, aggregate type, and degree of aging are summarized in Tables 4.1 and 4.2. Figures 4.1 and 4.2 show variations of fracture temperatures for short-term oven aging (STOA) and long-term oven aging (LTOA) depending on asphalt type, for RC and RH aggregate, respectively.

The 95 percent repeatability limit for fracture temperature ranged from 3 percent to 30 percent for all asphalts. The fracture temperatures exhibit a wide range of values, depending on the asphalt type. The fracture temperatures of specimens with RC aggregate ranged from -32.1°C to -18.6°C for STOA and from -27.8°C to -13.6°C for LTOA. For specimens with RH aggregate, fracture temperatures ranged from -32.2°C to -16.3°C for STOA and from -29.3°C to -13.6°C for LTOA.

The fracture temperatures are warmer for LTOA specimens than for STOA specimens. The difference in fracture temperatures between STOA and LTOA specimens with RC aggregate ranged from -6.5°C to -0.6°C, with an average of -3.8°C. For specimens with RH aggregate, the difference ranged from -5.5°C to -0.6°C, with an average of -2.9°C.

Table 4.1. Fracture temperature for short-term aged specimens

Asphalt	Aggregate	No. of Obs.	Minimum (°C)	Maximum (°C)	Mean (°C)	C.V. (%)	95% Repeatability Limit (%)
AAA-1	RC	3	-34.1	-30.7	-32.1	5.6	15.5
	RH	2	-32.4	-31.9	-32.2	1.7	
AAB-1	RC	5	-28.2	-22.1	-26.2	10.4	28.8
	RH	5	-27.9	-26.5	-27.1	2.1	5.8
AAC-1	RC	4	-26.7	-22.3	-24.3	7.6	21.0
	RH	5	-23.4	-20.6	-21.9	4.7	12.9
AAD-1	RC	3	-31.6	-29.9	-30.6	2.9	7.9
	RH	3	-28.7	-28.1	-28.4	1.1	2.9
AAF-1	RC	4	-20.7	-17.1	-18.6	8.3	23.0
	RH	3	-20.4	-17.7	-18.9	7.3	20.1
AAG-1	RC	4	-21.8	-18.4	-20.1	7.0	19.3
	RH	4	-17.9	-15.0	-16.3	7.8	21.7
AAK-1	RC	5	-26.8	-23.0	-24.9	7.0	19.3
	RH	4	-24.7	-23.0	-23.8	3.3	22.6
AAL-1	RC	2	-32.2	-31.3	-31.8	2.0	
	RH	4	-31.9	-29.8	-30.8	3.2	8.7
AAM-1	RC	4	-23.4	-19.6	-21.6	8.5	23.6
	RH	6	-21.8	-20.2	-20.8	2.6	7.2
AAV-1	RC	3	-28.6	-26.4	-27.5	4.0	11.1
	RH	4	-27.0	-25.6	-26.0	2.6	7.1
AAW-1	RC	3	-21.8	-20.9	-21.5	2.3	6.4
	RH	5	-22.3	-20.1	-21.6	4.0	11.2
AAX-1	RC	5	-22.3	-19.7	-21.4	4.7	13.1
	RH	4	-20.6	-19.1	-20.0	3.5	24.1
AAZ-1	RC	4	-23.0	-21.3	-22.2	4.1	11.2
	RH	5	-21.1	-18.2	-19.6	6.0	16.6
ABC-1	RC	2	-30.1	-28.7	-29.4	3.4	
	RH	2	-28.8	-28.2	-28.5	1.5	

Table 4.2. Fracture temperature for long-term aged specimens

Asphalt	Aggregate	No. of Obs.	Minimum (°C)	Maximum (°C)	Mean (°C)	C.V. (%)	95% Repeatability Limit (%)
AAA-1	RC	3	-28.2	-27.3	-27.8	1.7	4.7
	RH	2	-29.6	-28.9	-29.3	1.7	
AAB-1	RC	4	-24.4	-23.0	-23.8	2.4	6.8
	RH	2	-22.1	-22.0	-22.1	0.3	
AAC-1	RC	3	-24.1	-22.1	-22.9	4.6	12.8
	RH	6	-22.1	-19.6	-21.0	4.8	13.3
AAD-1	RC	2	-25.3	-21.6	-24.2	6.7	
	RH	5	-25.5	-23.0	-23.6	4.5	12.4
AAF-1	RC	4	-17.9	-13.5	-15.8	14.7	40.8
	RH	3	-15.8	-14.7	-15.1	3.9	10.7
AAG-1	RC	3	-15.8	-12.0	-13.6	14.6	40.6
	RH	4	-14.5	-12.6	-13.6	6.3	17.5
AAK-1	RC	4	-21.4	-18.2	-19.8	6.8	18.9
	RH	2	-21.2	-20.8	-21.0	1.4	
AAL-1	RC	2	-26.3	-24.4	-25.4	5.3	11.5
	RH	5	-26.9	-24.6	-25.8	4.2	19.1
AAM-1	RC	3	-22.7	-20.1	-21.0	6.9	10.1
	RH	5	-20.8	-19.0	-20.2	3.7	2.4
AAV-1	RC	3	-24.3	-23.9	-24.1	0.9	3.0
	RH	3	-23.8	-23.3	-23.6	1.1	10.0
AAW-1	RC	5	-19.9	-18.4	-19.2	3.6	15.2
	RH	4	-18.3	-16.0	-17.2	5.5	
AAX-1	RC	2	-18.5	-18.2	-18.4	1.2	15.1
	RH	3	-18.8	-17.0	-17.7	5.5	7.4
AAZ-1	RC	3	-17.5	-16.6	-17.1	2.7	9.5
	RH	4	-18.9	-17.4	-18.2	3.4	7.9
ABC-1	RC	3	-25.8	-24.4	-25.2	2.9	
	RH	2	-24.6	-23.1	-23.9	4.5	

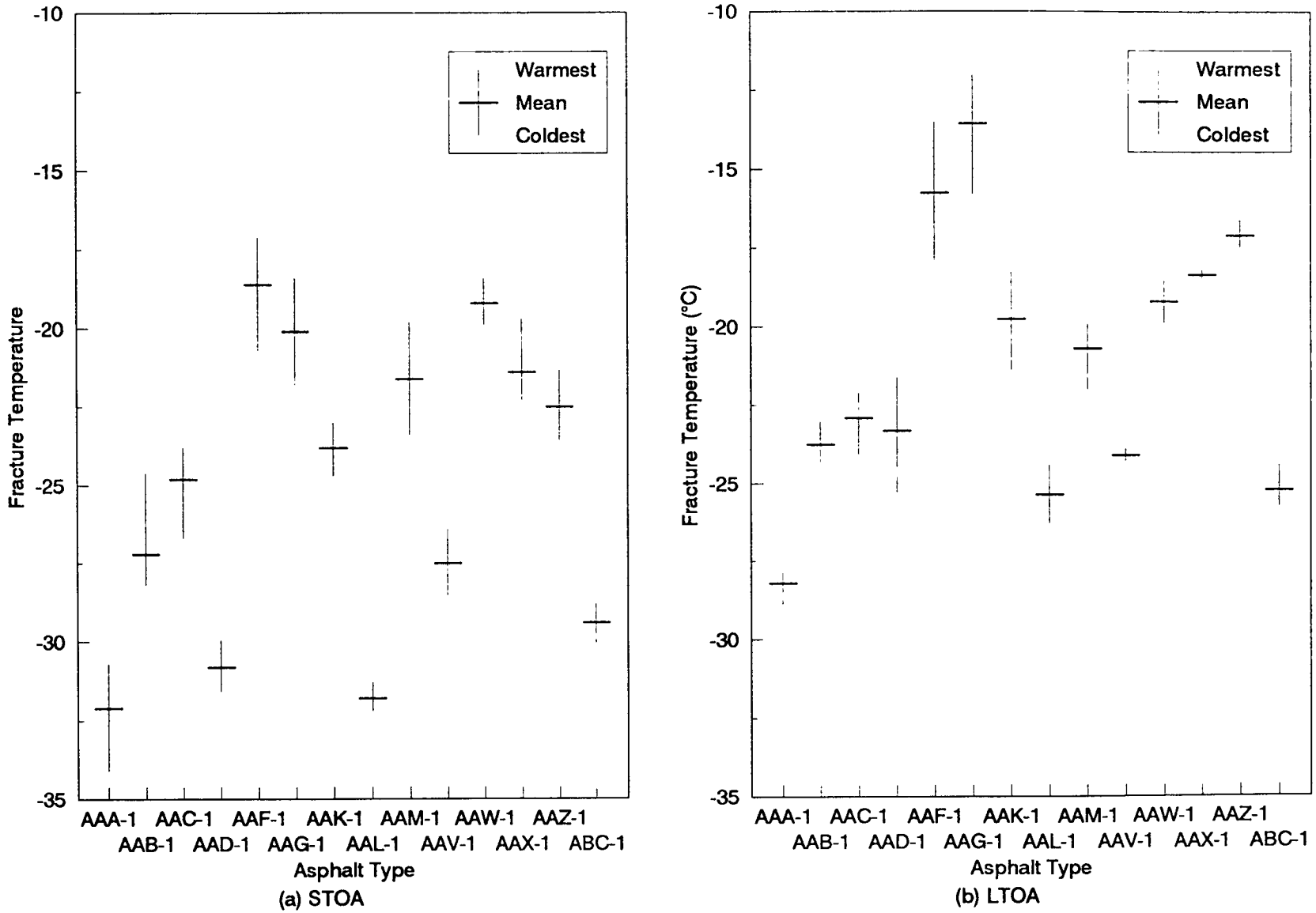

Figure 4.1. Mean and range of fracture temperature (RC)

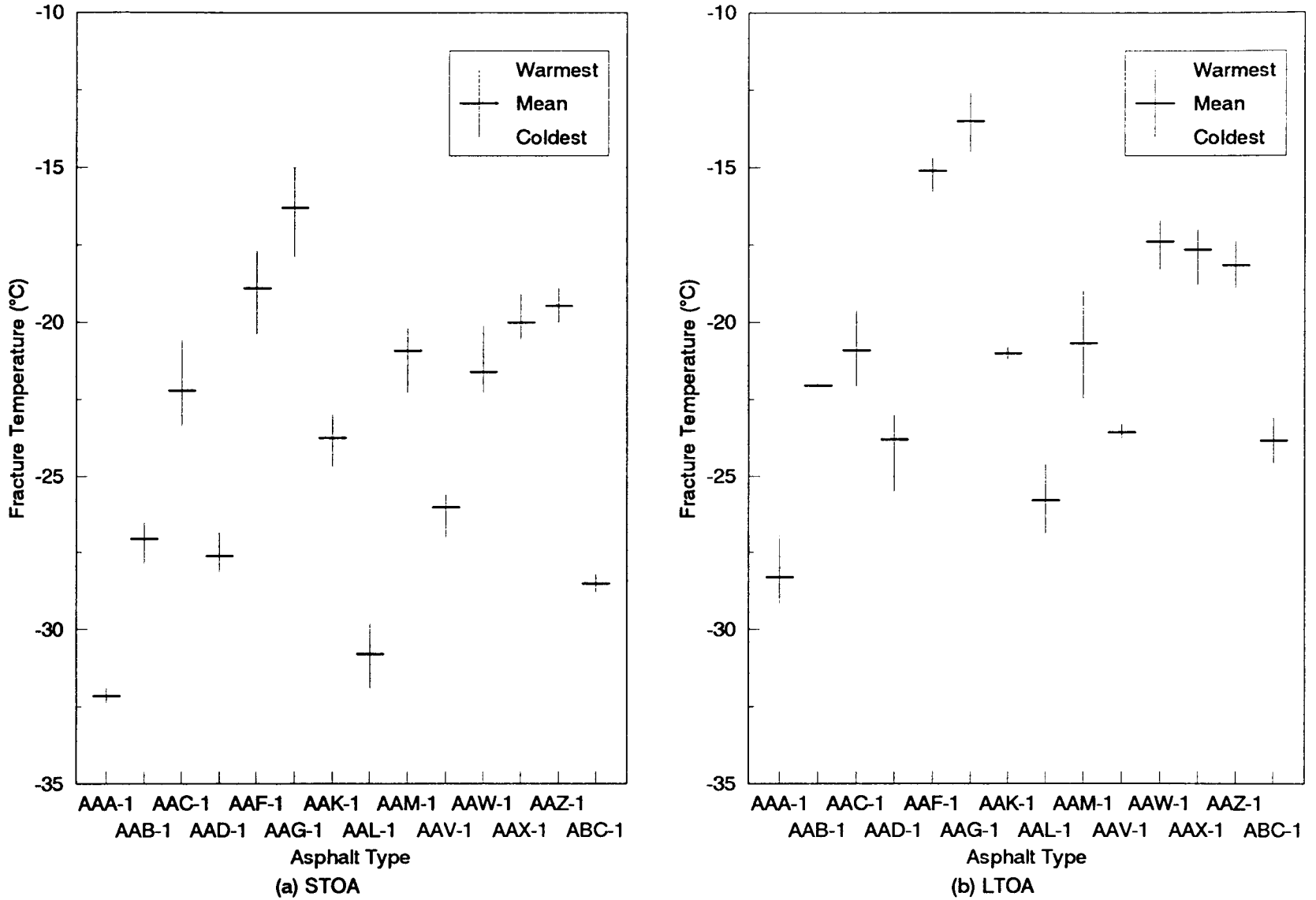

Figure 4.2. Mean and range of fracture temperature (RH)

The fracture temperature appears to be colder for specimens with RC aggregate compared with specimens with RH aggregate. The difference between STOA specimens with RC and RH aggregate ranged from -3.8°C to -0.9°C, with an average of -1.16°C. For LTOA specimens, the difference ranged from -2.0°C to 1.6°C, with an average of -0.42°C. Summary statistics for fracture temperature are given in Table 4.3.

4.2 Fracture Strength

Fracture strength is defined in terms of the maximum stress at fracture. Mean values and the coefficients of variation of fracture strength for a specific asphalt type, aggregate type, and degree of aging are summarized in Tables 4.4 and 4.5. Figures 4.3 and 4.4 show variations of fracture strengths for STOA and LTOA, depending on asphalt type for RC and RH aggregate, respectively.

The 95 percent repeatability limit for fracture strength was less than 50 percent for most of the asphalts. The fracture strengths exhibit a wide range of values, depending on asphalt type. The fracture strengths of specimens with RC aggregate ranged from 1.9 to 2.9 MPa for STOA and from 2.1 to 2.9 MPa for LTOA. For specimens with RH aggregate, fracture strengths ranged from 2.6 to 3.5 MPa for STOA and from 2.0 to 3.4 MPa for LTOA.

The fracture strengths for LTOA specimens with RC aggregate tend to be slightly higher than those for STOA specimens. The difference in fracture strengths between STOA and LTOA specimens with RC aggregate ranged from -0.67 to 0.73 MPa, with an average of 0.20 MPa. For specimens with RH aggregate, no significant differences between STOA and LTOA specimens were observed. The difference ranged from -0.63 to 0.38 MPa, with an average of -0.02 MPa.

The fracture strengths of specimens with RH aggregate are higher than those for specimens with RC aggregate. The difference in fracture strengths between STOA specimens with RC and those with RH aggregate ranged from -0.30 to 1.11 MPa, with an average of 0.47 MPa. For LTOA specimens, the difference ranged from -0.26 to 0.76 MPa, with an average of 0.25 MPa. Summary statistics for fracture strengths are given in Table 4.6.

4.3 Slope (dS/dT)

The slope of the thermally induced stress curve is defined as the maximum stress change per unit temperature change. It indicates the rate of accumulation of stresses in the specimen caused by cooling. It reflects the combined effect of the coefficient of thermal contraction and mixture stiffness. Mean values and the coefficients of variation of slope for a specific asphalt type, aggregate type, and degree of aging are summarized in Tables 4.7 and 4.8. Figures 4.5 and 4.6 show variations of slope for STOA and LTOA, depending on asphalt type, for RC and RH aggregate, respectively. The coldest and the warmest transition temperatures observed are plotted with the mean value for each asphalt type.

Table 4.3. Summary statistics for fracture temperature

Aggregate Type	Degree of Aging	Warmest Frac. Temp. (°C)	Coldest Frac. Temp. (°C)	Range (Warm-Cold)
RC	STOA	-18.6	-32.1	15.4
	LTOA	-13.6	-27.8	12.9
	Difference (STOA - LTOA)	Minimum -0.6	Maximum -6.5	Average -3.8
RH	STOA	-16.3	-32.2	15.7
	LTOA	-13.6	-29.3	14.8
	Difference (STOA - LTOA)	Minimum -0.6	Maximum -5.5	Average -2.9

Difference in STOA, °C (RC - RH)	Maximum:	-3.8
	Minimum:	0.9
	Average:	-1.16
Difference in LTOA, °C (RC - RH)	Maximum:	-2.0
	Minimum:	1.6
	Average:	-0.42

Table 4.4. Fracture strength for short-term aged specimens

Asphalt	Aggregate	No. of Obs.	Minimum (MPa)	Maximum (MPa)	Mean (MPa)	C.V. (%)	95% Repeatability Limit (%)
AAA-1	RC	3	2.436	2.836	2.617	15.6	21.3
	RH	2	3.485	3.540	3.512	1.1	N/A
AAB-1	RC	5	2.070	2.387	2.211	6.3	17.6
	RH	5	2.512	3.319	2.919	11.6	32.3
AAC-1	RC	4	1.884	2.498	2.177	11.5	32.0
	RH	5	2.201	2.629	2.472	5.7	15.7
AAD-1	RC	3	1.904	2.636	2.244	16.4	45.4
	RH	3	2.325	3.181	2.870	16.5	45.7
AAF-1	RC	4	1.663	2.008	1.884	8.0	22.3
	RH	3	2.484	2.836	2.617	7.3	20.2
AAG-1	RC	4	1.898	2.167	2.048	5.4	15.1
	RH	4	2.443	2.808	2.589	6.4	17.6
AAK-1	RC	5	1.771	2.254	1.971	11.7	32.5
	RH	4	2.884	3.388	3.076	7.1	19.7
AAL-1	RC	2	2.332	3.209	2.770	22.4	N/A
	RH	4	2.436	3.333	2.884	14.7	40.7
AAM-1	RC	4	2.719	3.257	2.922	8.6	23.8
	RH	6	3.050	3.202	3.127	2.2	6.1
AAV-1	RC	3	1.691	1.973	1.877	8.6	23.8
	RH	4	2.036	3.443	2.705	22.2	61.5
AAW-1	RC	3	2.381	2.650	2.413	9.2	25.6
	RH	5	2.229	3.098	2.742	13.3	36.9
AAX-1	RC	5	1.870	2.939	2.378	20.0	55.3
	RH	4	2.525	2.988	2.770	8.5	23.4
AAZ-1	RC	4	2.477	3.402	2.896	13.8	38.2
	RH	5	2.123	3.098	2.600	17.2	47.7
ABC-1	RC	2	2.505	2.712	2.608	5.6	N/A
	RH	2	2.250	2.919	2.584	18.3	N/A

Table 4.5. Fracture strength for long-term aged specimens

Asphalt	Aggregate	No. of Obs.	Minimum (MPa)	Maximum (MPa)	Mean (MPa)	C.V. (%)	95% Repeatability Limit (%)
AAA-1	RC	3	2.594	3.409	2.891	15.6	43.2
	RH	2	3.436	3.457	3.447	0.4	N/A
AAB-1	RC	4	2.443	3.195	2.663	13.4	37.2
	RH	2	2.815	3.098	2.957	6.8	N/A
AAC-1	RC	3	2.236	3.098	2.903	19.9	55.2
	RH	6	2.415	3.057	2.765	9.0	24.9
AAD-1	RC	2	2.760	3.063	2.898	6.7	N/A
	RH	5	2.394	3.105	2.921	9.9	26.8
AAF-1	RC	4	1.829	2.857	2.243	19.7	54.6
	RH	3	1.642	2.574	1.983	25.9	71.8
AAG-1	RC	3	1.484	3.071	2.153	38.2	105.8
	RH	4	2.132	2.864	2.460	15.6	43.2
AAK-1	RC	4	1.753	2.933	2.377	22.4	62.0
	RH	2	2.967	3.312	3.140	7.8	N/A
AAL-1	RC	2	2.622	2.926	2.774	7.7	N/A
	RH	5	2.125	2.912	2.710	8.1	22.5
AAM-1	RC	3	2.387	3.057	2.788	12.7	35.1
	RH	5	3.298	3.540	3.413	3.0	24.8
AAV-1	RC	3	2.153	2.981	2.456	18.6	51.4
	RH	3	2.415	3.326	2.870	15.9	43.9
AAW-1	RC	5	2.353	3.181	2.654	12.6	34.8
	RH	4	2.208	2.657	2.399	9.3	25.9
AAX-1	RC	2	2.470	2.788	2.629	8.5	N/A
	RH	3	2.581	2.843	2.705	4.9	13.5
AAZ-1	RC	3	1.822	2.546	2.226	16.6	46.0
	RH	4	2.884	3.071	2.979	2.8	7.7
ABC-1	RC	3	1.208	2.629	2.109	37.2	103.0
	RH	2	2.401	2.601	2.501	5.7	N/A

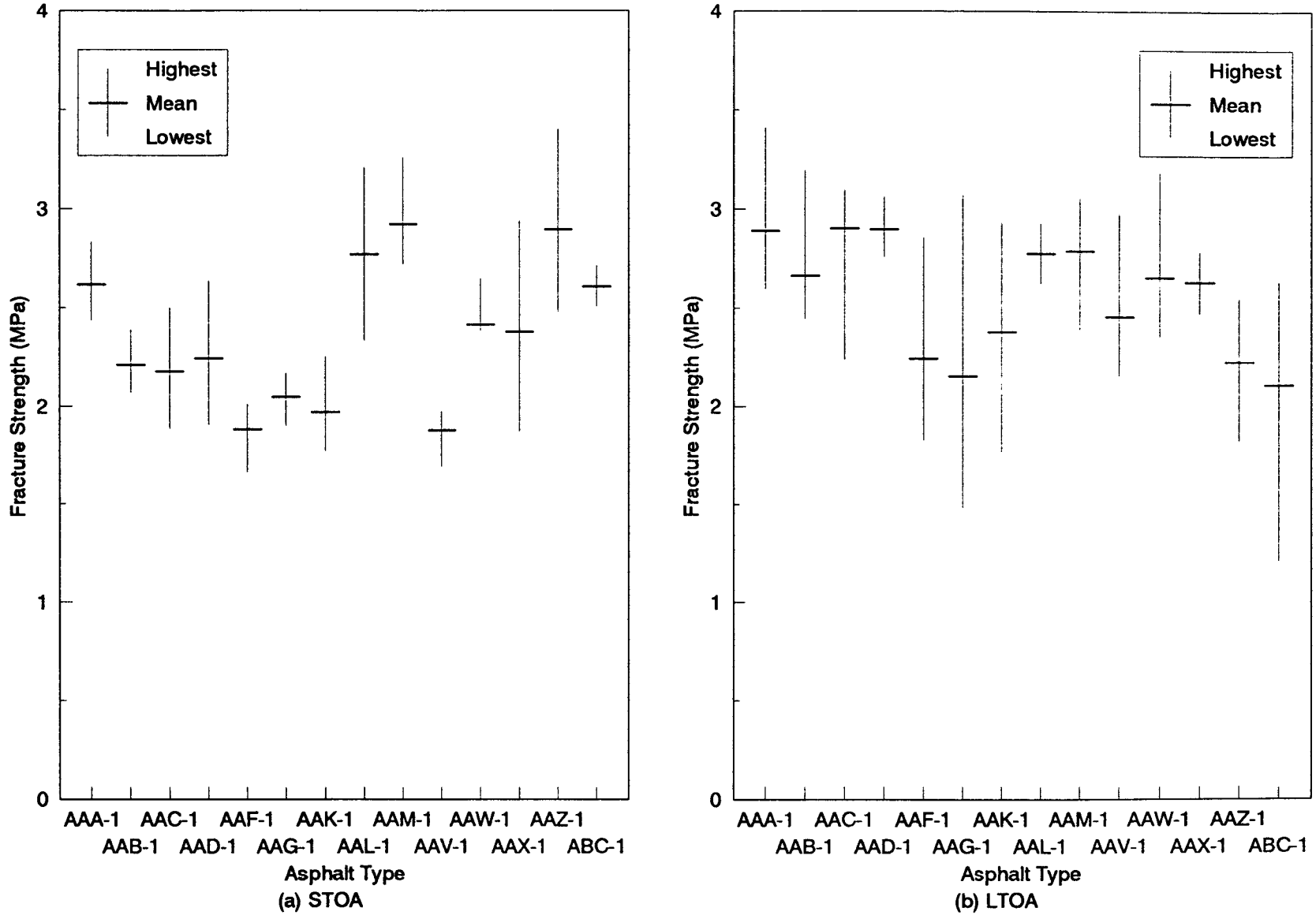

Figure 4.3. Mean and range of fracture strength (RC)

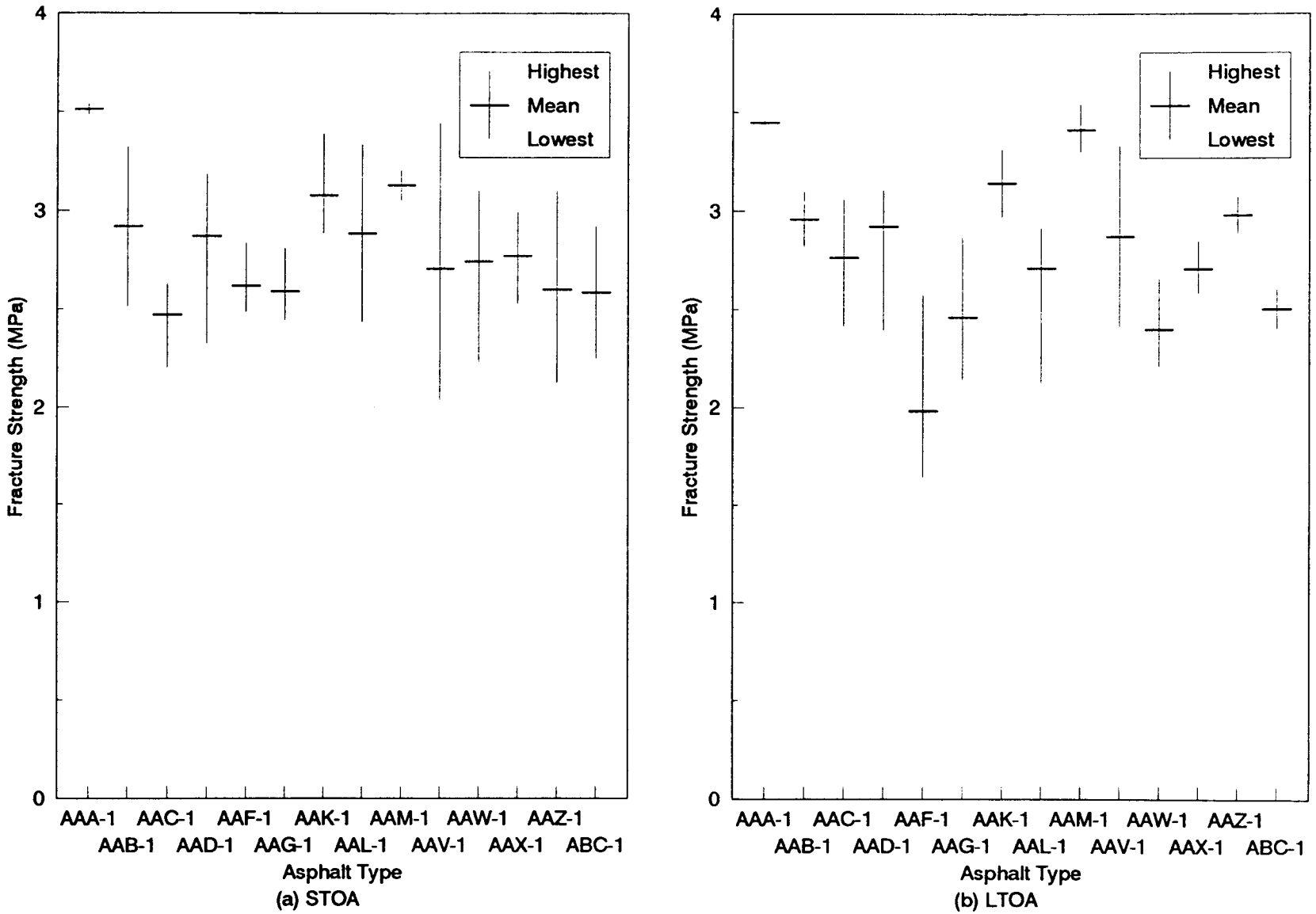

Figure 4.4. Mean and range of fracture strength (RH)

Table 4.6. Summary statistics for fracture strength

Aggregate Type	Degree of Aging	Max. Fracture Strength (MPa)	Min. Fracture Strength (MPa)	Range (Max.-Min.)
RC	STOA	2.922	1.877	1.045
	LTOA	2.903	2.109	0.794
	Difference (STOA - LTOA)	Maximum 0.726	Minimum -0.670	Average 0.20
RH	STOA	3.512	2.584	0.928
	LTOA	3.447	1.983	1.464
	Difference (STOA - LTOA)	Maximum 0.379	Minimum -0.634	Average -0.02

Difference in STOA, MPa (RH - RC)	Maximum:	1.105
	Minimum:	-0.296
	Average:	0.467
Difference in LTOA, MPa (RH - RC)	Maximum:	0.763
	Minimum:	-0.260
	Average:	0.249

Table 4.7. Slope for short-term aged specimens

Asphalt	Aggregate	No. of Obs.	Minimum (MPa/°C)	Maximum (MPa/°C)	Mean (MPa/°C)	C.V. (%)	95% Repeatability Limit (%)
AAA-1	RC	3	0.1380	0.1628	0.1488	8.3	23.1
	RH	2	0.2532	0.2581	0.2556	1.3	N/A
AAB-1	RC	5	0.1173	0.1808	0.1333	20.3	56.1
	RH	5	0.1649	0.2070	0.1955	8.9	24.5
AAC-1	RC	4	0.1063	0.1566	0.1358	15.4	42.6
	RH	5	0.1925	0.2381	0.2128	9.2	25.6
AAD-1	RC	3	0.1056	0.1359	0.1240	13.0	36.1
	RH	3	0.1628	0.2194	0.1930	14.8	40.9
AAF-1	RC	4	0.1070	0.1484	0.1325	13.5	37.5
	RH	3	0.1808	0.2346	0.1999	15.1	41.8
AAG-1	RC	4	0.1304	0.1573	0.1468	8.0	22.1
	RH	4	0.2070	0.2691	0.2431	12.3	34.2
AAK-1	RC	5	0.1035	0.1373	0.1225	12.8	35.5
	RH	4	0.2043	0.2401	0.2234	6.7	18.6
AAL-1	RC	2	0.1394	0.1656	0.1525	12.2	N/A
	RH	4	0.1794	0.2174	0.1918	12.5	34.7
AAM-1	RC	4	0.1622	0.2208	0.1858	15.1	41.8
	RH	6	0.2222	0.2429	0.2360	3.6	9.9
AAV-1	RC	3	0.1111	0.1332	0.1256	10.0	27.7
	RH	4	0.1691	0.2622	0.2090	19.6	54.2
AAW-1	RC	3	0.1421	0.1559	0.1495	4.6	12.9
	RH	5	0.1573	0.2215	0.1943	13.0	36.1
AAX-1	RC	5	0.1070	0.1566	0.1383	16.7	46.1
	RH	4	0.2091	0.2346	0.2203	6.1	17.0
AAZ-1	RC	4	0.1710	0.2249	0.1923	12.6	34.8
	RH	5	0.1856	0.2553	0.2187	16.2	44.9
ABC-1	RC	2	0.1283	0.1566	0.1425	14.0	N/A
	RH	2	0.1463	0.1808	0.1632	14.7	N/A

Table 4.8. Slope for long-term aged specimens

Asphalt	Aggregate	No. of Obs.	Minimum (MPa/°C)	Maximum (MPa/°C)	Mean (MPa/°C)	C.V. (%)	95% Repeatability Limit (%)
AAA-1	RC	3	0.1421	0.1856	0.1587	14.2	39.3
	RH	2	0.1152	0.2456	0.1804	51.1	N/A
AAB-1	RC	4	0.1380	0.1766	0.1489	12.5	34.7
	RH	2	0.2236	0.2346	0.2291	3.4	N/A
AAC-1	RC	3	0.1263	0.2015	0.1760	24.5	67.7
	RH	6	0.1835	0.2429	0.2134	12.0	33.2
AAD-1	RC	2	0.1380	0.1628	0.1553	6.9	N/A
	RH	5	0.1504	0.2036	0.1898	10.6	29.5
AAF-1	RC	4	0.1249	0.1822	0.1430	18.8	51.7
	RH	1	0.1987	0.1987	0.1987	N/A	N/A
AAG-1	RC	3	0.0925	0.1594	0.1265	26.5	73.3
	RH	4	0.2208	0.2519	0.2343	5.6	15.4
AAK-1	RC	4	0.1035	0.1656	0.1408	22.9	63.4
	RH	2	0.2001	0.2249	0.2118	8.8	N/A
AAL-1	RC	2	0.1525	0.1980	0.1753	18.4	N/A
	RH	5	0.1421	0.2167	0.1909	13.7	38.0
AAM-1	RC	3	0.1628	0.1822	0.1766	2.9	8.2
	RH	5	0.2243	0.2677	0.2432	7.8	21.7
AAV-1	RC	3	0.1470	0.1766	0.1608	9.3	25.7
	RH	3	0.1863	0.2636	0.2259	17.1	47.4
AAW-1	RC	5	0.1352	0.1877	0.1537	13.2	36.5
	RH	4	0.1484	0.1946	0.1665	14.8	41.0
AAX-1	RC	2	0.1594	0.1704	0.1649	4.7	N/A
	RH	3	0.1697	0.2298	0.2031	10.8	29.9
AAZ-1	RC	3	0.1428	0.1746	0.1603	10.1	27.8
	RH	4	0.2070	0.2415	0.2215	7.8	21.7
ABC-1	RC	3	0.0566	0.1401	0.1095	42.0	116.3
	RH	2	0.1642	0.1656	0.1649	0.6	N/A

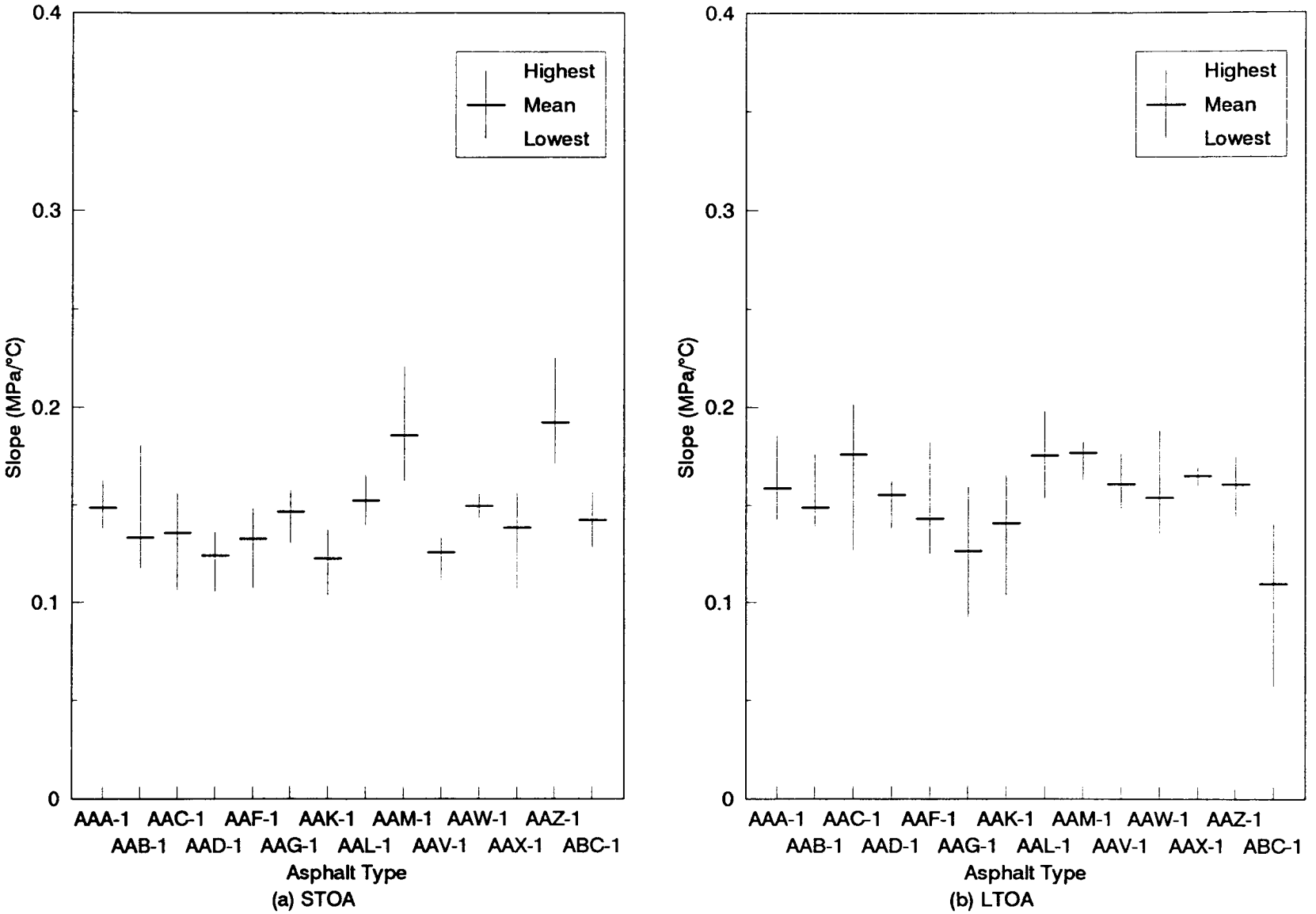

Figure 4.5. Mean and range of slope (RC)

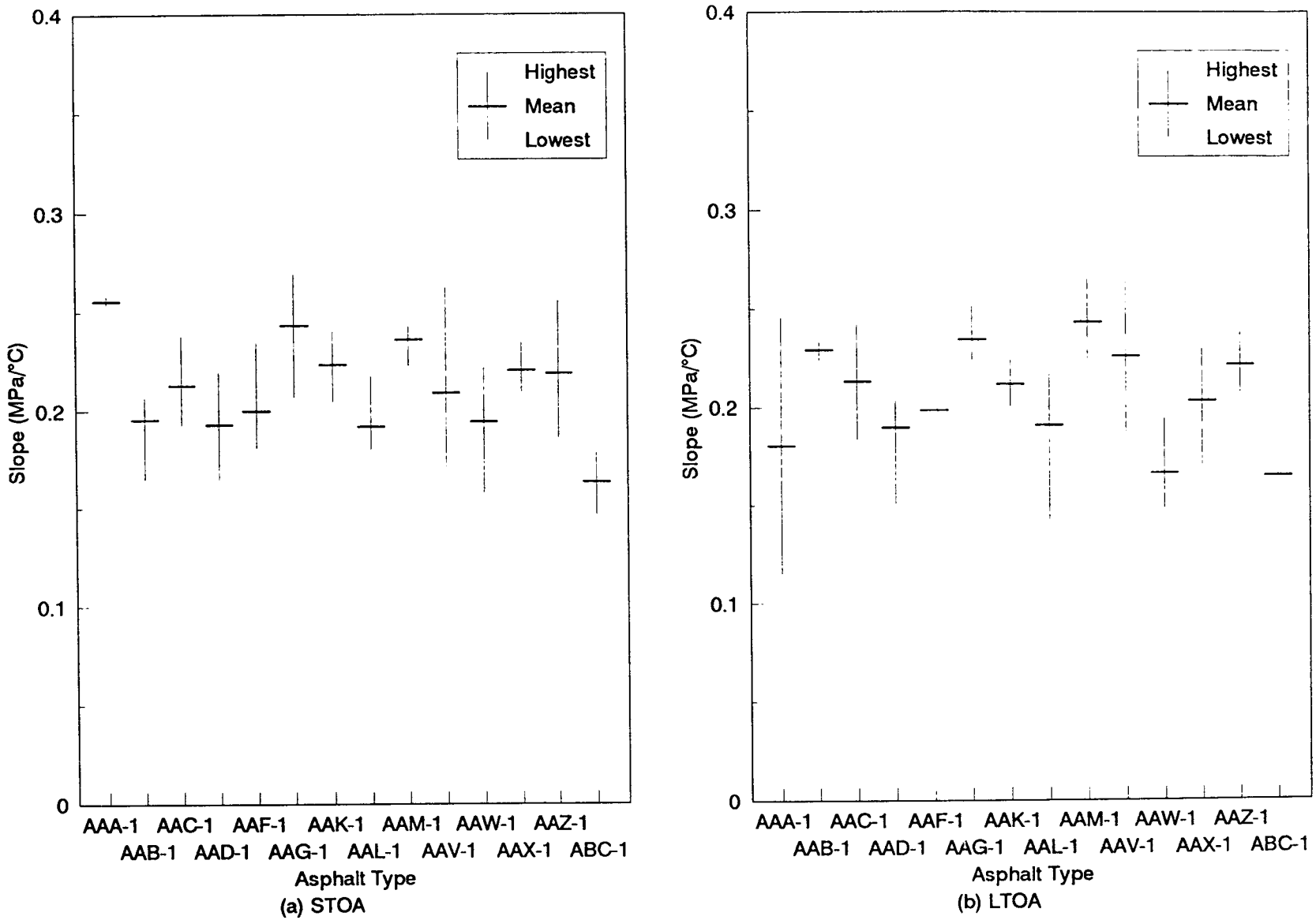

Figure 4.6. Mean and range of slope (RH)

The 95 percent repeatability limit for slope ranged from 25 percent to 50 percent for the majority of the asphalts. The slopes of specimens with RC aggregate ranged from 0.1225 to 0.1923 MPa/°C for STOA and from 0.1095 to 0.1766 M/Pa°C for LTOA. For specimens with RH aggregate, the slopes ranged from 0.1632 to 0.2556 MPa/°C for STOA and from 0.1649 to 0.2432 MPa/°C for LTOA.

The slopes of specimens with RH aggregate are greater than those for specimens with RC aggregate. The difference in slopes between STOA specimens with RC and RH aggregate ranged from 0.0207 to 0.1068 MPa/°C, with an average of 0.066 MPa/°C. For LTOA specimens, the difference ranged from 0.0128 to 0.1078 MPa/°C, with an average of 0.052 MPa/°C.

No consistent trend in slope between STOA and LTOA specimens was observed. The difference (LTOA minus STOA) in slopes between LTOA and STOA specimens with RC aggregate ranged from -0.0330 to 0.0402 MPa/°C, with an average of 0.0081 MPa/°C. For specimens with RH aggregate, the difference ranged from -0.0752 to 0.0366 MPa/°C, with an average of -0.0140 MPa/°C. Summary statistics for slopes are given in Table 4.9.

4.4 Transition Temperature

The transition temperature is defined as the temperature at which the slope becomes maximum. At temperatures warmer than the transition temperature, thermal stresses induced in the specimen are relaxed. At temperatures colder than the transition temperature, thermal stresses accumulated in the specimen are not relaxed (to any appreciable extent). Mean values and the coefficients of variation of transition temperature for a specific asphalt type, aggregate type, and degree of aging are summarized in Tables 4.10 and 4.11. Figures 4.7 and 4.8 show variations of transition temperatures for STOA and LTOA, depending on asphalt type, for RC and RH aggregate, respectively. The coldest and the warmest transition temperatures observed are plotted with the mean value for each asphalt type.

The 95 percent repeatability limit for transition temperature was less than 20 percent for most of the asphalts. The transition temperatures of specimens with RH aggregate ranged from -10.6°C to -25.7°C for STOA and from -8.7°C to -22.4°C for LTOA. For specimens with RC aggregate, the transition temperatures ranged from -10.9°C to -22.5°C for STOA and from -7.1°C to -19.6°C for LTOA.

The transition temperatures of LTOA specimens are warmer than for STOA specimens. The difference in transition temperatures between STOA and LTOA specimens with RC aggregate ranged from 1.0°C to 6.9°C with an average of 3.5°C. For specimens with RH aggregate, the difference ranged from -0.1°C to 5.3°C, with an average of 2.8°C. These trends were anticipated since the effect of aging is to increase mixture stiffness and cause a mix to be more susceptible to low-temperature cracking.

Table 4.9. Summary statistics for slope

Aggregate Type	Degree of Aging	Max. Slope (MPa/°C)	Min. Slope (MPa/°C)	Range (Max.-Min.)
RC	STOA	0.1923	0.1225	0.0698
	LTOA	0.1766	0.1095	0.0671
	Difference (LTOA - STOA)	Maximum 0.0402	Minimum -0.0330	Average 0.0081
RH	STOA	0.2556	0.1632	0.0924
	LTOA	0.2432	0.1649	0.0783
	Difference (LTOA - STOA)	Maximum 0.0336	Minimum -0.0752	Average -0.0140

Difference in STOA, MPa/°C (RH - RC)	Maximum:	0.1068
	Minimum:	0.0207
	Average:	0.066
Difference in LTOA, MPa/°C (RH - RC)	Maximum:	0.1078
	Minimum:	0.0128
	Average:	0.052

Table 4.10. Transition temperature for short-term aged specimens

Asphalt	Aggregate	No. of Obs.	Minimum (°C)	Maximum (°C)	Mean (°C)	C.V. (%)	95% Repeatability Limit (%)
AAA-1	RC	3	-23.5	-21.8	-22.5	3.9	10.7
	RH	2	-26.0	-26.4	-25.7	1.7	N/A
AAB-1	RC	5	-17.4	-16.5	-16.9	2.2	0.6
	RH	5	-18.8	-18.4	-18.6	1.1	3.1
AAC-1	RC	4	-17.1	-15.9	-16.6	3.2	8.8
	RH	5	-17.4	-15.5	-16.5	3.1	8.5
AAD-1	RC	3	-20.9	-20.7	-20.8	1.5	4.1
	RH	3	-21.5	-21.0	-21.2	1.2	3.3
AAF-1	RC	4	-11.6	-10.3	-11.0	5.0	13.9
	RH	3	-13.6	-13.2	-13.4	1.6	4.3
AAG-1	RC	4	-11.8	-10.5	-10.9	5.6	15.4
	RH	4	-10.7	-10.3	-10.6	1.8	5.0
AAK-1	RC	5	-16.4	-16.0	-16.2	0.9	2.6
	RH	4	-17.9	-17.0	-17.5	2.2	6.2
AAL-1	RC	2	-22.9	-22.3	-22.6	1.9	N/A
	RH	4	-22.7	-22.5	-22.6	0.4	1.2
AAM-1	RC	4	-15.7	-15.2	-15.4	1.5	4.3
	RH	6	-16.0	-15.0	-15.4	2.3	6.4
AAV-1	RC	3	-18.9	-18.2	-18.5	2.1	5.7
	RH	4	-20.4	-19.8	-20.1	1.3	3.6
AAW-1	RC	3	-12.7	-12.1	-12.4	3.0	8.4
	RH	5	-15.2	-15.0	-15.1	0.6	1.6
AAX-1	RC	5	-14.1	-13.6	-13.8	1.7	4.8
	RH	4	-14.6	-14.1	-14.4	1.5	4.3
AAZ-1	RC	4	-14.5	-14.1	-14.3	1.2	3.3
	RH	5	-15.0	-14.6	-14.8	1.3	3.6
ABC-1	RC	2	-20.6	-19.4	-20.0	4.2	N/A
	RH	2	-21.5	-21.2	-21.3	1.3	N/A

Table 4.11. Transition temperature for long-term aged specimens

Asphalt	Aggregate	No. of Obs.	Minimum (°C)	Maximum (°C)	Mean (°C)	C.V. (%)	95% Repeatability Limit (%)
AAA-1	RC	3	-20.1	-19.1	-19.6	2.6	7.1
	RH	2	-22.7	-22.1	-22.4	1.9	N/A
AAB-1	RC	4	-15.1	-15.0	-15.0	0.4	1.1
	RH	2	-15.3	-15.0	-15.2	1.4	N/A
AAC-1	RC	3	-15.0	-14.1	-14.6	3.1	8.6
	RH	6	-16.0	-15.0	-15.3	3.4	9.3
AAD-1	RC	2	-14.4	-13.2	-13.9	2.0	N/A
	RH	5	-16.6	-16.1	-16.4	2.4	6.6
AAF-1	RC	4	-8.8	-7.4	-8.0	8.4	23.1
	RH	1	-10.3	-10.3	-10.3	N/A	N/A
AAG-1	RC	3	-7.2	-6.9	-7.1	2.2	6.0
	RH	4	-9.0	-8.1	-8.7	4.7	12.9
AAK-1	RC	4	-11.0	-10.0	-10.4	4.6	12.8
	RH	2	-13.6	-13.5	-13.6	0.5	N/A
AAL-1	RC	2	-17.4	-17.0	-17.2	1.6	N/A
	RH	5	-19.1	-18.2	-18.7	1.9	5.3
AAM-1	RC	3	-15.0	-14.0	-14.4	3.8	10.6
	RH	5	-15.7	-15.2	-15.5	2.0	5.6
AAV-1	RC	3	-17.4	-16.7	-17.1	2.2	6.1
	RH	3	-18.4	-17.5	-18.0	2.5	7.0
AAW-1	RC	5	-10.3	-10.0	-10.2	1.6	4.5
	RH	4	-11.2	-11.0	-11.1	1.0	2.9
AAX-1	RC	2	-10.1	-10.0	-10.1	0.7	N/A
	RH	3	-12.0	-11.6	-11.8	1.8	4.9
AAZ-1	RC	3	-10.6	-10.3	-10.4	1.7	4.6
	RH	4	-12.7	-12.3	-12.5	1.4	3.8
ABC-1	RC	3	-17.5	-10.6	-15.0	25.6	70.9
	RH	2	-16.4	-15.5	-16.0	4.0	N/A

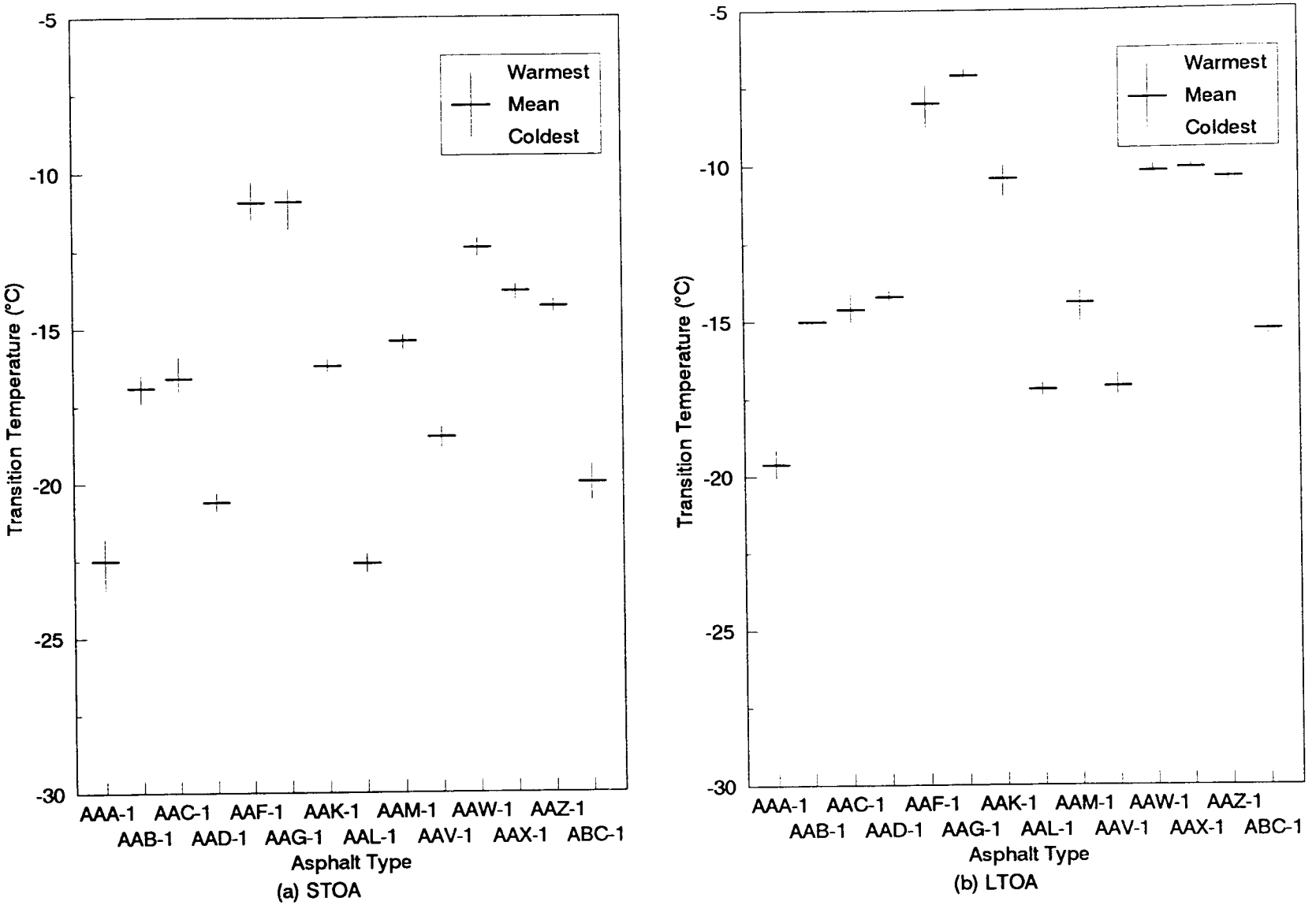

Figure 4.7. Mean and range of transition temperature (RC)

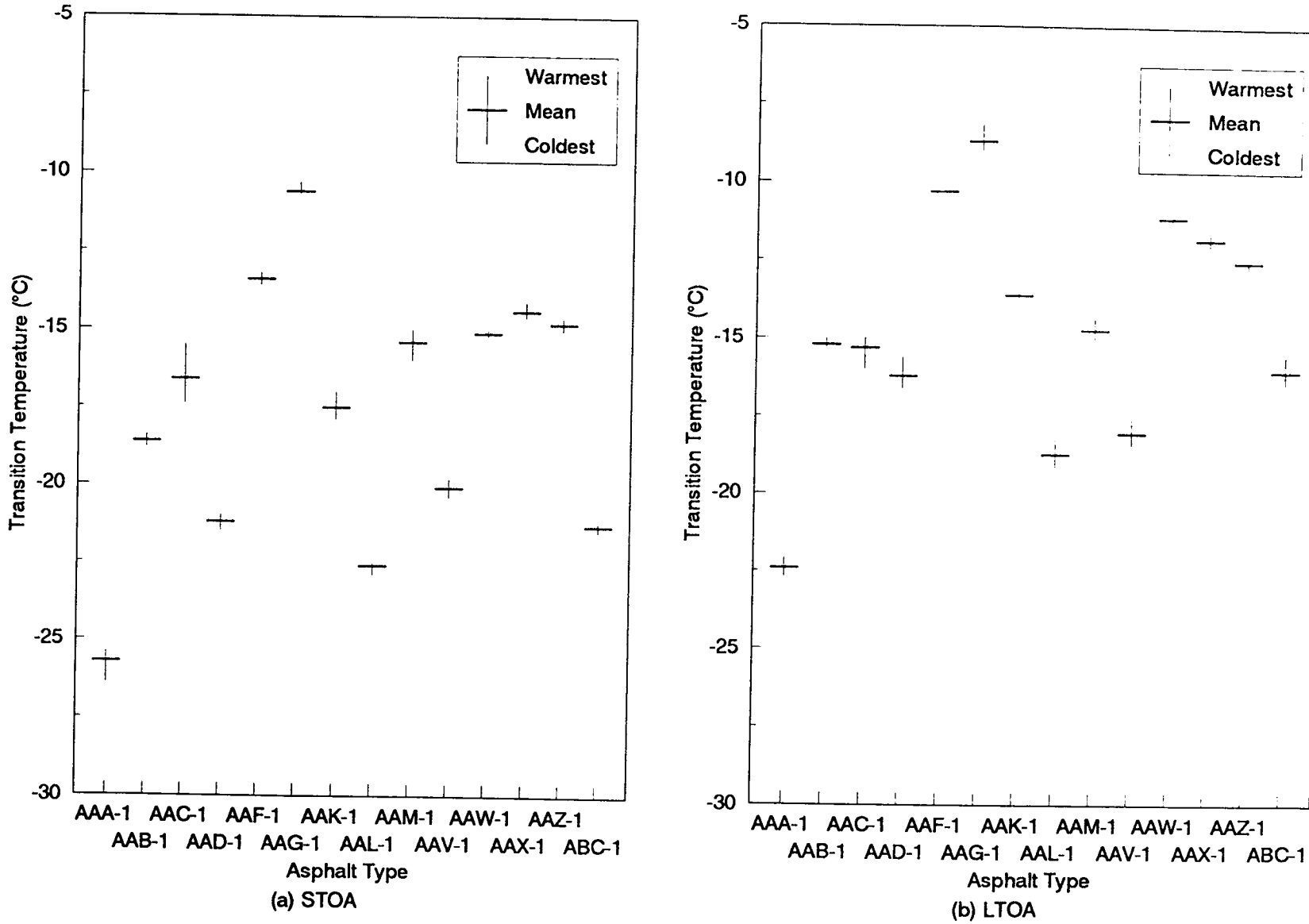

Figure 4.8. Mean and range of transition temperature (RH)

The transition temperatures of specimens with RH aggregate are slightly colder than those for specimens with RC aggregate. The difference in transition temperatures for STOA specimens with RC and RH aggregate ranged from -0.6°C to 3.2°C, with an average of 0.88°C. For LTOA specimens, the difference ranged from 0.2°C to 3.2°C, with an average of 1.6°C. Summary statistics for transition temperatures are presented in Table 4.12.

4.5 Summary of Results

The repeatability of the TSRST is estimated as good for fracture and transition temperature, and reasonable for fracture strength and slope. The coefficients of variation for fracture and transition temperature were close to or below 10 percent, and for fracture strength and slope were close to or below 20 percent.

The TSRST results expressed in terms of fracture temperature, fracture strength, slope, and transition temperature were strongly dependent on asphalt type. That is, asphalt type was identified as the dominant factor related to the low-temperature cracking characteristics of asphalt concrete mixes.

Fracture temperature increases significantly as the degree of aging increases. The fracture temperatures for LTOA specimens were warmer than those for STOA specimens. There are small differences in fracture temperatures related to aggregate type and air void content. Fracture temperature is slightly warmer for low air void content mixtures. Fracture temperatures for mixtures with RH aggregate are warmer than fracture temperatures for mixtures with RC aggregate. The differences in fracture temperatures related to aggregate type and air void content are not significant compared to the differences due to asphalt type and aging.

Transition temperatures for long-term aged mixtures were warmer than transition temperatures of short-term aged mixtures. Transition temperatures are slightly colder for mixtures with RH aggregate.

There are significant differences in fracture strengths and slope related to aggregate type. Fracture strength and slope are also greater for mixtures with RH aggregate. Fracture strength and slope are slightly higher for LTOA mixtures. Some differences also exist in fracture strength and slope depending on asphalt type, but the differences are not significant compared to differences related to aggregate type and air void content.

Table 4.12. Summary statistics for transition temperature

Aggregate Type	Degree of Aging	Warmest Tran. Temp. (°C)	Coldest Tran. Temp. (°C)	Range (Warm-Cold)
RC	STOA	-10.9	-22.5	11.6
	LTOA	-7.1	-19.6	12.5
	Difference (LTOA - STOA)	Maximum 6.9	Minimum 1.0	Average 3.5
RH	STOA	-10.3	-25.7	15.1
	LTOA	-8.7	-22.4	13.7
	Difference (LTOA - STOA)	Maximum 5.3	Minimum -0.1	Average 2.8

Difference in STOA, °C (RC - RH)	Maximum: 3.2 Minimum: -0.6 Average: 0.88
Difference in LTOA, °C (RC - RH)	Maximum: 3.2 Minimum: 0.2 Average: 1.6

5

Statistical Analysis of TSRST Results

Statistical analyses were performed on the thermal stress restrained specimen test (TSRST) results using general linear model procedures included in the Statistical Analysis System (SAS) software package (SAS Institute Inc., 1991). The specific analyses included (1) analysis of covariance, (2) analysis of least squares means, and (3) Waller-Duncan T-test.

5.1 Data Description

The source variables considered in the model were asphalt type (AAA-1 through ABC-1), aggregate type (RC and RH), degree of aging (short-term [ST] and long-term [LT]), and air void content. The dependent variables in the model were fracture temperature, fracture strength, slope (dS/dT), and transition temperature. The source and dependent variables considered in the analysis are described in Table 5.1.

The experiment design included a total of 14 × 2 × 2 × 2 × 2 experiments. In reality, it was difficult to achieve the target air void contents of 4 percent and 8 percent, because of difficulties in compaction with the aggregates selected. The resulting air void contents ranged from 2 percent to 15 percent. In addition, for the target air void content of 4 percent, a significant amount of aggregate breakage occurred during compaction, particularly for the RC aggregate. Consequently, several specimens from the 224 identified in the original experiment design were discarded. A total of 201 test results were included in the analysis.

5.2 Analysis of Covariance

Since the air void contents were not fully controlled, a source variable (VOID) was considered to be a covariate (continuous variable) in the analysis. The analysis of covariance was performed using a general linear model (GLM) procedure. The analysis of covariance combined some of the features of regression and analysis of variance. Typically, the covariate was introduced in the model of an analysis of variance.

Table 5.1. Description of variables

Source Variables	Levels	Description
ASP	AAA-1, AAB-1, AAC-1, AAD-1, AAF-1, AAG-1, AAK-1, AAL-1, AAM-1 AAV-1, AAW-1, AAX-1, AAZ-1, ABC-1	Asphalt Type
AGG	RC, RH	Aggregate Type
AGE	ST (Short-Term Aging) LT (Long-Term Aging)	Degree of Aging
VOID	Covariate	Air void content

Dependent Variables	Description
FRTEMP	Fracture Temperature
FRSTRE	Fracture Strength
SLOPE	Slope (dS/dT)
TRTEMP	Transition Temperature

The GLM procedure provides both Type I and Type III hypothesis tests. Type I mean squares indicate the influence of that factor after the effects of the factors listed before it in the model have been removed. Type III mean squares indicate the influence of that factor after the effects of all the other factors in the model have been removed. The procedure can also provide least squares means (LSMEAN). LSMEAN of a variance are estimated for a given level of a given effect and adjusted for the covariate. That is, LSMEAN of fracture temperature and strength, slope, and transition temperature for a specific asphalt type are mean values of these variables adjusted for the average air void content, which considered the effect of aggregate type and degree of aging.

The procedure followed in the analysis was as follows: (1) consider the full model, which included all possible factors, (2) perform the analysis of covariance for the model, (3) select and delete insignificant factors in the model, (4) repeat the analysis for the reduced model without insignificant factors until reasonable factors can be selected, and (5) finalize the model.

5.2.1 Fracture Temperature Model

From the full model analysis for the dependent variable FRTEMP, the Type III $P_r > F$ values for all the factors are significant. However, the Type III mean square for the factor ASP*AGG was not significant compared with other factors. Thus, the factor ASP*AGG was dropped from the model.

The first reduced model included ASP, AGE, AGG, VOID, ASP*AGE, and AGG*AGE. The mean square error for the model was 1.267. The Type III $P_r > F$ values for all the factors in the model were still less than 0.05, but the Type III mean square for AGG*AGE was not significant. Therefore, the factor AGG*AGE was dropped from the model.

The second reduced model included factors ASP, AGE, AGG, VOID, and ASP*AGE. The mean square error for the model was 1.303. The Type III $P_r > F$ values were significant for all the factors in the model, but the Type III mean square for AGG was not significant. The factor AGG was dropped from the model.

The third reduced model consisted of factors ASP, AGE, VOID, and ASP*AGE. The mean square error for the model was 1.385. Both the Type III $P_r > F$ values and mean squares for all the factors in the model were significant. The factors ASP, AGE, VOID, and ASP*AGE were included in the fracture temperature model.

The ranking for the factors considered in the third reduced model based on Type III mean squares was AGE> ASP> VOID> ASP*AGE. The Type III mean squares for AGE and ASP were much greater compared to VOID and ASP*AGE. Thus, degree of aging and asphalt type had a substantial influence on fracture temperature, while air void content and the interaction between asphalt type and degree of aging had a minor influence. The mean square errors for the full model and the reduced models are given in Table 5.2.

Table 5.2. Mean square errors for fracture temperature models

Model	Factors Involved	Mean Square Errors
Full Model	ASP, AGE, AGG, VOID, ASP*AGE, ASP*AGG, AGG*AGE	1.141
Reduced Model I	ASP, AGE, AGG, VOID, ASP*AGE, AGG*AGE	1.267
Reduced Model II	ASP, AGE, AGG, VOID, ASP*AGE	1.303
Reduced Model III	ASP, AGE, VOID, ASP*AGE	1.385

LSMEAN of fracture temperature for the effect ASP ranged from -15.8°C to -30.3°C. Fracture temperature for long-term oven aging (LTOA) specimens was warmer than short-term oven aging (STOA) specimens. The difference in the LSMEAN of fracture temperature for specimens with RC aggregate ranged from 2.1°C to 6.7°C, with an average of 4.7°C. For specimens with RH aggregate, the difference ranged from 0.6°C to 5.1°C, with an average of 3.4°C.

LSMEAN of fracture temperature for STOA and LTOA specimens are compared in Figure 5.1. LSMEAN for the factor AGG shows no significant difference in fracture temperature between RC and RH aggregate. The fracture temperature of specimens with RH aggregate is slightly warmer than for specimens with RC aggregate. LSMEAN of fracture temperature for specimens with RC and RH aggregates are compared in Figure 5.2.

5.2.2 Fracture Strength Model

ASP*AGG was not a significant factor in the full model because the Type III $P_r > F$ value was 0.1461 > 0.05. The factor ASP*AGG can be dropped from the model.

The first reduced model consisted of ASP, AGE, AGG, VOID, ASP*AGE, and AGG*AGE. The mean square error for the model was 1570.1. The Type III $P_r > F$ values for all the factors in the model were significant, but the Type III mean squares for ASP*AGE were not significant. The factor ASP*AGE was dropped from the model.

The second reduced model included ASP, AGE, AGG, VOID, and AGG*AGE. The mean square error for the model was 1681.8. The Type III $P_r > F$ values for all the factors in the model were significant, but the Type III mean square for the factor AGE was not significant. The factor AGE was dropped from the model.

The third reduced model included ASP, AGG, VOID, and AGG*AGE. Both the Type III $P_r > F$ values and mean squares for all the factors in the model were significant. Mean square error for the model was 1681.8. The factors ASP, AGG, VOID, and AGG*AGE were included in the fracture strength model.

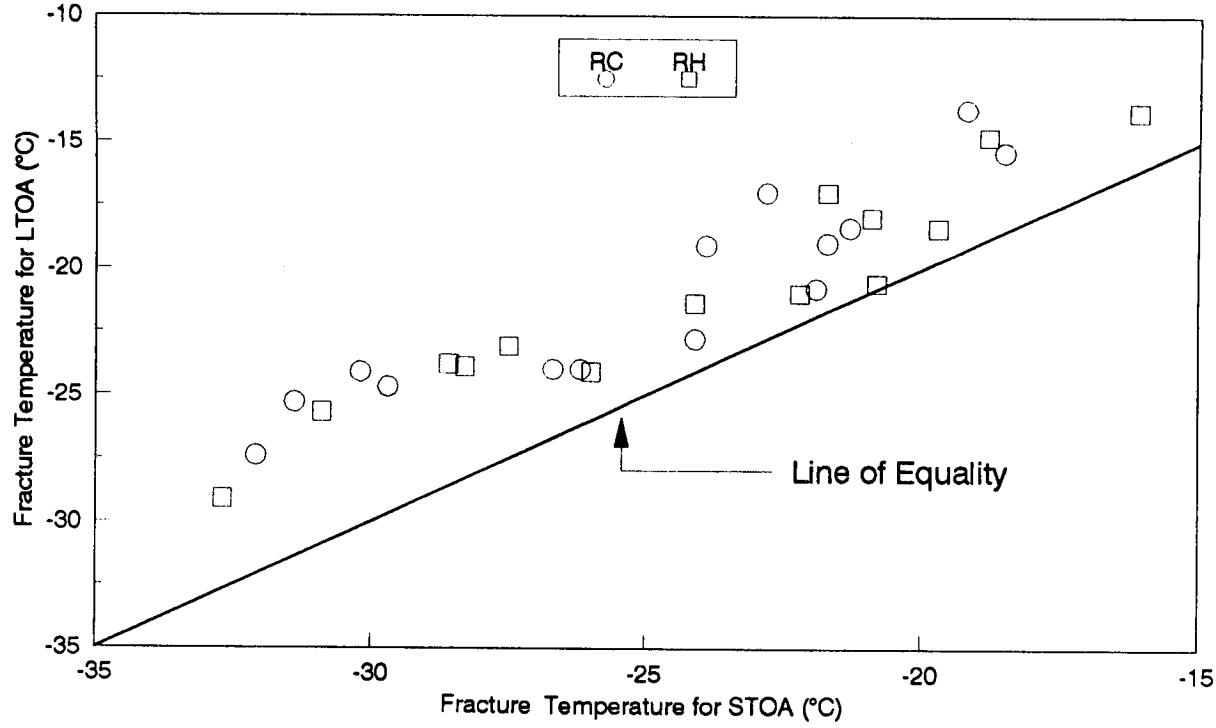

Figure 5.1. Comparison of fracture temperature for STOA and LTOA specimens

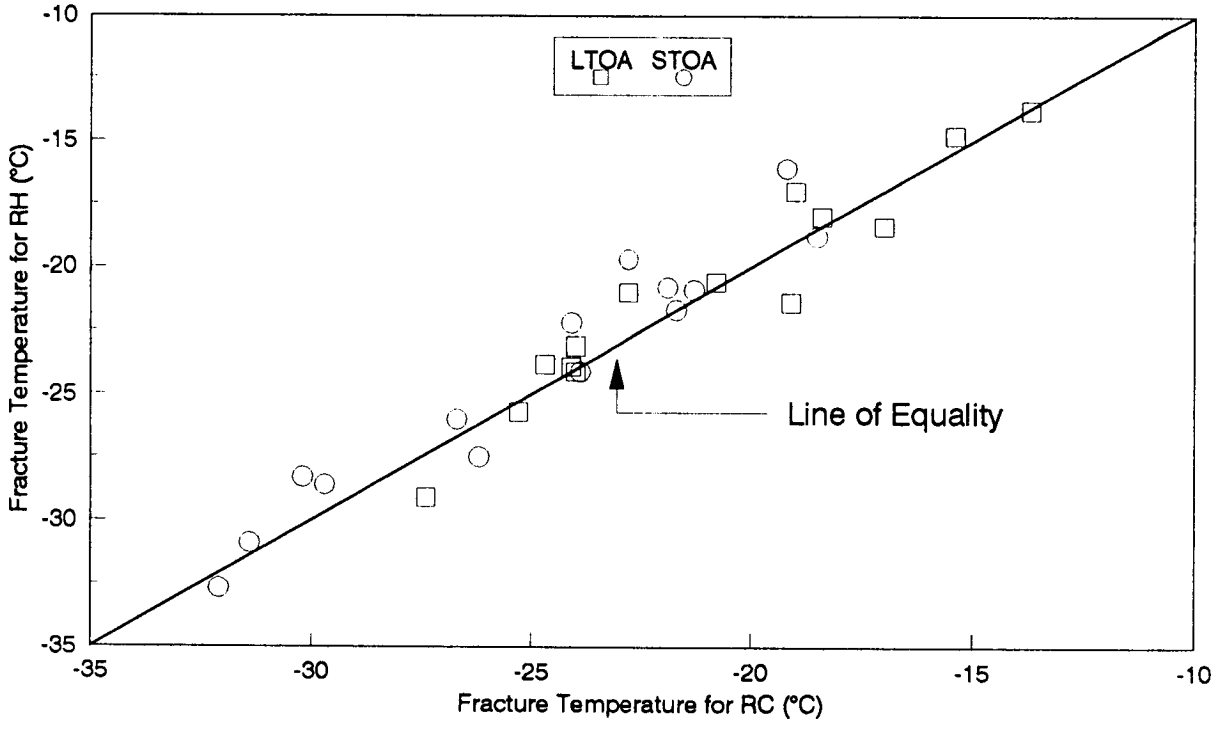

Figure 5.2. Comparison of fracture temperature for RC and RH aggregates

The ranking for the factors considered in the third reduced model based on the Type III mean squares was VOID> AGG> AGG*AGE> ASP. The Type III mean squares for VOID and AGG were much greater than AGG*AGE and ASP. Thus, fracture strength was highly affected by air void content and aggregate type, and affected by asphalt type and by the interaction between aggregate type and degree of aging to a much lesser extent. Table 5.3 shows the mean square errors for all the models considered.

LSMEAN of fracture strength for the effect ASP ranged from 2275 kPa to 3135 kPa (330 to 455 psi). LSMEAN for the effect AGE shows that the fracture strength of LTOA specimens is greater than STOA by 131 kPa (19 psi). LSMEAN of fracture strength for STOA and LTOA specimens are compared in Figure 5.3. LSMEAN for the effect AGG shows that the fracture strength of specimens with RH aggregate is greater than RC aggregate by 220 kPa (32 psi). LSMEAN of fracture strength for specimens with RC and RH aggregates are compared in Figure 5.4.

Since the air void contents were not fully controlled, the test results were divided into two groups; high and low air voids. Low air void contents were less than 6 percent. High air void contents were greater than 6 percent. LSMEAN of fracture strength for high and low air void contents were obtained for specimens with a specific asphalt type and which had at least two observations for each air void group. Figure 5.5 compares fracture strength for high and low air voids. As indicated, fracture strengths are greater for specimens with low air voids.

5.2.3 Slope (dS/dT) Model

From the analysis for the dependent variable SLOPE, the Type III $P_r > F$ value for the factor AGE was 0.1413 > 0.05. AGE was not a significant factor in the full model. The factor AGE was dropped from the model.

The first reduced model consisted of ASP, AGG, VOID, ASP*AGE, ASP*AGG, and AGG*AGE. The mean square error for the model was 5.580. The Type III $P_r > F$ values for all the factors in the model were significant, but the Type III mean square for ASP*AGE was not significant. The factor ASP*AGE was dropped from the model.

The second reduced model included ASP, AGG, VOID, ASP*AGG, and AGG*AGE. The mean square error for the model was 6.296. The Type III $P_r > F$ values for all the factors in the model were significant, but the Type III mean square for the factor ASP*AGG was not significant. The factor ASP*AGG was dropped from the model.

The third reduced model included ASP, AGG, VOID, and AGG*AGE. Both the Type III $P_r > F$ values and mean squares for all the factors in the model were significant. The mean square error for the model was 6.893. The factors ASP, AGG, VOID, and AGG*AGE were included in the slope model.

Table 5.3. Mean square errors for fracture strength models

Model	Factors	Mean Square Errors
Full Model	ASP, AGE, AGG, VOID, ASP*AGE, ASP*AGG, AGG*AGE	1518.8
Reduced Model I	ASP, AGG, AGE, VOID, ASP*AGE, AGG*AGE	1570.1
Reduced Model II	ASP, AGG, AGE, VOID, AGG*AGE	1681.8
Reduced Model III	ASP, AGG, VOID, AGG*AGE	1681.8

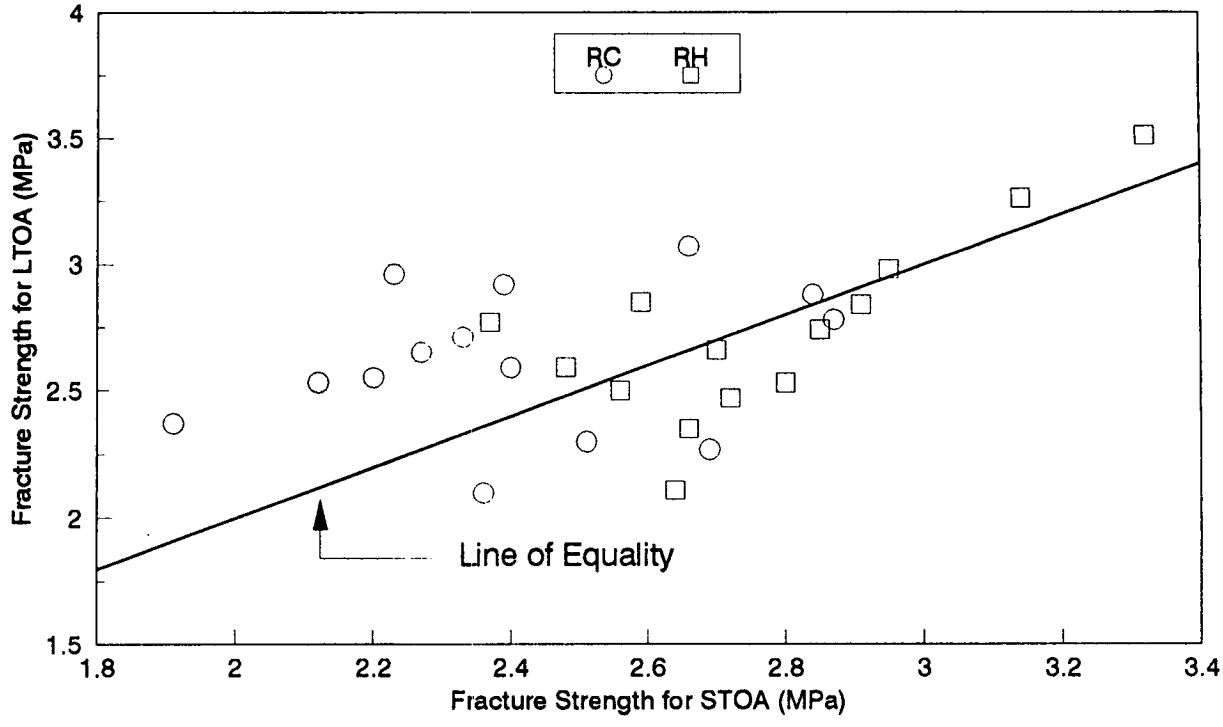

Figure 5.3. Comparison of fracture strength for STOA and LTOA specimens

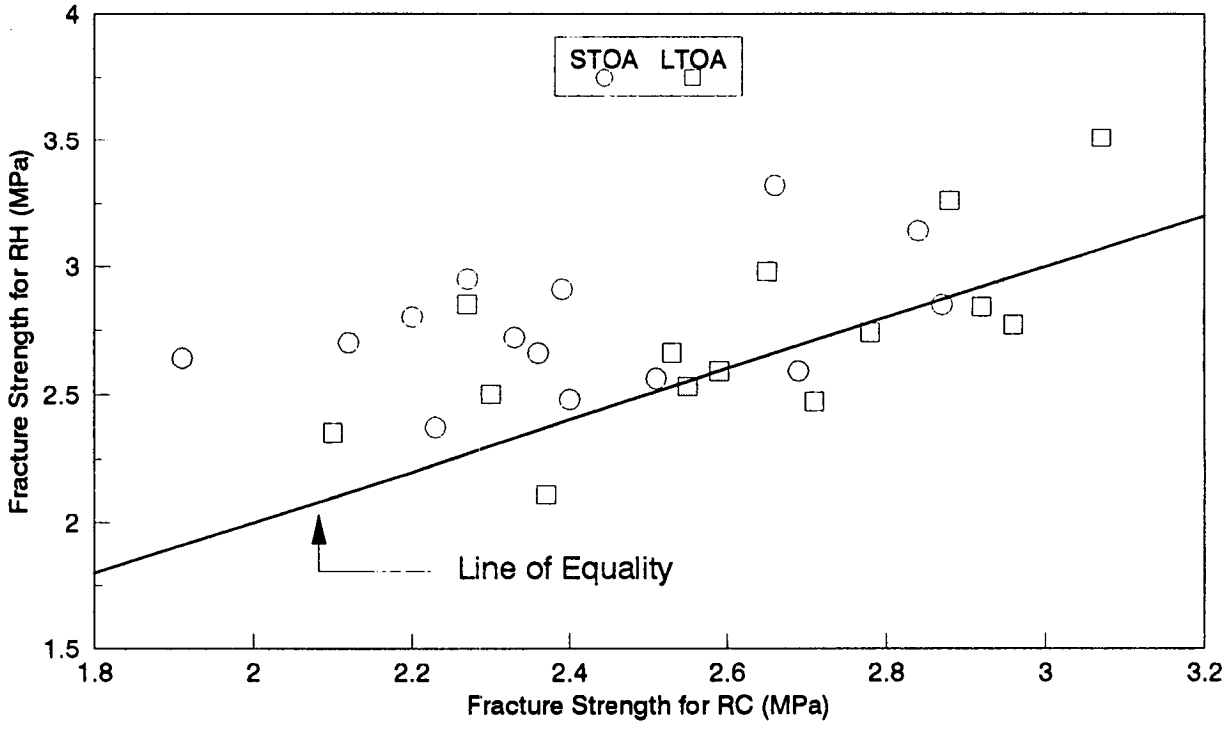

Figure 5.4. Comparison of fracture strength for RC and RH aggregates

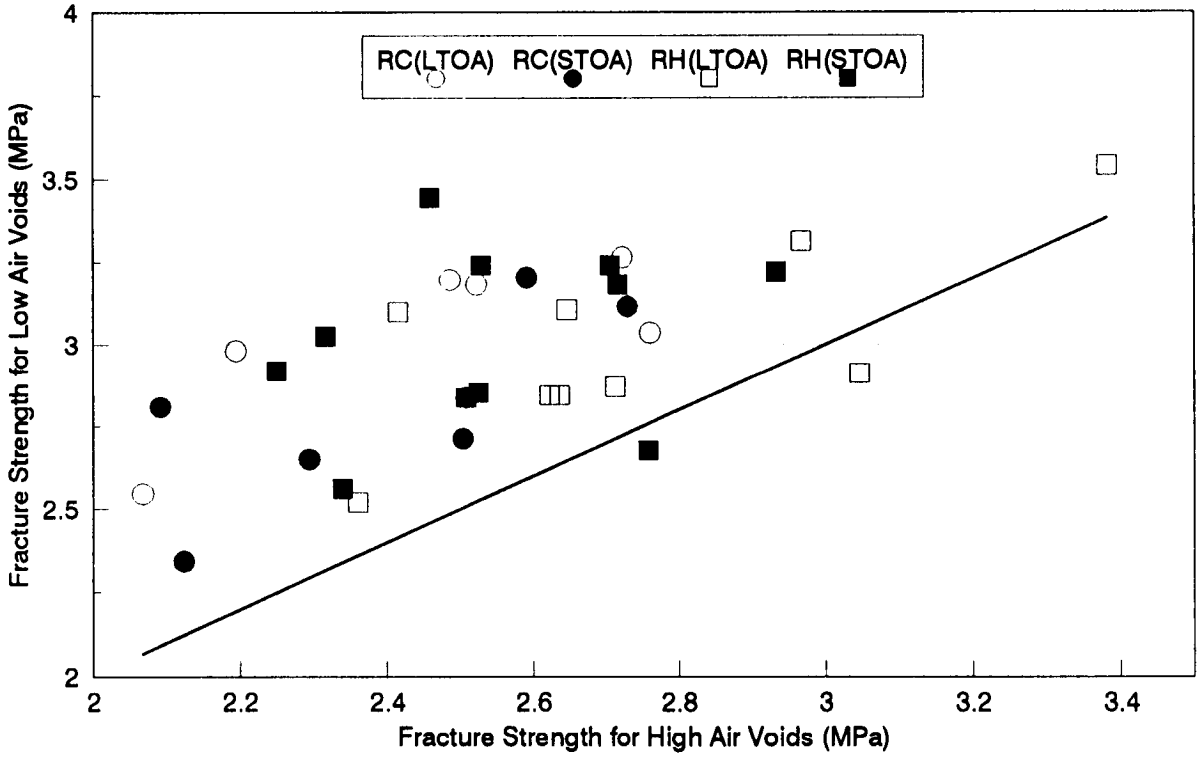

Figure 5.5. Comparison of fracture strength for high and low air voids

The ranking for the factors considered in the third reduced model based on the Type III mean squares was AGG> VOID> AGG*AGE> ASP. The Type III mean squares for AGG and VOID were much greater than for AGG*AGE and ASP. Thus, slope was highly affected by aggregate type and air void content, and was much less affected by asphalt type and the interaction between aggregate type and degree of aging. Table 5.4 shows the mean square errors for all the models considered.

LSMEAN of slope for the effect ASP ranged from 146 kPa/°C to 207 kPa/°C (21.2 psi/°C to 30.1 psi/°C). LSMEAN for the effect AGE shows no significant difference in slope for STOA and LTOA specimens. LSMEAN of slope for STOA and LTOA specimens are compared in Figure 5.6. LSMEAN for the effect AGG shows that slope for specimens with RH aggregate is greater than RC aggregate by 48 kPa/°C (7 psi/°C). LSMEAN of slope for specimens with RC and RH aggregates are compared in Figure 5.7.

LSMEAN of slope for high and low air void contents were obtained for specimens with a specific asphalt type and that had at least two observations for each air voids group. Slopes for high and low air voids are compared in Figure 5.8. As shown, the slopes are greater for specimens with low air voids.

5.2.4 Transition Temperature Model

From the full model analysis for the dependent variable TRTEMP, the Type III $P_r > F$ value for the factor VOID was 0.5701 > 0.05. The factor VOID was not significant and was dropped from the model.

The first reduced model consisted of ASP, AGE, AGG, ASP*AGE, ASP*AGG, and AGG*AGE. The mean square error for the model was 0.430. The Type III $P_r > F$ value for the factor AGG*AGE was greater than 0.05. The factor AGG*AGE was dropped from the model.

The second reduced model included factors ASP, AGE, AGG, ASP*AGE, and ASP*AGG. The mean square error for the model was 0.438. The Type III $P_r > F$ values were significant for all the factors in the model, but the Type III mean square for ASP*AGG was not significant. The factor ASP*AGG was dropped from the model.

The third reduced model consisted of factors ASP, AGE, AGG, and ASP*AGE. The mean square error for the model was 0.541. Both the Type III $P_r > F$ values and mean squares for all the factors in the model were significant. The factors ASP, AGE, AGG, and ASP*AGE were included in the transition temperature model.

The ranking for the factors considered in the third reduced model based on Type III mean squares was AGE> ASP> AGG> ASP*AGE. The Type III mean squares for AGE, ASP, and AGG were much greater than those for ASP*AGE. Thus, degree of aging, asphalt type, and aggregate type had a substantial influence on transition temperature, whereas the

Table 5.4. Mean square errors for slope (dS/dT) models

Model	Factors	Mean Square Errors
Full Model	ASP, AGE, AGG, VOID, ASP*AGE, ASP*AGG, AGG*AGE	5.580
Reduced Model I	ASP, AGG, VOID, ASP*AGE, ASP*AGG, AGG*AGE	5.580
Reduced Model II	ASP, AGG, VOID, ASP*AGG, AGG*AGE	6.296
Reduced Model III	ASP, AGG, VOID, AGG*AGE	6.893

Table 5.5. Mean square errors for transition temperature models

Model	Factors	Mean Square Errors
Full Model	ASP, AGE, AGG, VOID, ASP*AGE, ASP*AGG, ASP*AGE	0.432
Reduced Model I	ASP, AGE, AGG, ASP*AGE, ASP*AGG, AGG*AGE	0.430
Reduced Model II	ASP, AGE, AGG, ASP*AGE, ASP*AGG	0.438
Reduced Model III	ASP, AGE, AGG, ASP*AGE	0.541

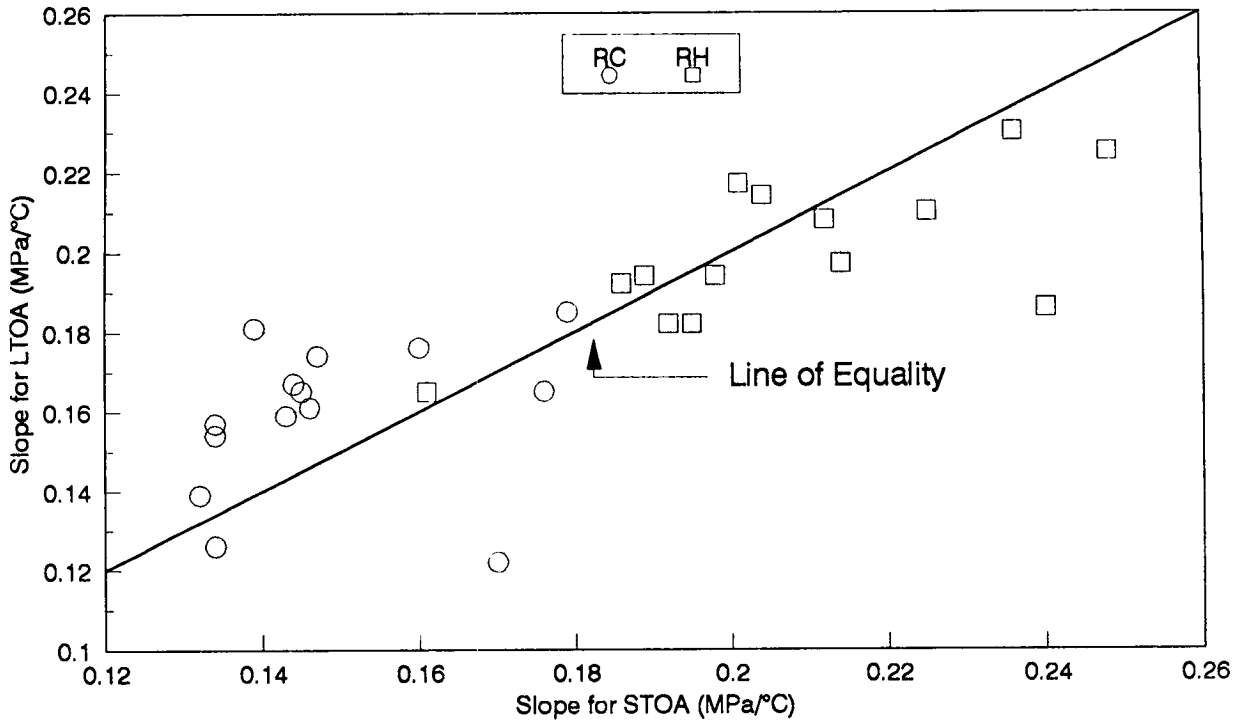

Figure 5.6. Comparison of slope for STOA and LTOA specimens

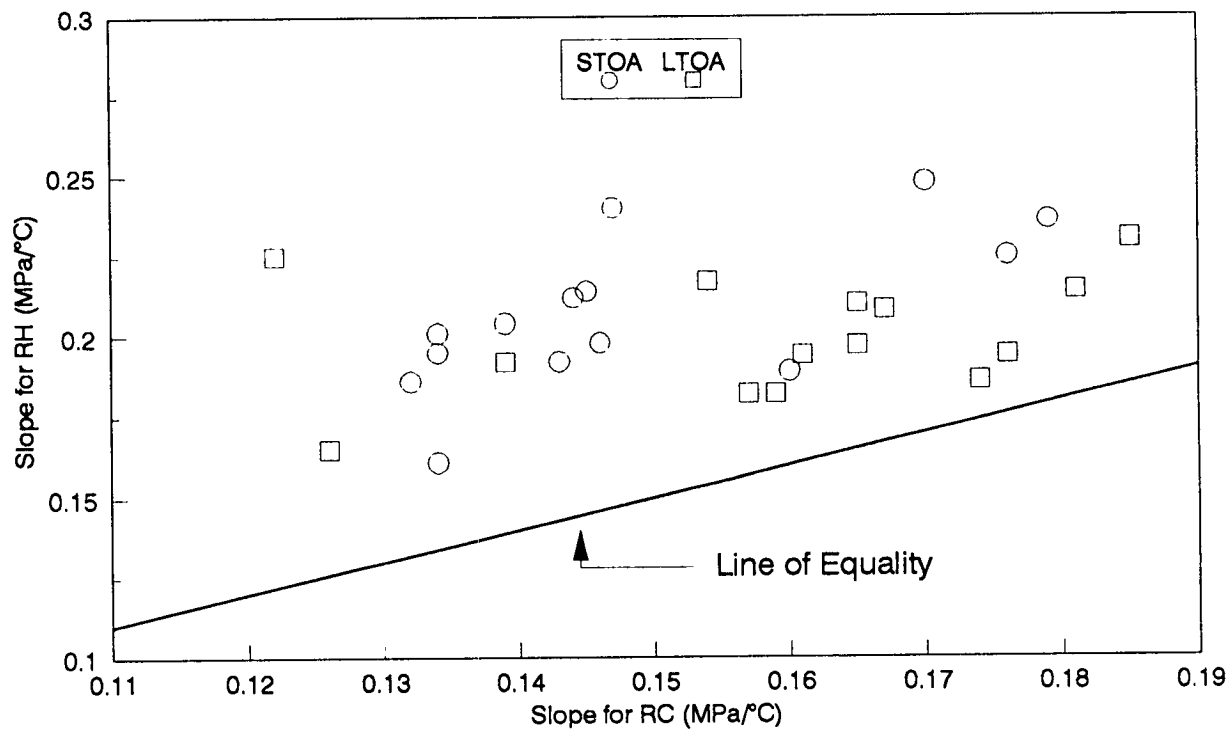

Figure 5.7. Comparison of slope for RC and RH aggregates

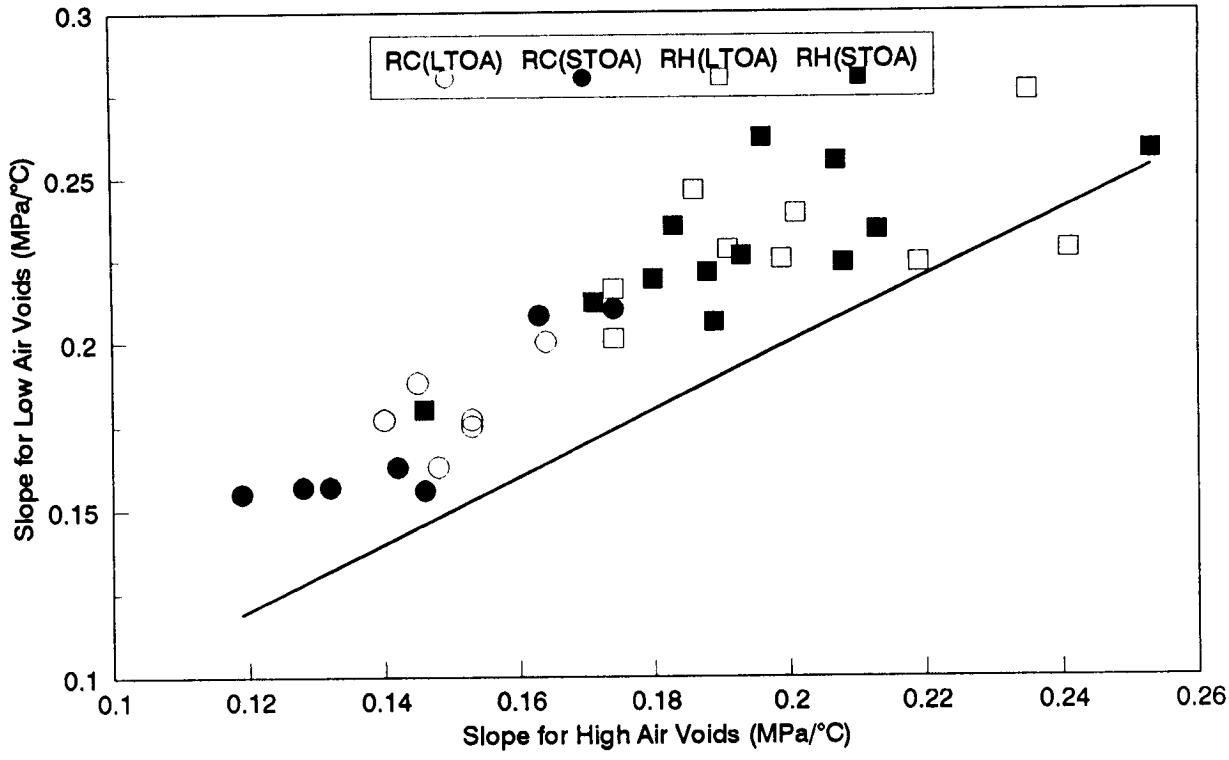

Figure 5.8. Comparison of slope for high and low air voids

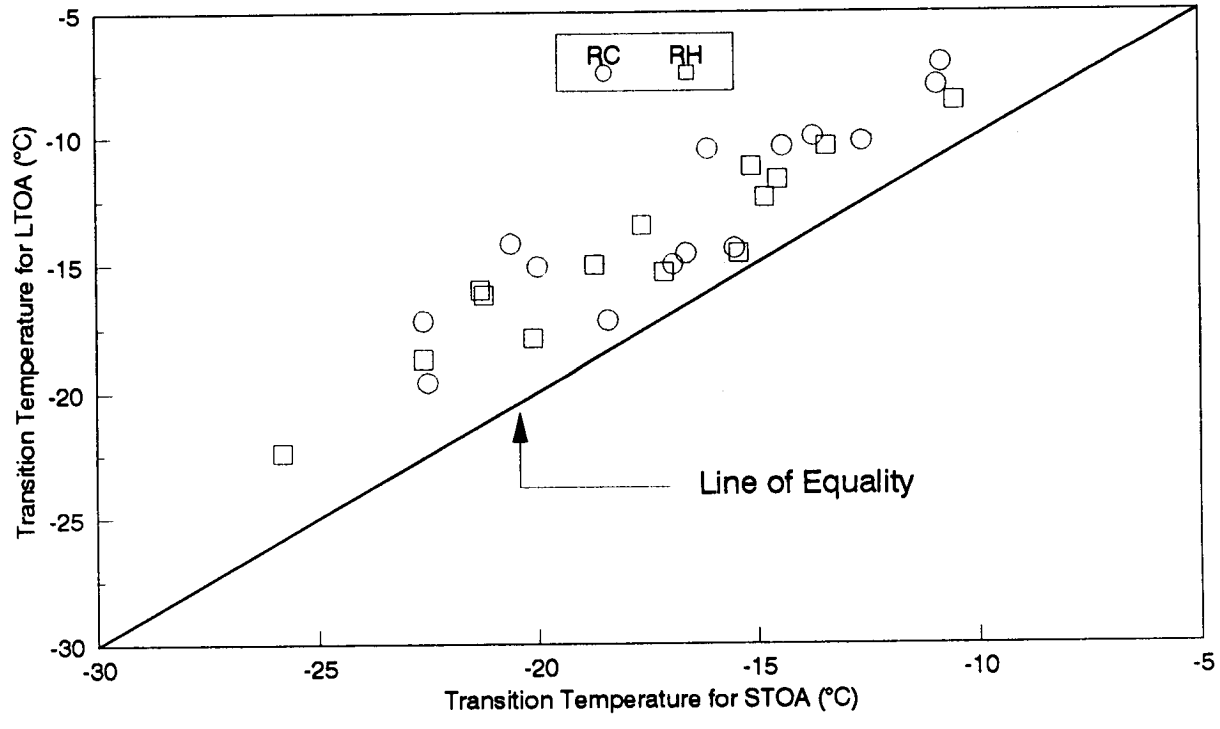

Figure 5.9. Comparison of transition temperature for STOA and LTOA specimens

interaction between asphalt type and degree of aging had a minor influence. The mean square errors for the full model and the reduced models are given in Table 5.5.

LSMEAN of transition temperature for the effect ASP ranged from -9.3°C to -22.6°C. LSMEAN for the effect AGE showed that the transition temperature of LTOA specimens was warmer than STOA by 3.2°C. LSMEAN of transition temperature for STOA and LTOA specimens are compared in Figure 5.9. LSMEAN for the effect AGG showed that the transition temperature of specimens with RC aggregate was warmer than RH aggregate by 1.3°C. LSMEAN of transition temperature for specimens with RC and RH aggregates are compared in Figure 5.10.

5.3 Waller-Duncan t-test

The Waller-Duncan t-test was performed to separate asphalt types showing similar response for a specific dependent variable (SAS Institute Inc. 1991). The Waller-Duncan t-test is a multiple comparison method that provides information about the differences among the means with unequal cell sizes. The test provides Waller's grouping of asphalts at a specified significance level.

The test was performed on the dependent variables fracture temperature (FRTEMP), fracture stress (FRSTRE), slope (SLOPE), and transition temperature (TRTEMP) for a specific asphalt type at a significance level of 0.05. Waller's groupings of asphalts for each dependent variable are presented for a specific aggregate type in Figures 5.11 through 5.18. Asphalts with the same letter are not significantly different at a significance level of 0.05. As indicated, asphalts are well divided into several groups for fracture and transition temperatures. For fracture strength and slope, the asphalts are divided into three to six groups. Each group includes a wide range of asphalts, and the groups overlap with one another.

5.4 Discussion of Results

Asphalt type, aggregate type, degree of aging, and air void content have a substantial influence on the low-temperature cracking resistance of asphalt concrete mixtures; interactions among them have a minor influence.

Fracture temperature was significantly influenced by asphalt type and degree of aging, and much less influenced by aggregate type and air void content. LSMEAN of fracture temperature for LTOA mixtures was warmer than for STOA mixtures. LSMEAN of fracture temperature showed no significant difference between aggregate types.

Fracture strength was highly dependent on air void content and aggregate type, and less dependent on asphalt type and degree of aging. LSMEAN of fracture strength for RH aggregate was greater than that for RC aggregate. LSMEAN of fracture strength for LTOA

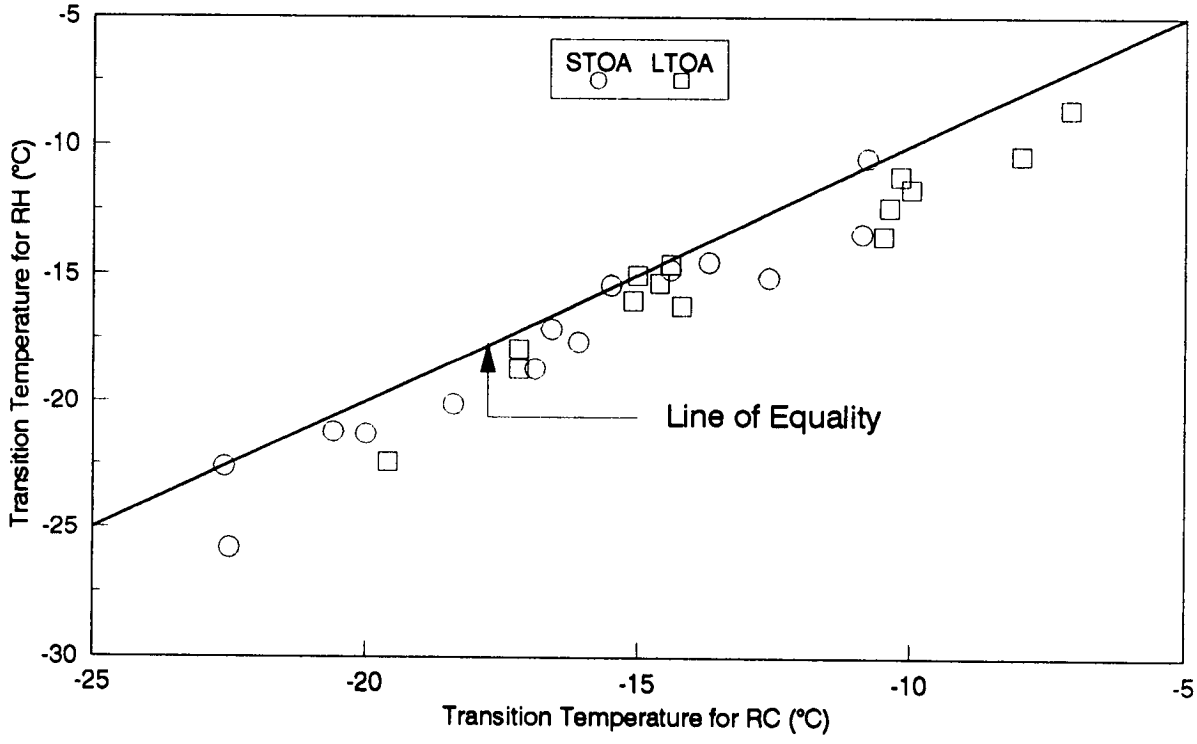

Figure 5.10. Comparison of transition temperature for RC and RH aggregates

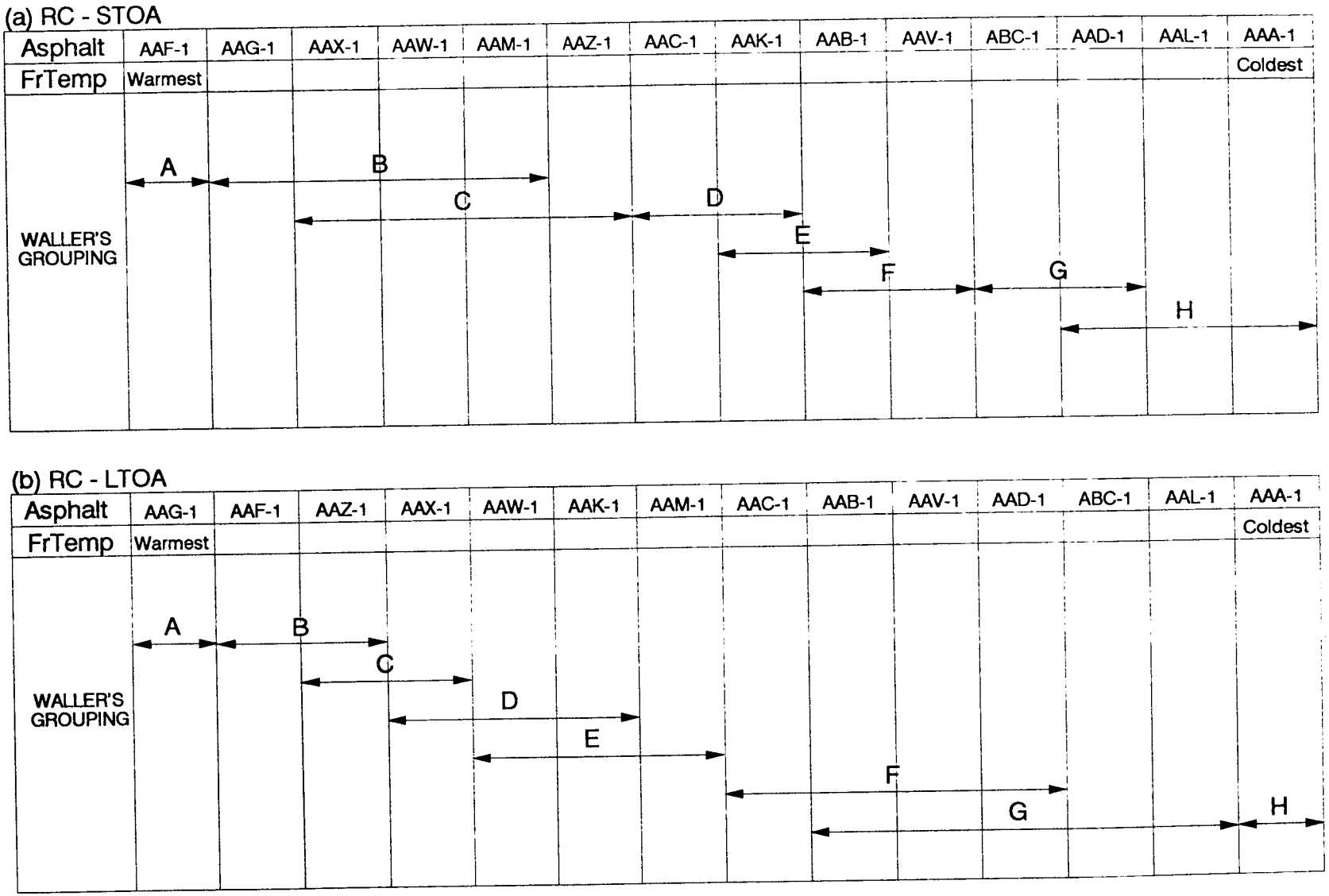

Figure 5.11. Waller's grouping of asphalts for fracture temperature (RC)

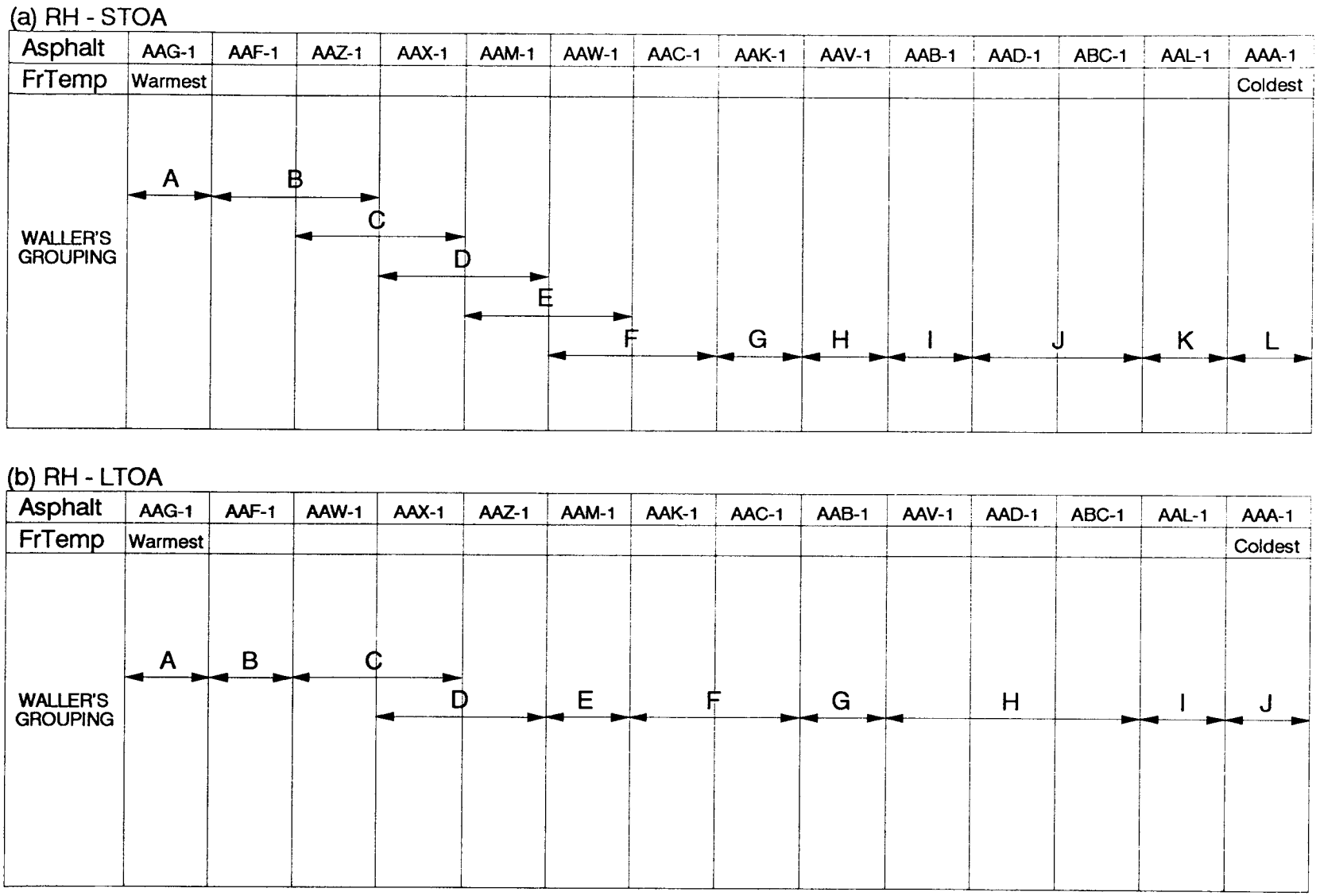

Figure 5.12. Waller's grouping of asphalts for fracture temperature (RH)

(a) RC - STOA

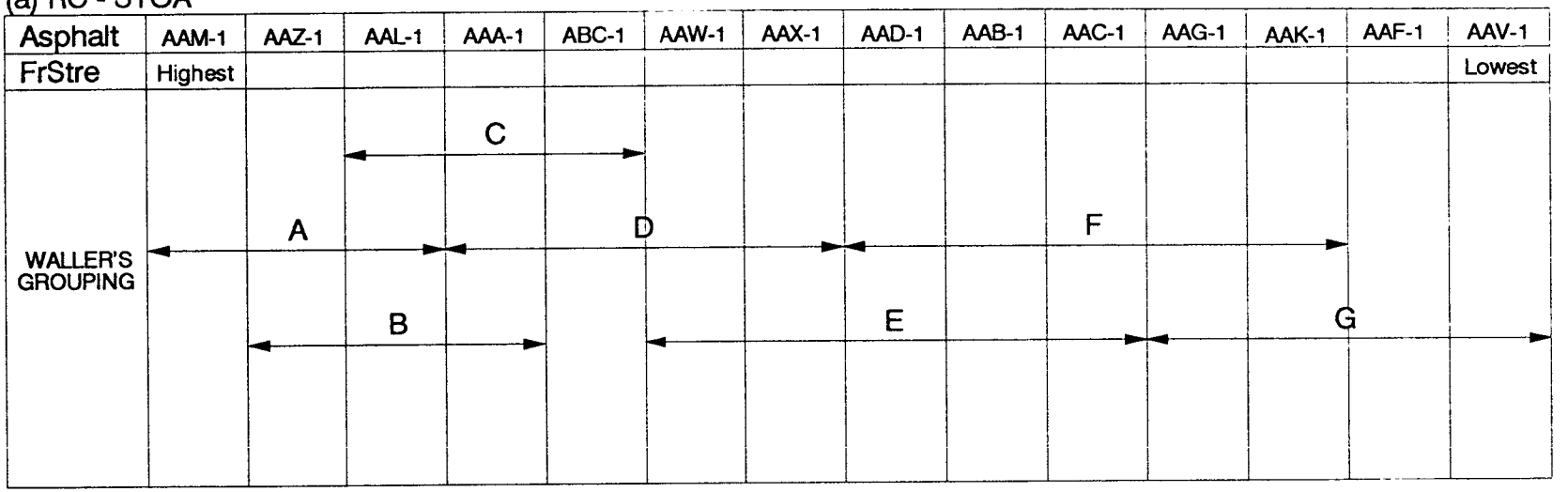

(b) RC - LTOA

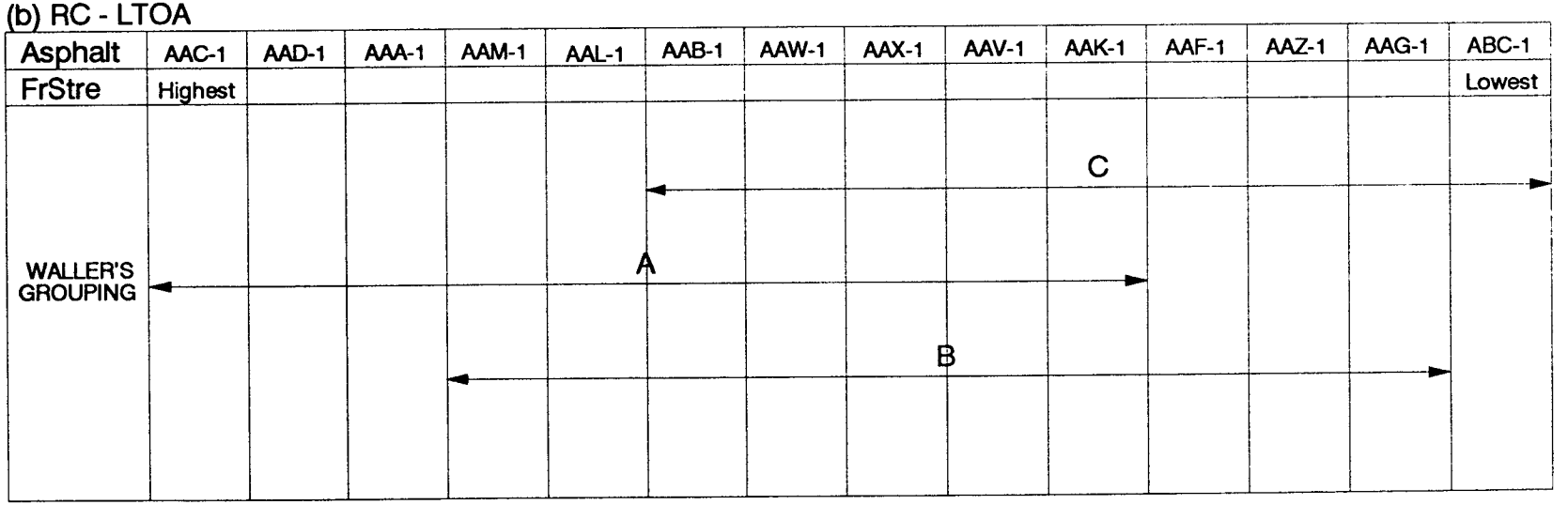

Figure 5.13. Waller's grouping of asphalts for fracture strength (RC)

(a) RH - STOA

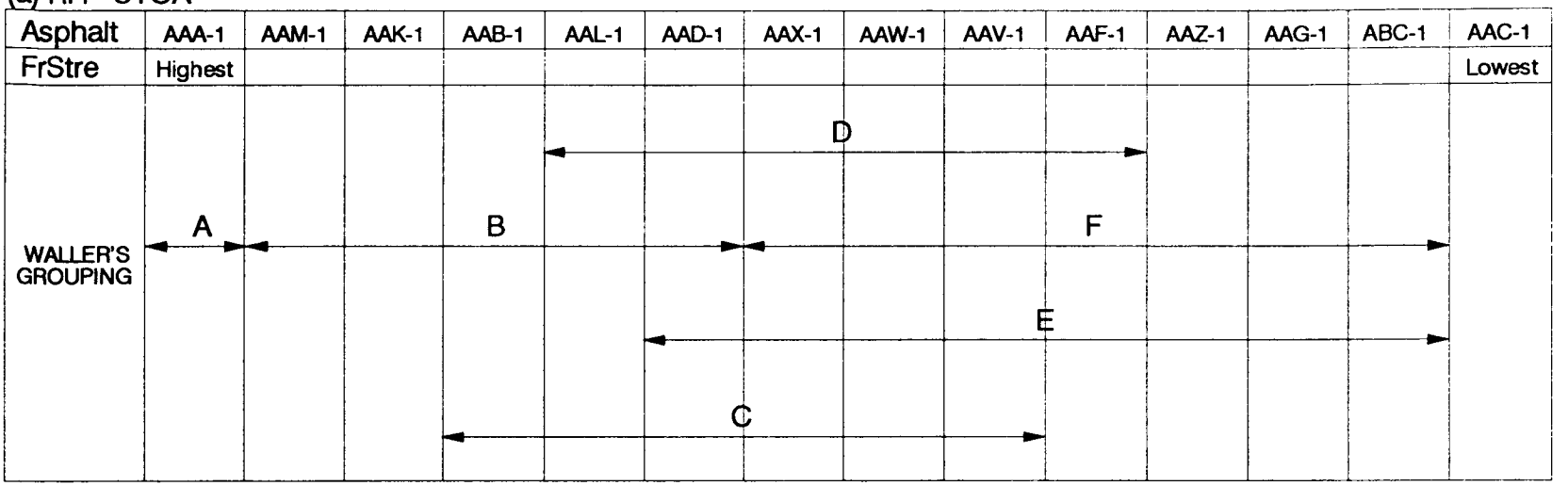

(b) RH - LTOA

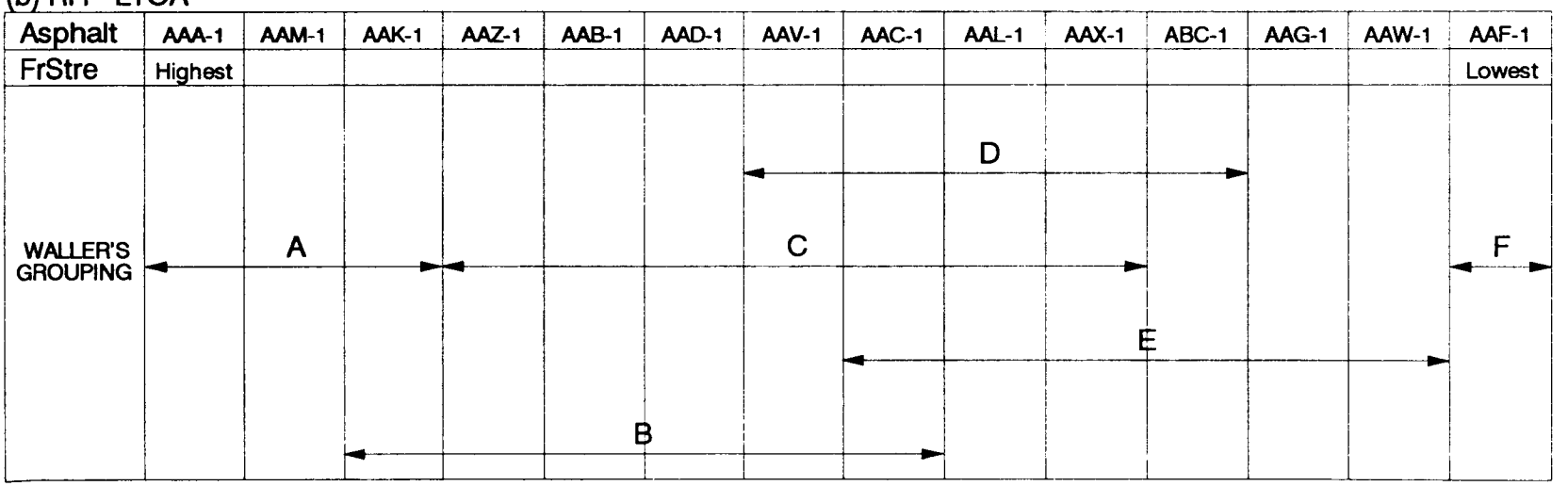

Figure 5.14. Waller's grouping of asphalts for fracture strength (RH)

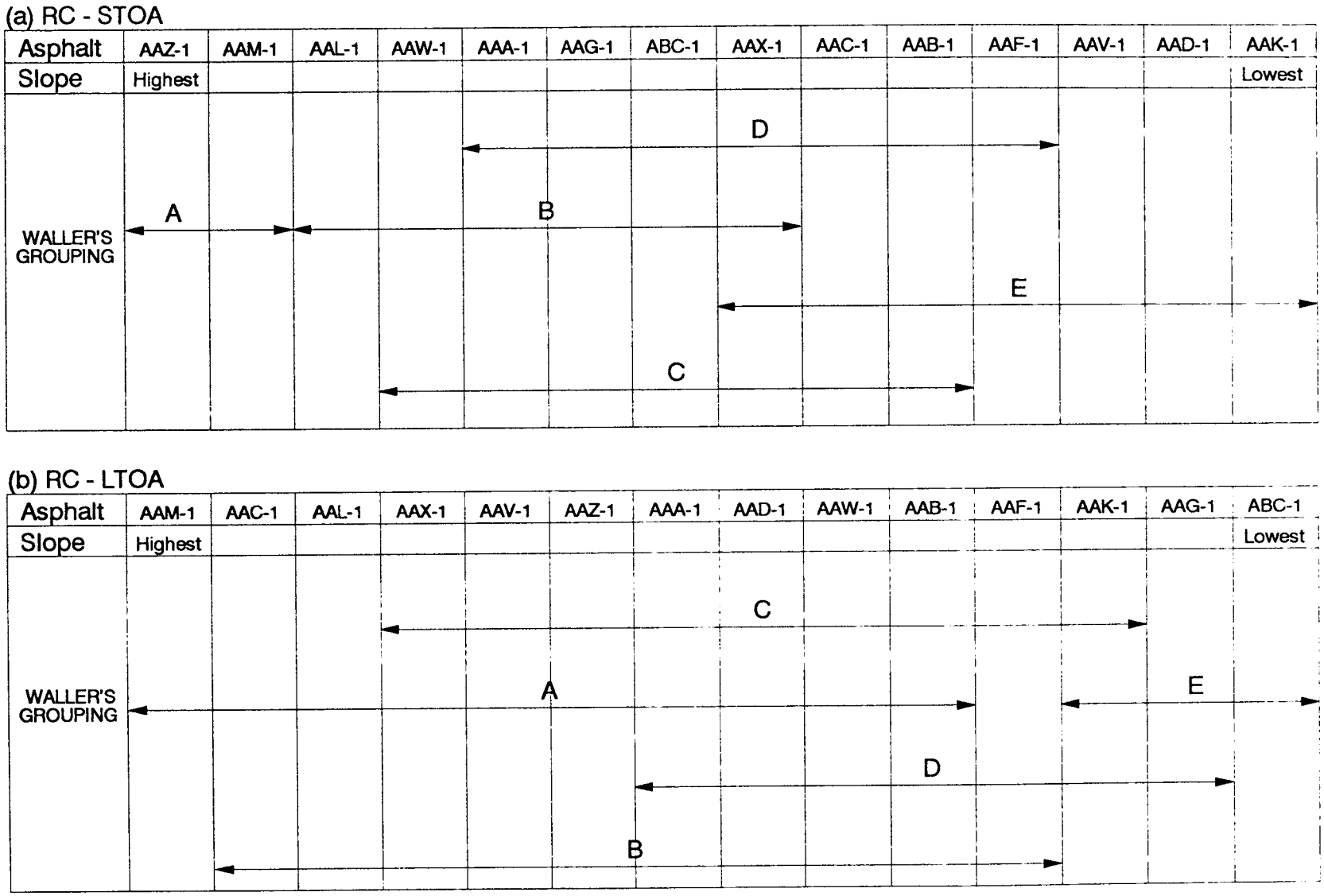

Figure 5.15. Waller's grouping of asphalts for slope (RC)

(a) RH - STOA

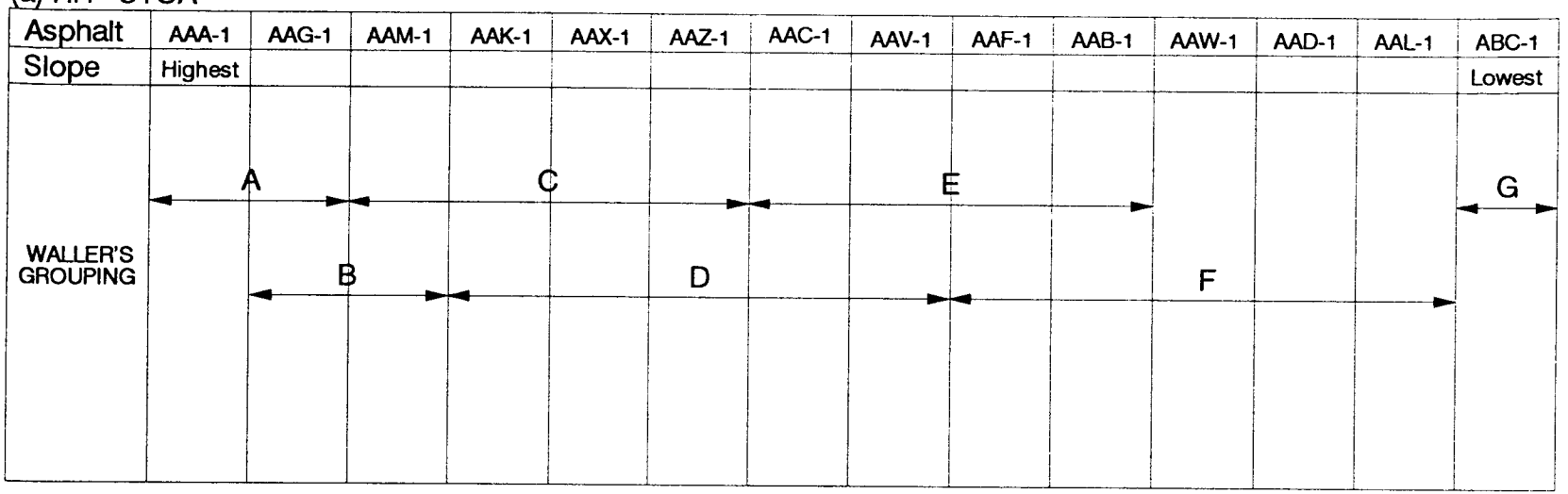

(b) RH - LTOA

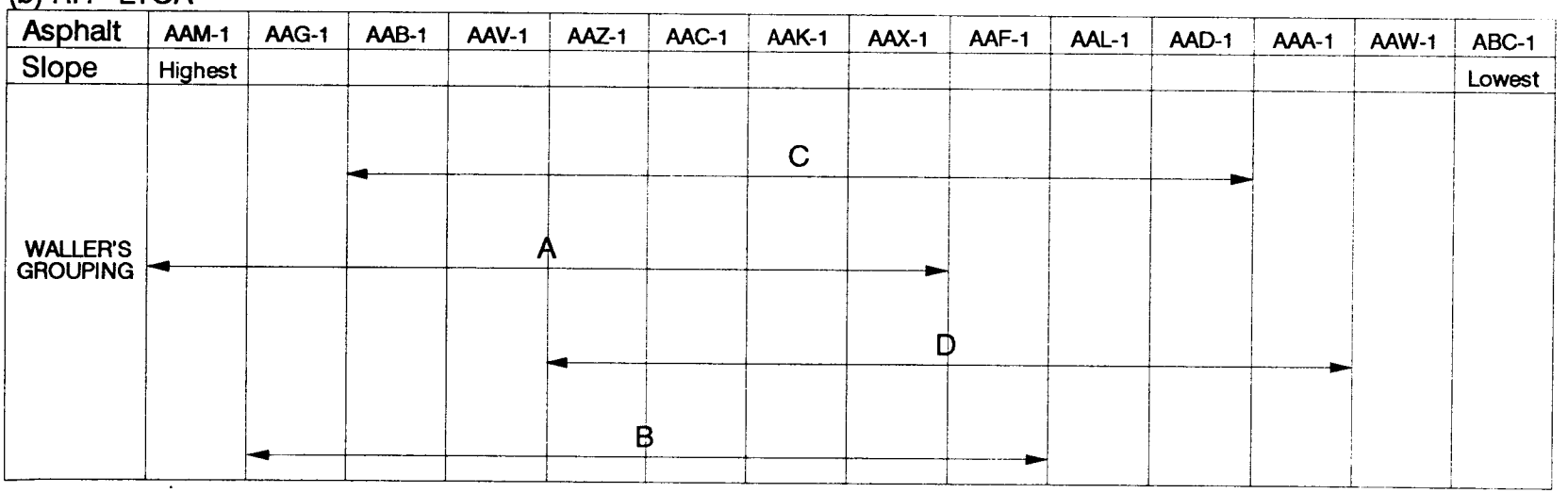

Figure 5.16. Waller's grouping of asphalts for slope (RH)

(a) RC - STOA

Asphalt	AAG-1	AAF-1	AAW-1	AAX-1	AAZ-1	AAM-1	AAK-1	AAC-1	AAB-1	AAV-1	ABC-1	AAD-1	AAL-1	AAA-1
TrTemp	Warmest													Coldest
WALLER'S GROUPING	A		B	C		D	E	F		G	H	I	J	K

(a) RC - LTOA

Asphalt	AAG-1	AAF-1	AAX-1	AAW-1	AAK-1	AAZ-1	AAD-1	AAM-1	AAC-1	ABC-1	AAB-1	AAV-1	AAL-1	AAA-1
TrTemp	Warmest													Coldest
WALLER'S GROUPING	A			B					C				D	E

Figure 5.17. Waller's grouping of asphalts for transition temperature (RC)

(a) RH - STOA

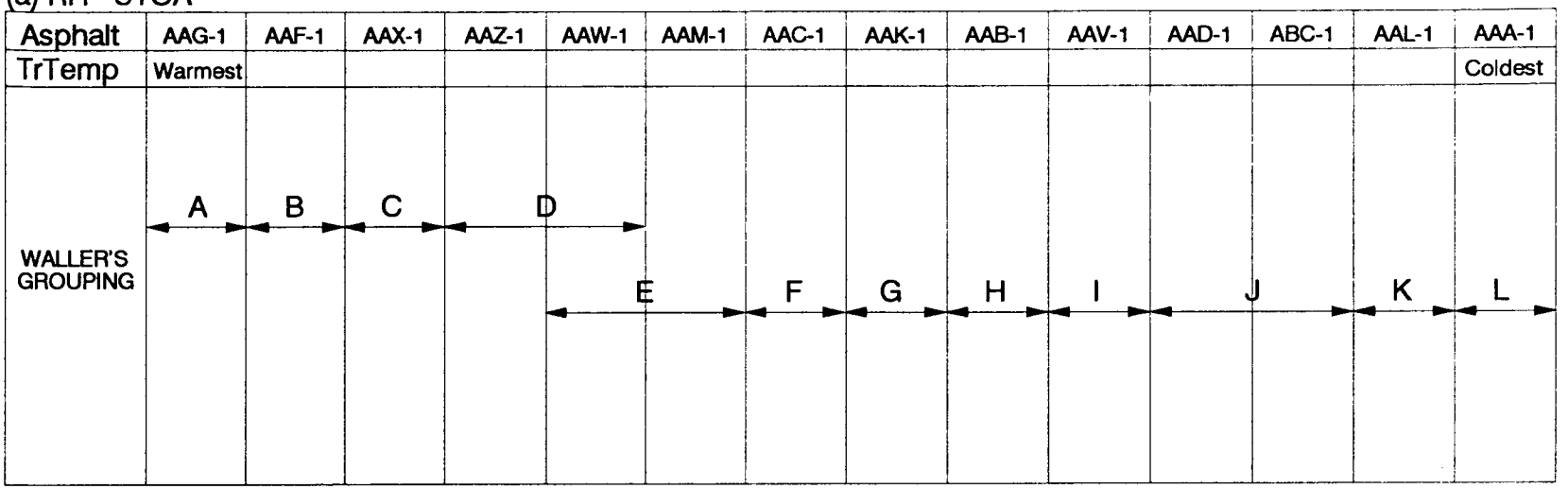

(b) RH - LTOA

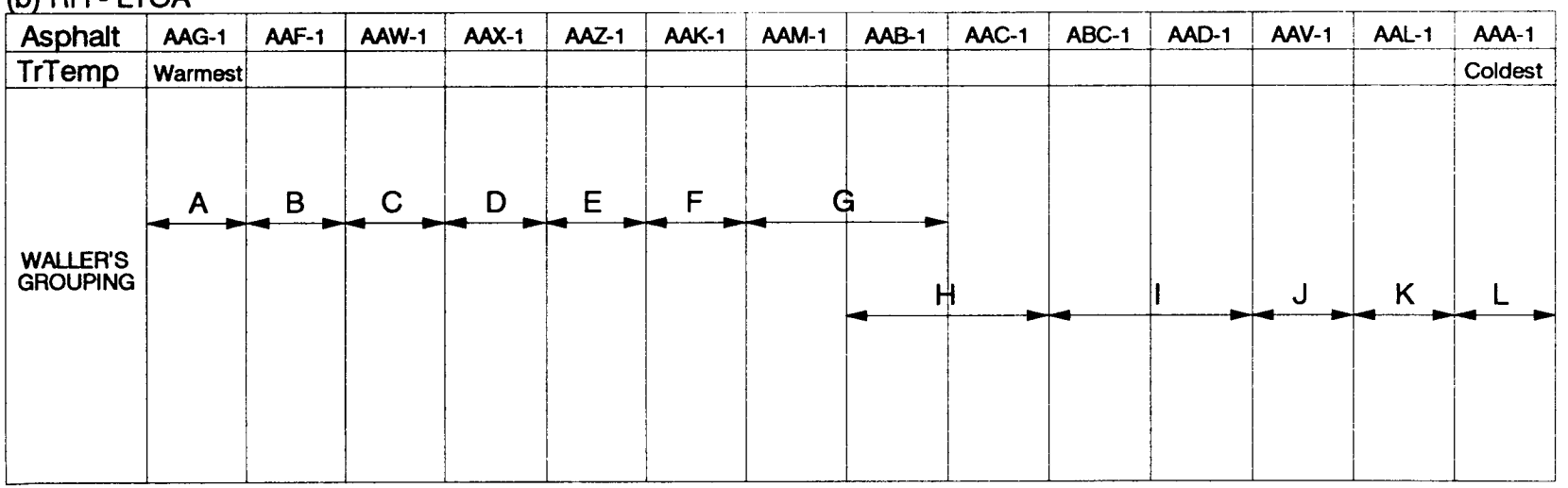

Figure 5.18. Waller's grouping of asphalts for transition temperature (RH)

mixtures was slightly greater than for STOA mixtures. However, as shown in Figure 5.3, the fracture strength was lower for a few LTOA mixtures.

The slope of the thermally induced stress curve was most affected by aggregate type and air void content, and much less affected by the interaction between aggregate and degree of aging and asphalt type. LSMEAN of slope for RH aggregate was greater than for RC aggregate. LSMEAN of slope showed no significant difference between STOA and LTOA mixtures. However, as shown in Figure 5.6, slope for STOA mixtures could not be correlated to slope for LTOA mixtures.

Transition temperature was most affected by the degree of aging, asphalt type, and aggregate type. It was affected by the interaction between asphalt and degree of aging to a much lesser extent. LSMEAN of transition temperature for LTOA mixtures was warmer than for STOA mixtures. LSMEAN of transition temperature was warmer for RC aggregate than for RH aggregate.

The low-temperature cracking resistance of asphalt concrete mixtures may be affected by the characteristics of aggregates in several ways. For example, the aggregate may influence thermal regime and stiffness of the mix and aging characteristics of the asphalt cement. The RC aggregate is more porous and thus may have a lower thermal conductivity which leads to lower thermal conductivity of mixtures with the RC aggregate. It will take longer for the mixture with RC aggregate to reach thermal equilibrium. The temperature within the mixtures with RC aggregate will be warmer and the asphalt cement in those mixtures will be softer than in those mixtures with RH aggregate under the same thermal condition (cooling rate and surface temperature). Thus, in the mixture with RC aggregate, the period of stress relaxation will be extended to colder temperatures, and additional stress will be relaxed. Beyond the transition temperature, in the mixture with RH aggregate, the thermal stresses will accumulate at a faster rate and the slope of the thermally induced stress curve will be steeper. Also, since the stress relaxation in the mixture with RH aggregate will cease at warmer temperatures and less stress will be relaxed, the fracture strength of mixtures with RH aggregate will be greater.

The low-temperature cracking resistance of an asphalt concrete mixture can also be significantly affected by aging of the asphalt cement. As the asphalt concrete mixture ages, the asphalt cement becomes stiffer. This increased stiffness will affect the temperature susceptibility of the mixture. When subjected to cooling, the asphalt cement in the LTOA mixtures will be stiffer than that in the STOA mixtures, and more stresses will accumulate. The thermally induced stress in the mixture will exceed the strength of the mixture at warmer temperatures. Finally, fracture will occur at a warmer temperature.

To summarize, asphalt type, aggregate type, degree of aging, and air void content are significant factors in the low-temperature cracking characteristics of asphalt concrete mixtures. However, at this time, the effects of the degree of aging on fracture strength and slope are inconclusive.

6

Rankings of Asphalts and Aggregates, and Comparison of A-002A and A-003A Results

The A-003A performance rankings of asphalts and aggregates for resistance to low-temperature cracking were compared with the rankings based on fundamental properties of asphalt cement given by A-002A (Materials Reference Library [MRL] Asphalt Properties, 4/29/92, 6/26/92, 10/22/92). Also, the mixture fracture temperature was related to the A-002A index test results and asphalt cement properties (Robertson et al., 1991; MRL Asphalt Properties, 4/29/92, 6/26/92, 10/22/92). Linear regression analyses were performed to correlate mixture fracture temperature to A-002A index test results and asphalt cement properties.

6.1 Rankings of Asphalts and Aggregates

The A-003A performance rankings of asphalts and aggregates for resistance to low-temperature cracking were determined using the LSMEAN of the mixture fracture temperature. For the ranking of asphalts, a score ranging from 1 to 14 was assigned to each asphalt. A lower score is associated with a colder fracture temperature. The ranking of aggregates was also based on the LSMEAN of fracture temperature.

The A-003A ranking of asphalts is presented with the ranking based on fundamental properties of asphalt cement given by A-002A in Table 6.1. The ranking of asphalts based on mixture fracture temperature compares favorably with a ranking based on fundamental properties of asphalt cement given by A-002A. The ranking of aggregates is presented in Table 6.2.

Table 6.1. Ranking of asphalts for resistance to low-temperature cracking indicated by A-003A and A-002A

Asphalt Type	Fracture Temperature, °C	A-003A Rank	A-002A Rank
AAA-1	-30.27	1	1
AAL-1	-28.34	2	2
AAD-1	-26.70	3	3
ABC-1	-26.67	4	4
AAB-1	-25.41	5	5
AAV-1	-25.24	6	8
AAC-1	-22.48	7	7
AAK-1	-22.07	8	6
AAM-1	-21.01	9	9
AAW-1	-19.95	10	9
AAX-1	-19.59	11	13
AAZ-1	-19.48	12	12
AAF-1	-16.86	13	11
AAG-1	-15.83	14	14

Table 6.2. Ranking of aggregates for resistance to low-temperature cracking indicated by A-003A

Aggregate Type	Fracture Temperature, °C	Rank
RC	-23.08	1
RH	-22.62	2

6.2 Relationship Between Fracture Temperature and A-002A Low-Temperature Index Test Results

Fracture temperature of both short- and long-term aged mixtures was compared with A-002A low-temperature index test results, — specifically the limiting stiffness temperature, the m-value and the creep stiffness from the bending beam rheometer test, and the ultimate strain at failure from the direct tension test. The low-temperature index test results were obtained for both unaged and aged asphalt cements. Linear regression analyses were performed. Summary statistics of linear regression analyses are presented in Table 6.3.

Figures 6.1 and 6.2 show relationships between the fracture temperature of short- and long-term aged mixtures (RC and RH aggregates) and the limiting stiffness temperature (S[t] = 200 MPa at 2 hours) of unaged and aged asphalt cements, respectively. Fracture temperature of both short- and long-term aged mixtures exhibit good correlations with the limiting stiffness temperature of both unaged and aged asphalt cements. Limiting stiffness temperature of both aged and unaged asphalt cements shows better correlations with fracture temperature of short-term aged mixtures. As indicated in Table 6.3, R-squared values are greater and mean square errors (MSE) and coefficients of variation (C.V.) are smaller for linear relationships with the fracture temperature of short-term aged mixtures.

Figures 6.3 and 6.4 show relationships between the fracture temperature of short- and long-term aged mixtures (RC and RH aggregates) and the m-value of unaged (at 0°C) and aged (at -10°C) asphalt cements, respectively. The m-value at 0°C of unaged asphalt cement exhibits better correlation with fracture temperature of both short- and long-term aged mixtures than the m-value at -10°C of aged asphalt cement. As indicated in Table 6.3, R-squared values are greater and MSE and C.V. are smaller for linear relationships between fracture temperature and m-value of unaged asphalt cements. The m-values of both unaged and aged asphalt cements exhibit better correlations with the fracture temperature of short-term aged mixtures than with that of long-term aged mixtures.

Figure 6.5 shows relationships between the fracture temperature of short- and long-term aged mixtures (RC and RH aggregates) and the creep stiffness (at -10°C) of aged asphalt cement. Fracture temperatures of both short- and long-term aged mixtures exhibit good correlation with the creep stiffness at -10°C of aged asphalt cement. As indicated in Figure 6.5 and Table 6.3, the correlation with the fracture temperature of long-term aged mixtures is somewhat better than with that of short-term aged mixtures. R-squared values are 0.88 for both linear relationships, but MSE and C.V. are smaller for the linear relationship with the fracture temperature of long-term aged mixtures.

Figures 6.6 and 6.7 present relationships between the fracture temperature of short- and long-term aged mixtures (RC and RH aggregates) and the ultimate strain at failure of unaged (at -26°C) and aged (at -10°C) asphalt cements, respectively. Fracture temperature of short-term aged mixtures exhibits a good correlation with the ultimate strain at failure (at -26°C) of unaged asphalt cement. The ultimate strain at failure (at -10°C) of aged asphalt cement does not exhibit good correlation with the fracture temperatures of both short- and long-term aged mixtures.

Table 6.3. Summary statistics of linear regression analyses with the A-002A index test results

Asphalt Binder Properties	Fracture Temp.	Parameter Estimates		MSE	C.V. (%)	F Value	R^2
		Intercept	Slope				
Limiting Stiffness Temperature (unaged)	STOA	0.492	1.019	2.2	5.9	118.1	0.91
	LTOA	0.817	0.874	2.9	8.1	65.8	0.85
Limiting Stiffness Temperature after PAV (aged)	STOA	-7.933	1.349	1.3	4.5	165.2	0.95
	LTOA	-7.058	1.118	4.1	9.3	36.2	0.82
m-Value @ 0°C(unaged)	STOA	-7.423	-45.831	3.7	7.7	64.3	0.84
	LTOA	-6.463	-37.980	5.0	10.6	33.2	0.73
m-Value @ -10°C after PAV (aged)	STOA	1.683	-80.306	5.7	8.9	21.4	0.73
	LTOA	-3.139	-55.726	4.6	9.4	12.8	0.61
Creep Stiffness @ -10°C after PAV (aged)	STOA	-34.889	0.064	2.5	6.0	58.1	0.88
	LTOA	-29.036	0.048	1.4	5.2	60.5	0.88
Ultimate Strain @ -26°C (unaged)	STOA	-14.304	-6.253	4.0	8.0	59.3	0.83
	LTOA	-21.086	-5.040	5.9	11.5	26.2	0.69
Ultimate Strain @ -10°C after PAV (aged)	STOA	-24.020	-0.621	13.7	13.6	2.9	0.29
	LTOA	-20.976	-0.460	6.4	10.8	3.4	0.33

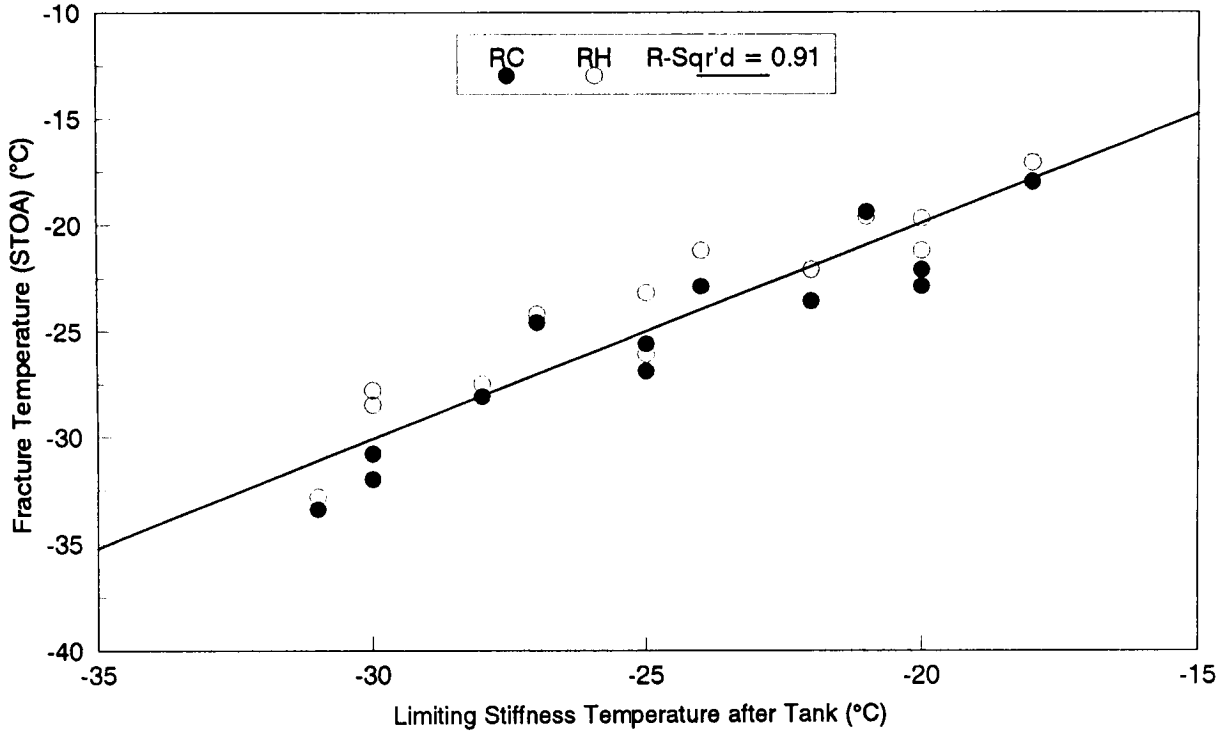

(a) Fracture Temperature of Short-Term Aged Mixes

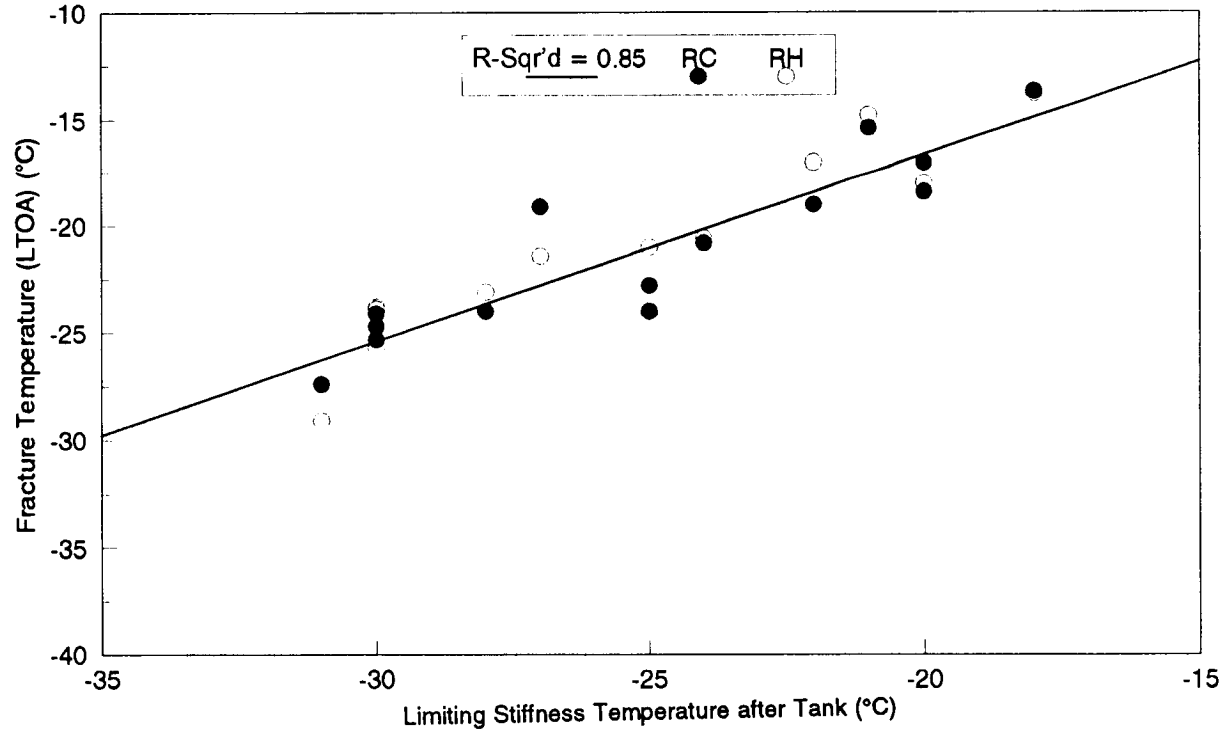

(b) Fracture Temperature of Long-Term Aged Mixes

Figure 6.1. Relationship between fracture temperature and limiting stiffness temperature after tank (unaged)

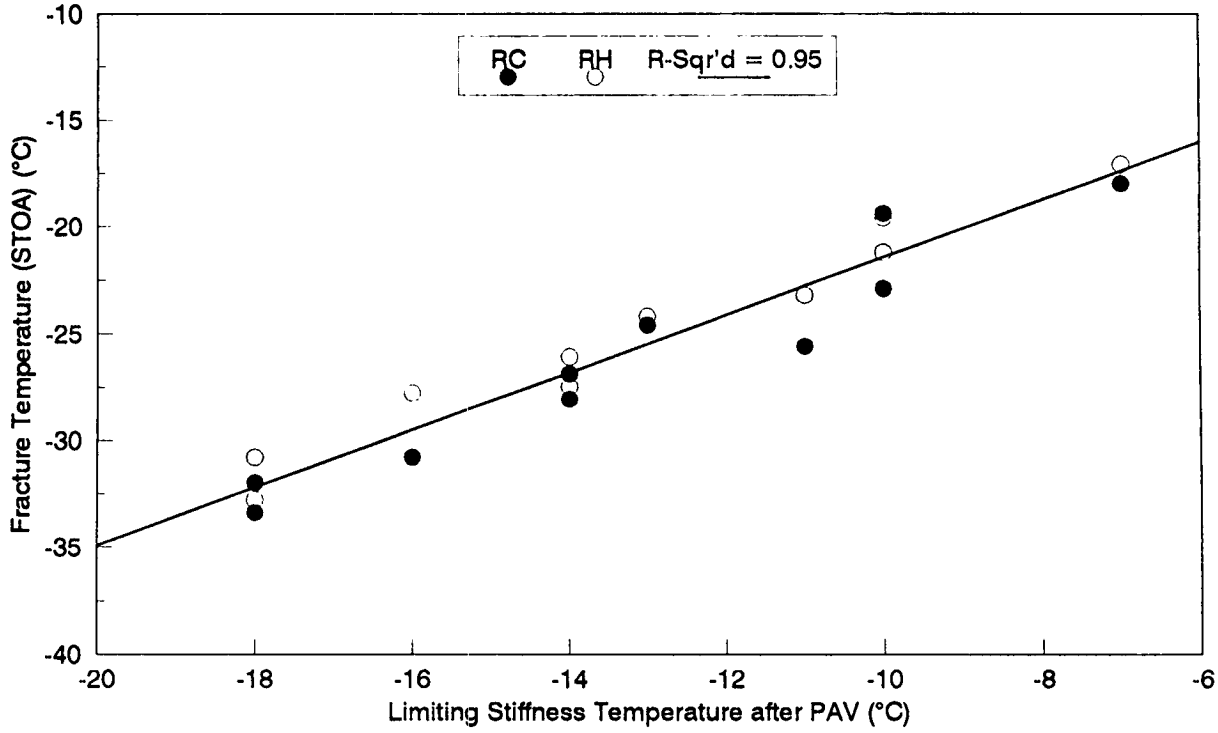

(a) Fracture Temperature of Short-Term Aged Mixes

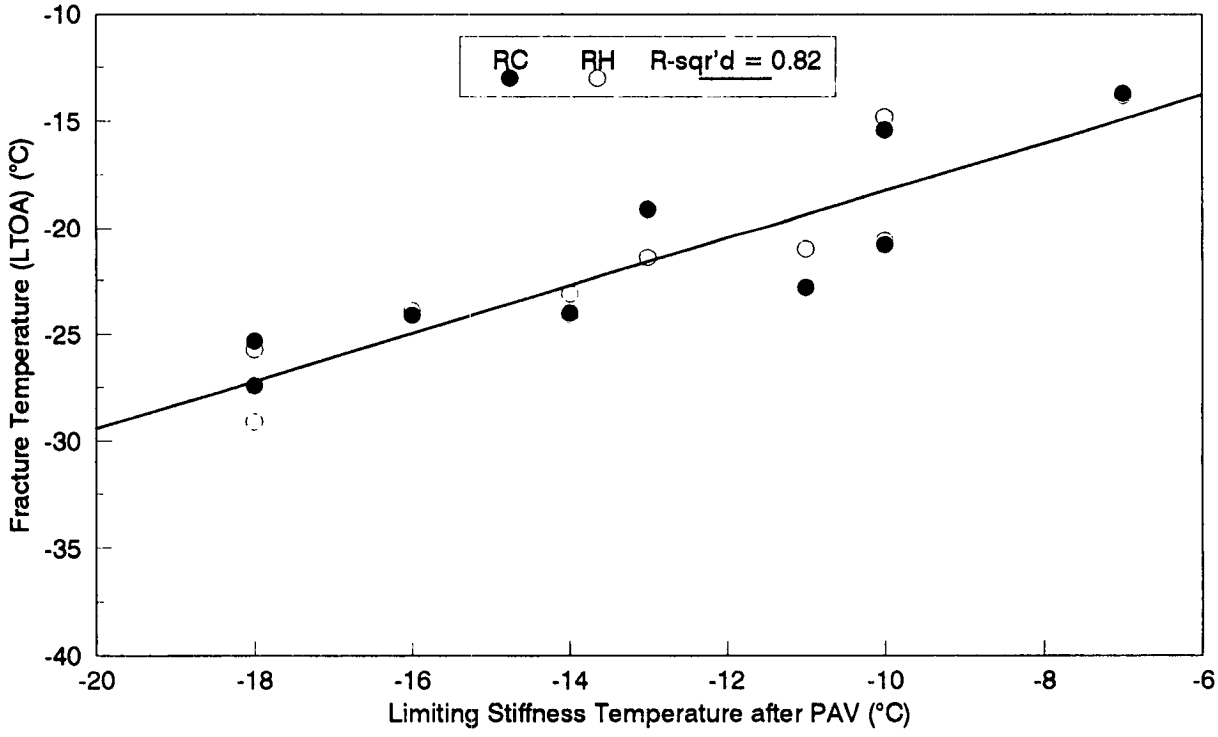

(b) Fracture Temperature of Long-Term Aged Mixes

Figure 6.2. Relationship between fracture temperature and limiting stiffness temperature after PAV (aged)

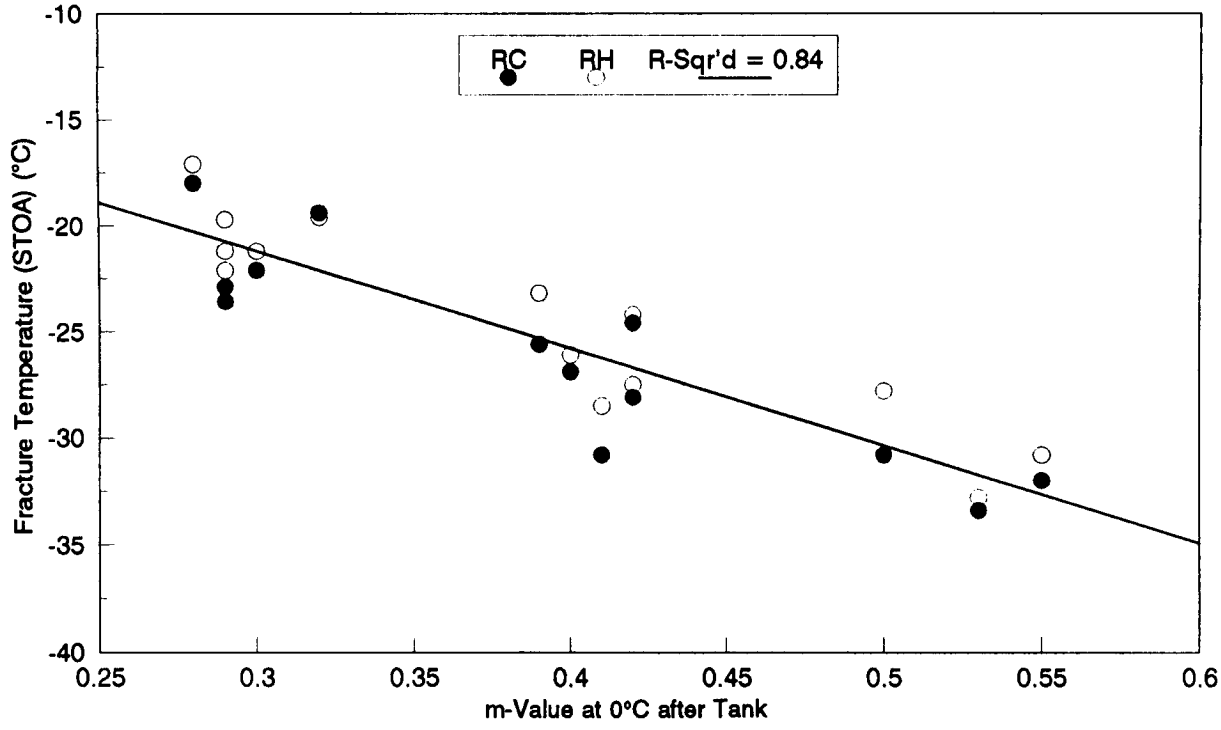

(a) Fracture Temperature of Short-Term Aged Mixes

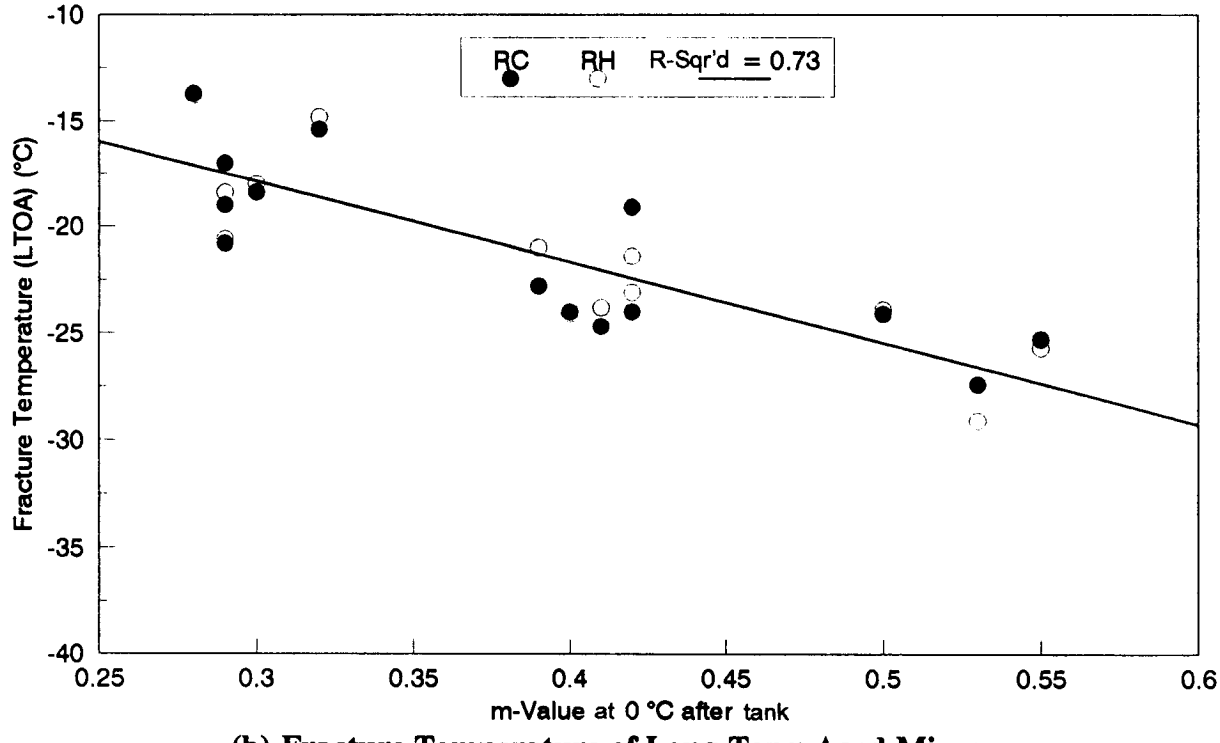

(b) Fracture Temperature of Long-Term Aged Mixes

Figure 6.3 **Relationship between fracture temperature and m-value at 0°C after tank (unaged)**

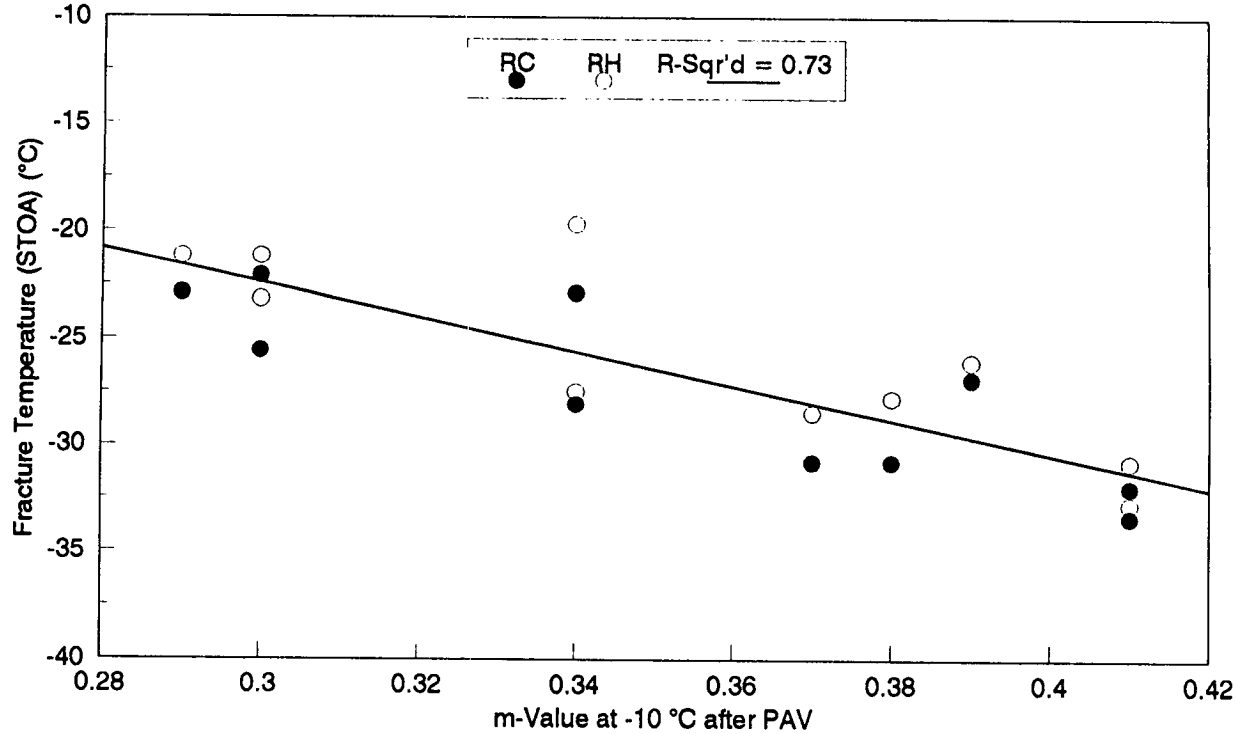

(a) Fracture Temperature of Short-Term Aged Mixes

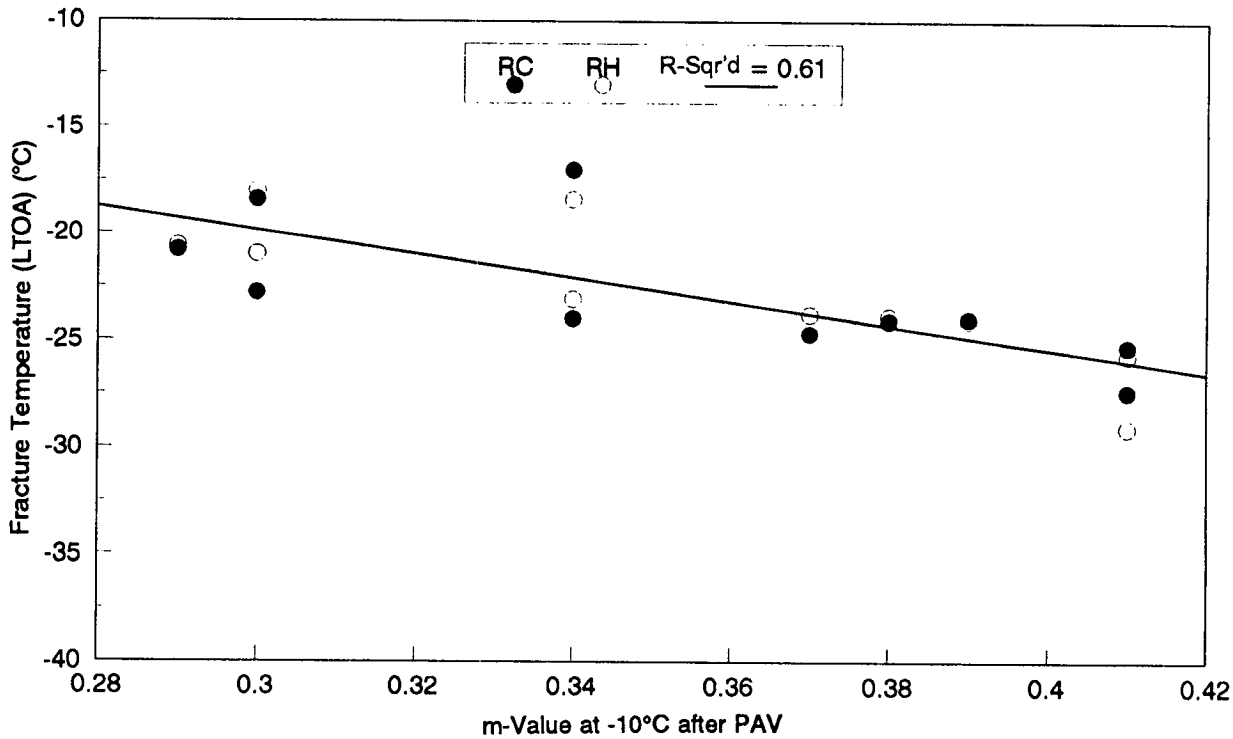

(b) Fracture Temperature of Long-Term Aged Mixes

Figure 6.4. Relationship between fracture temperature and m-value at -10°C after PAV (aged)

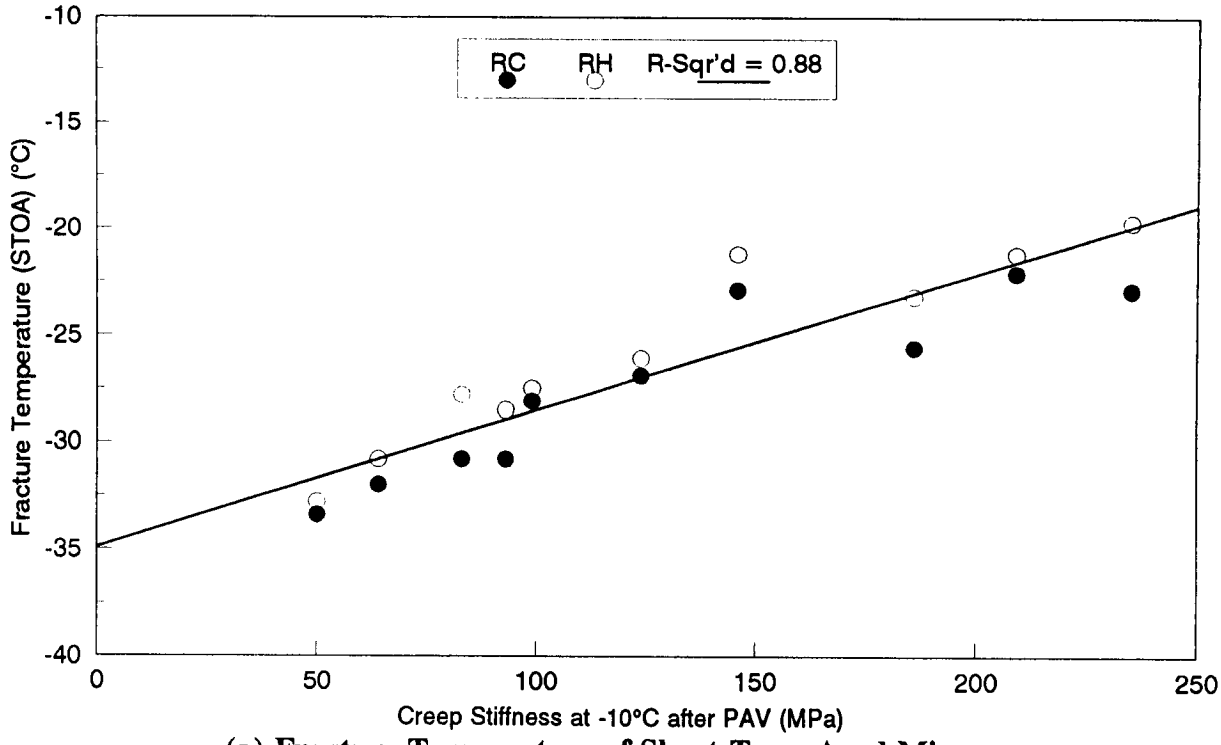

(a) Fracture Temperature of Short-Term Aged Mixes

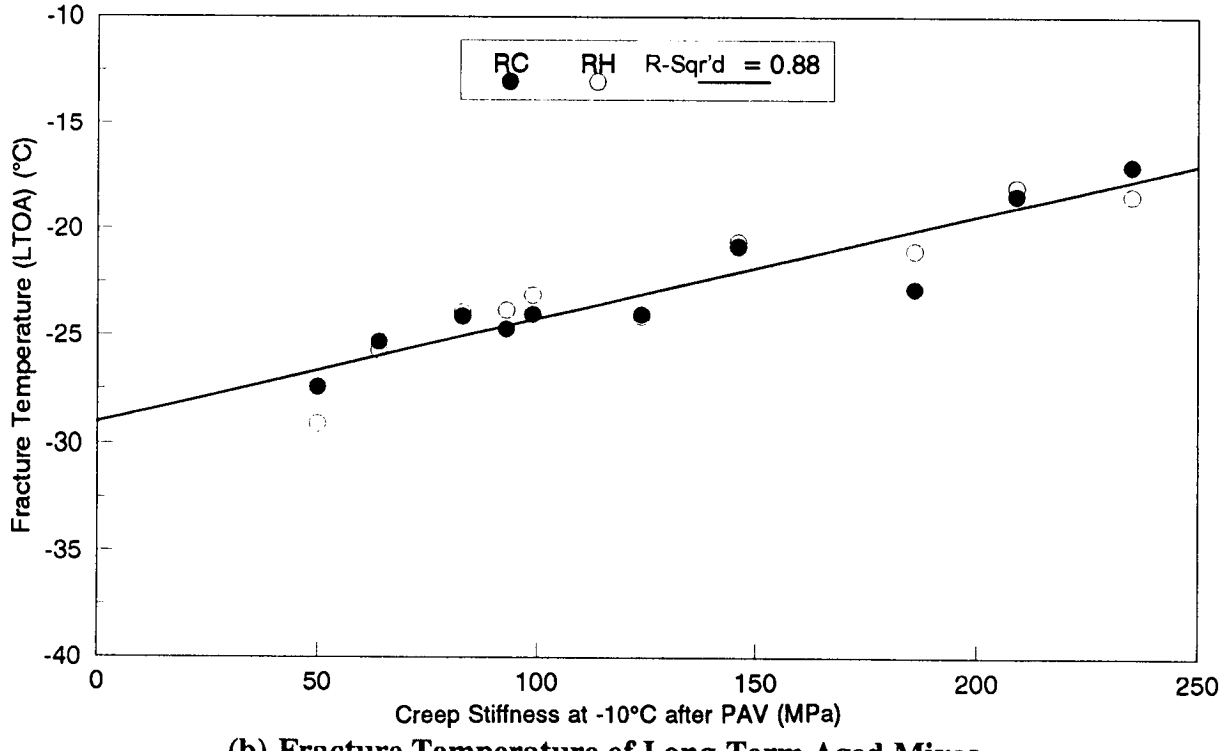

(b) Fracture Temperature of Long-Term Aged Mixes

Figure 6.5. Relationship between fracture temperature and creep stiffness at -10°C after PAV (aged)

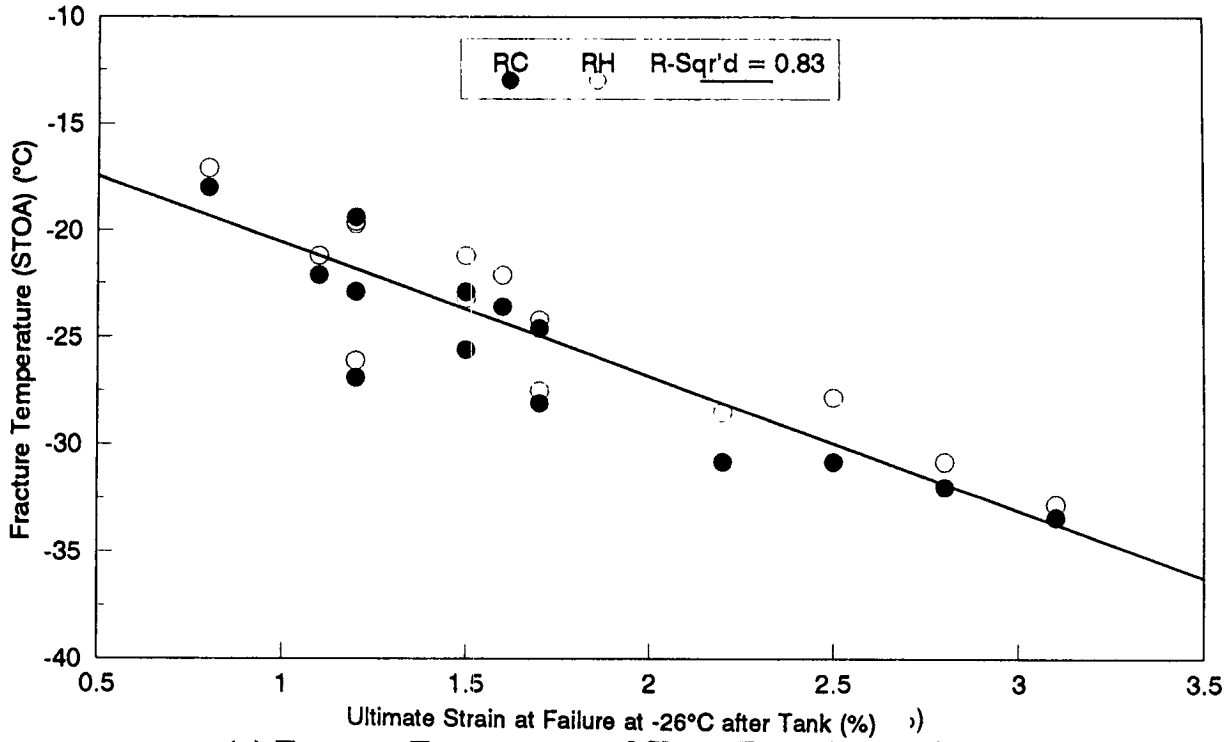

(a) Fracture Temperature of Short-Term Aged Mixes

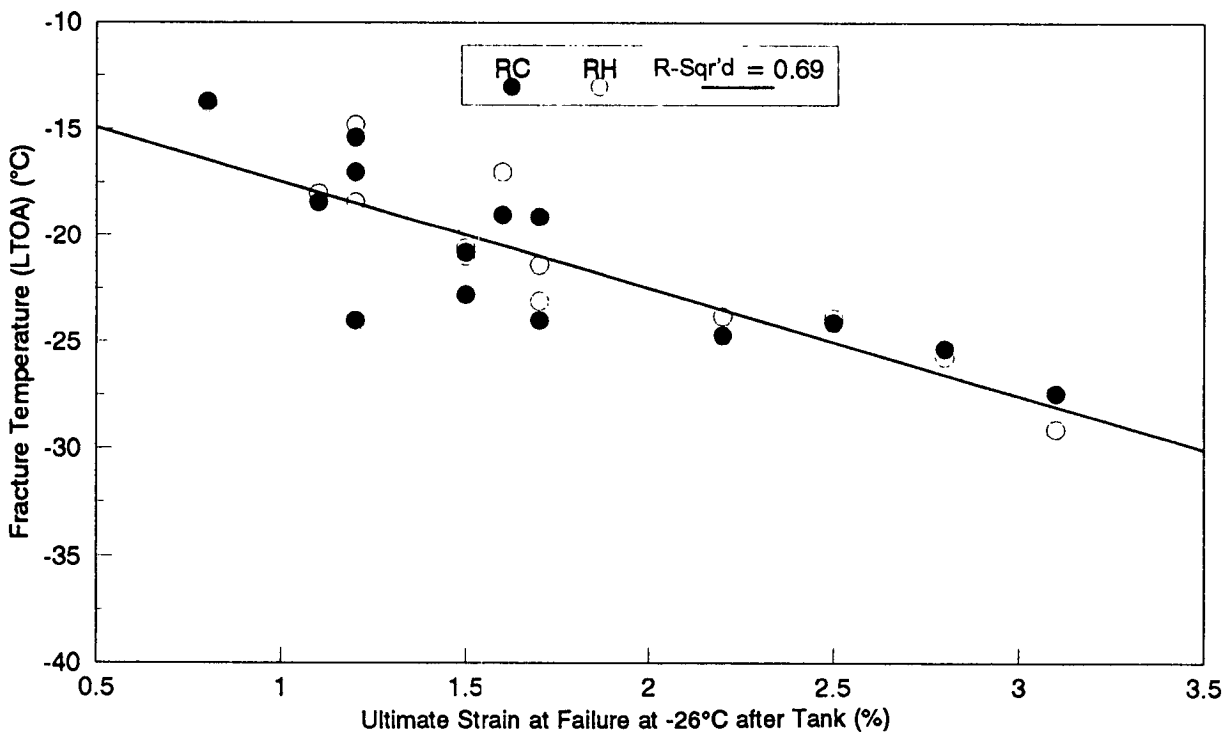

(b) Fracture Temperature of Long-Term Aged Mixes

Figure 6.6. Relationship between fracture temperature and ultimate strain at failure at -26°C after tank (unaged)

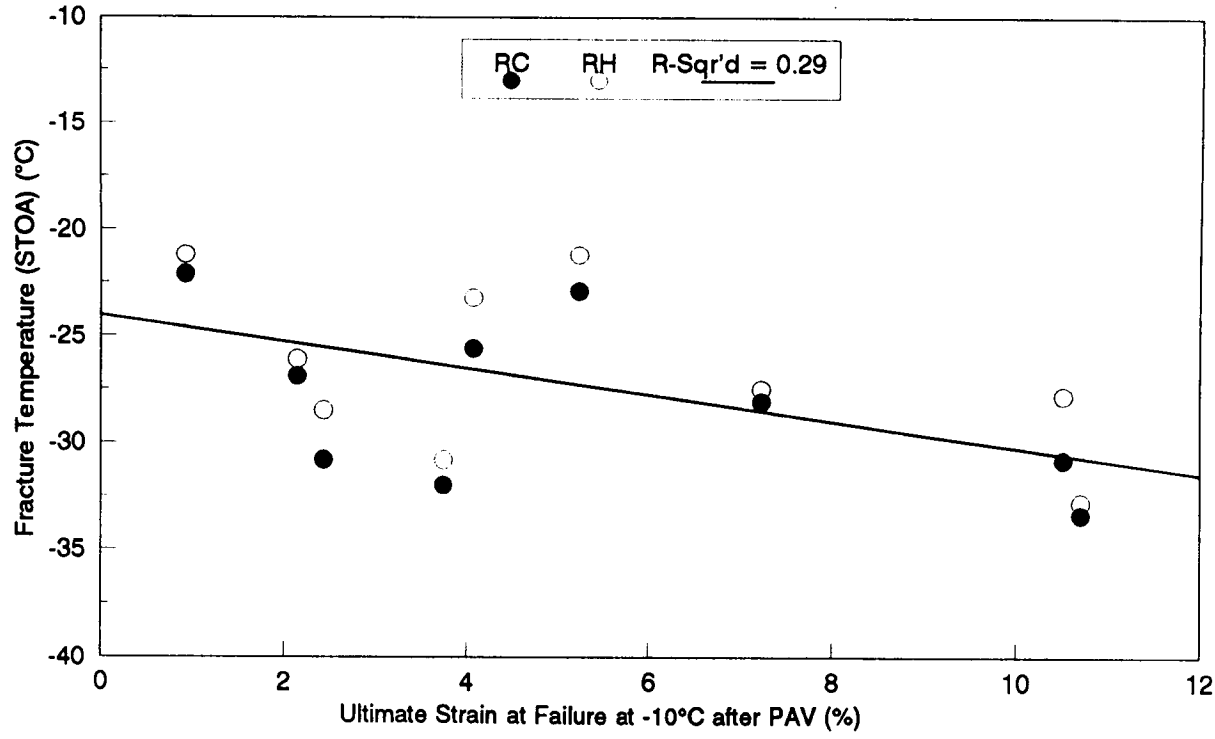

(a) Fracture Temperature of Short-Term Aged Mixes

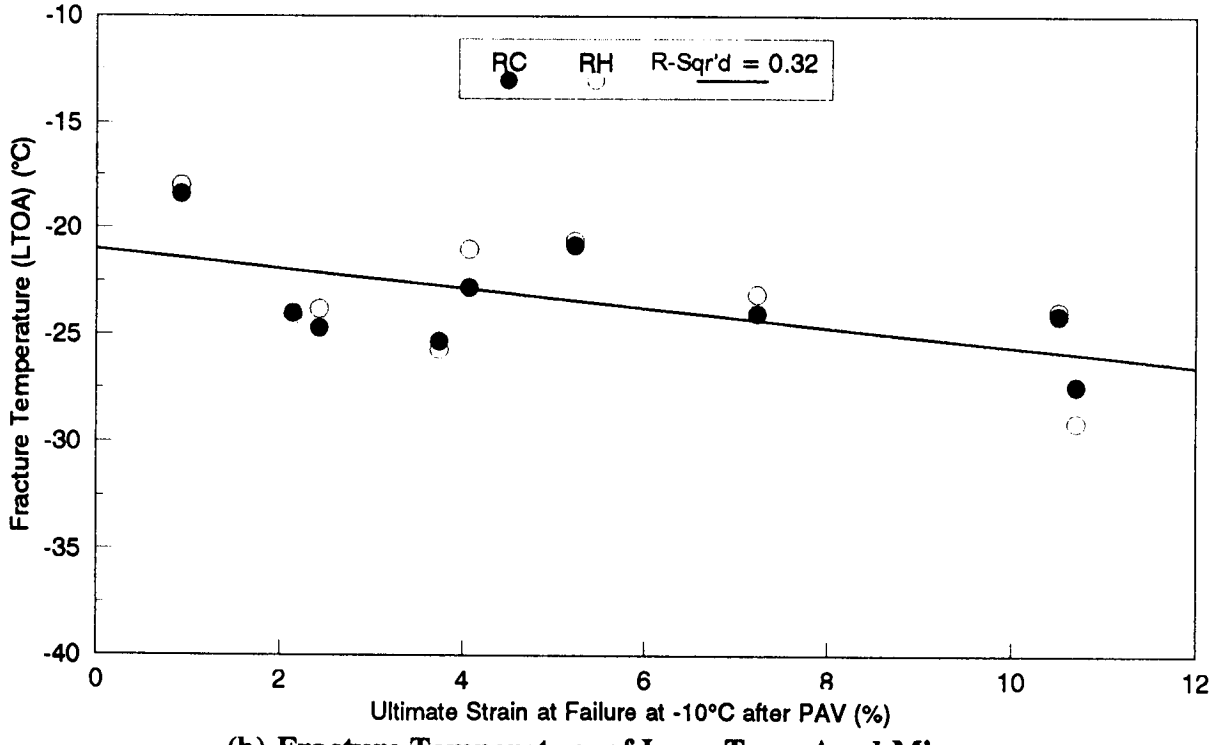

(b) Fracture Temperature of Long-Term Aged Mixes

Figure 6.7. Relationship between fracture temperature and ultimate strain at failure at -10°C after PAV (aged)

Figures 6.8 and 6.9 compare the measured fracture temperatures of short- and long-term aged mixtures, respectively, with the predicted fracture temperature with the A-002A low-temperature index test results. For short-term aged mixtures, standard errors between the measured fracture temperature and the predicted value (using the limiting stiffness temperature of unaged and aged asphalt cements, the m-value at 0°C of unaged asphalt cement and the creep stiffness at -10°C of aged asphalt cement) ranged from 0.37 to 1.0, depending on the asphalt type. For long-term aged mixtures, standard errors between the measured fracture temperature and the predicted value (using the limiting stiffness temperature of unaged asphalt cement and the creep stiffness at -10°C of aged asphalt cement) ranged from 0.37 to 0.78. Those with the m-value at 0°C of unaged asphalt cement and the ultimate strain at failure at -26°C of unaged asphalt cement ranged from 0.52 to 1.5, depending the asphalt type.

6.3 Relationship Between Fracture Temperature and A-002A Asphalt Cement Properties

Fracture temperature of both short- and long-term aged mixtures was compared to asphalt cement properties determined by A-002A researchers (Robertson et al. 1991). Linear regression analyses were performed. Summary statistics of linear regression analyses are presented in Table 6.4.

Relationships between the fracture temperature of short- and long-term aged mixtures (RC and RH aggregates) and the penetration of asphalt cement at 15°C after tank (unaged) are shown in Figure 6.10. Fracture temperature of both short- and long-term aged mixtures exhibits good correlations with the penetration of unaged asphalt cement at 15°C. R-squared values are 0.87 for the linear relationship with the fracture temperature of short-term aged mixes and 0.81 for long-term aged mixtures. The fracture temperature is colder for mixtures with softer asphalt cements.

Fracture temperature of both short- and long-term aged mixtures (RC and RH aggregates) for the eight SHRP core asphalts were compared with the penetration of aged asphalt cements at 15°C after the thin film oven test (TFOT) and pressure aging vessel (PAV). Relationships between the fracture temperature of short- and long-term aged mixtures and the penetration of aged asphalt cements are shown in Figures 6.11 and 6.12, respectively. Both the penetration of aged asphalt cements at 15°C after TFOT and PAV exhibit good correlations with the fracture temperature of short-term aged and long-term aged mixtures. As indicated in Figures 6.11 and 6.12 and Table 6.4, the penetration of aged asphalt cements exhibits better correlation with the fracture temperature of short-term aged mixtures. R-squared values are 0.94 for the linear relationship with the penetration of asphalt cement after TFOT, and 0.97 for the penetration of asphalt cement after PAV. For the fracture temperature of long-term aged mixtures, R-squared values are 0.86 for the linear relationship with the penetration of asphalt cement after TFOT, and 0.91 for the penetration of asphalt cement after PAV. Also, the penetration of asphalt cement after PAV exhibits better correlation with the fracture temperatures of both short- and long-term aged mixtures than the penetration after TFOT. Fracture temperature of both short-term and long-term aged

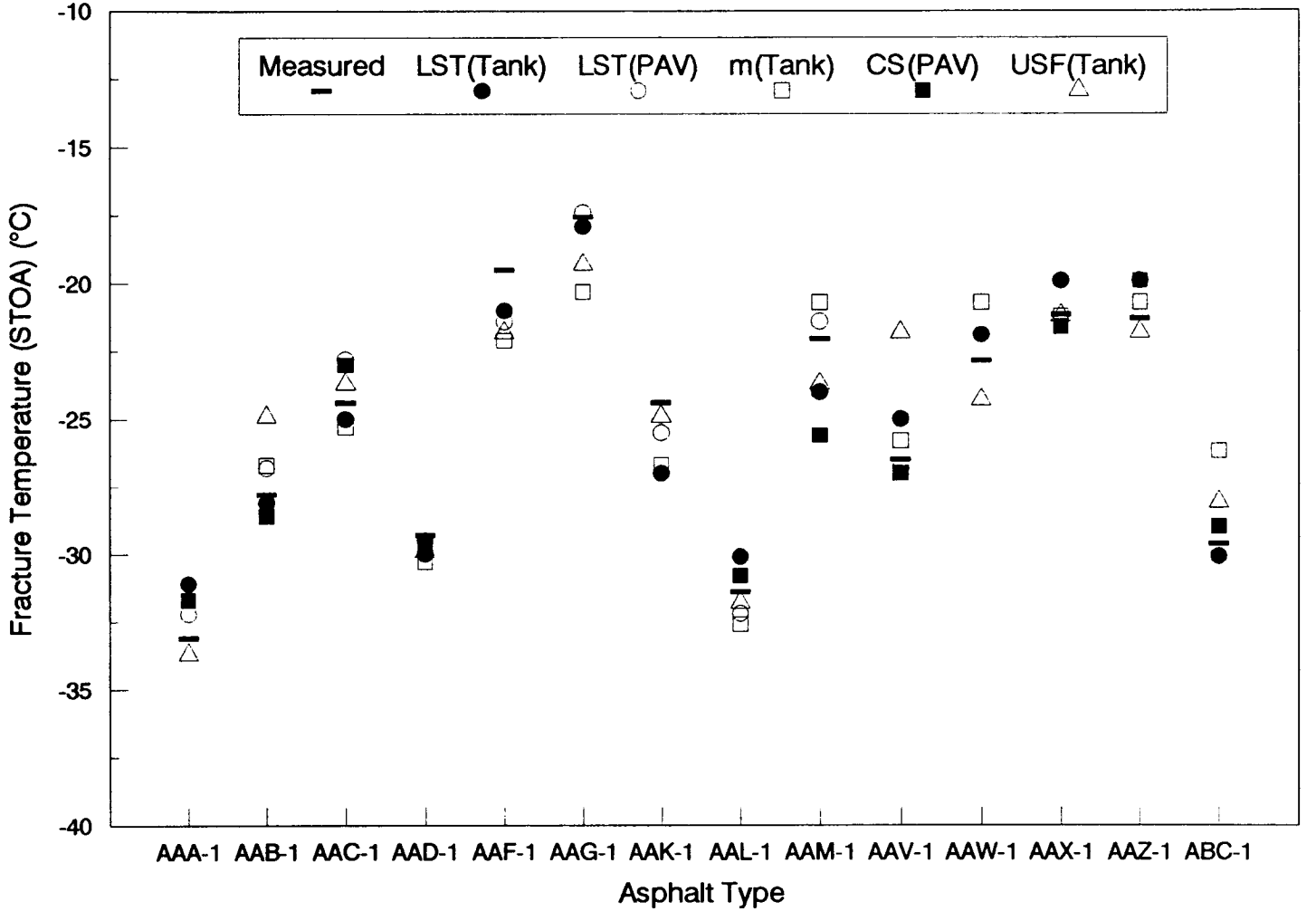

Figure 6.8. Comparison of fracture temperature (STOA) predicted with A-002A index test results

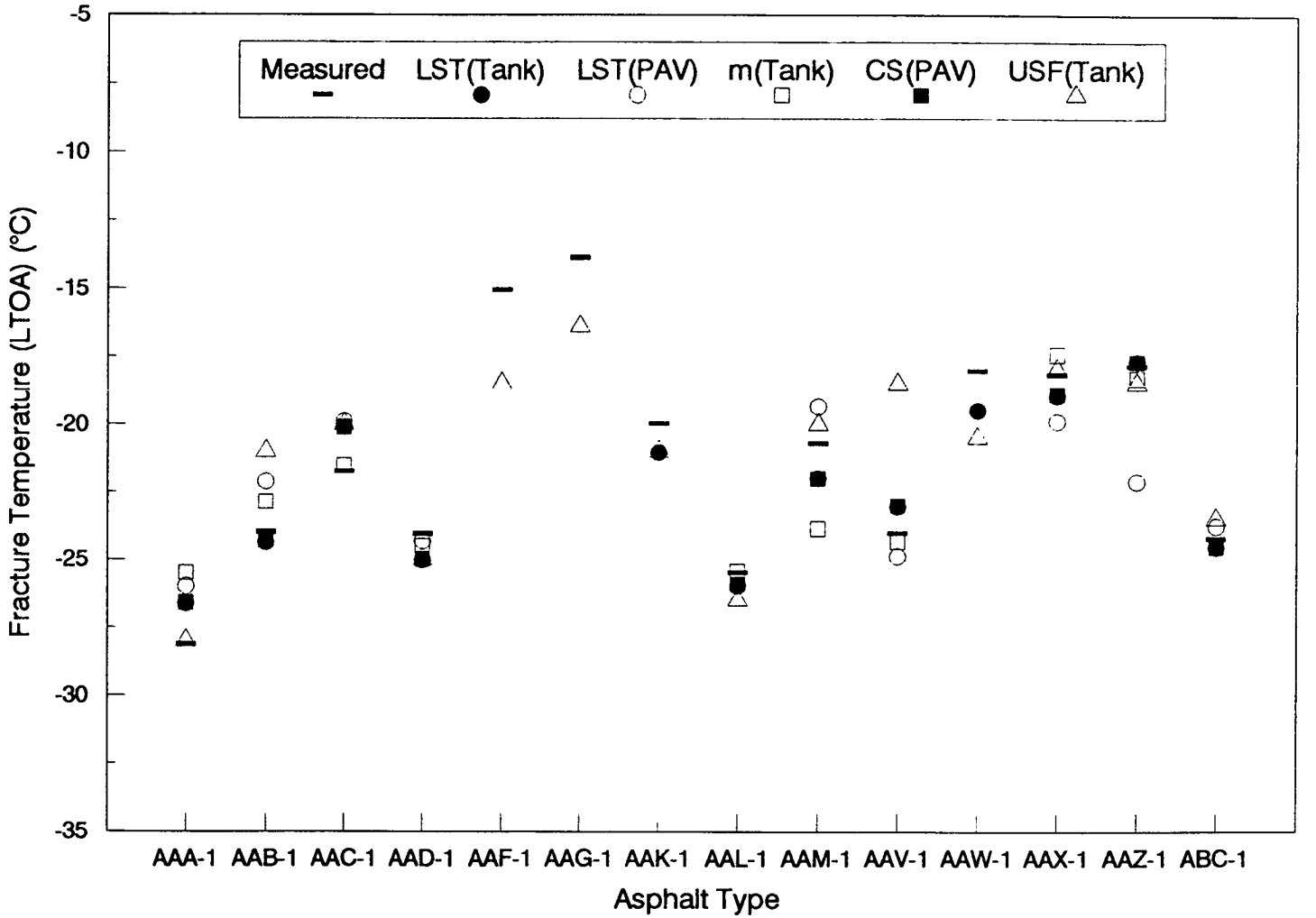

Figure 6.9. Comparison of fracture temperature (LTOA) predicted with A-002A index test results

Table 6.4. Summary statistics of linear regression analyses with the A-002A asphalt cement properties

Asphalt Binder Properties	Fracture Temp.	Parameter Estimates		MSE	C.V. (%)	F Value	R^2
		Intercept	Slope				
Penetration at 15°C after tank (unaged)	STOA	-16.205	-0.319	3.2	7.0	73.9	0.87
	LTOA	-13.390	-0.276	3.7	9.0	46.6	0.81
Penetration at 15°C after TFOT (aged)	STOA	-14.273	-0.603	1.8	5.5	95.5	0.94
	LTOA	-11.722	-0.530	3.6	9.0	38.2	0.86
Penetration at 15°C after PAV (aged)	STOA	-13.014	-1.093	1.0	3.9	190.3	0.97
	LTOA	-10.491	-0.972	2.3	7.2	62.2	0.91
Fraass Brittle Point after tank (unaged)	STOA	-16.752	0.763	5.5	9.5	27.9	0.82
	LTOA	-13.074	0.749	1.5	5.8	100.7	0.94

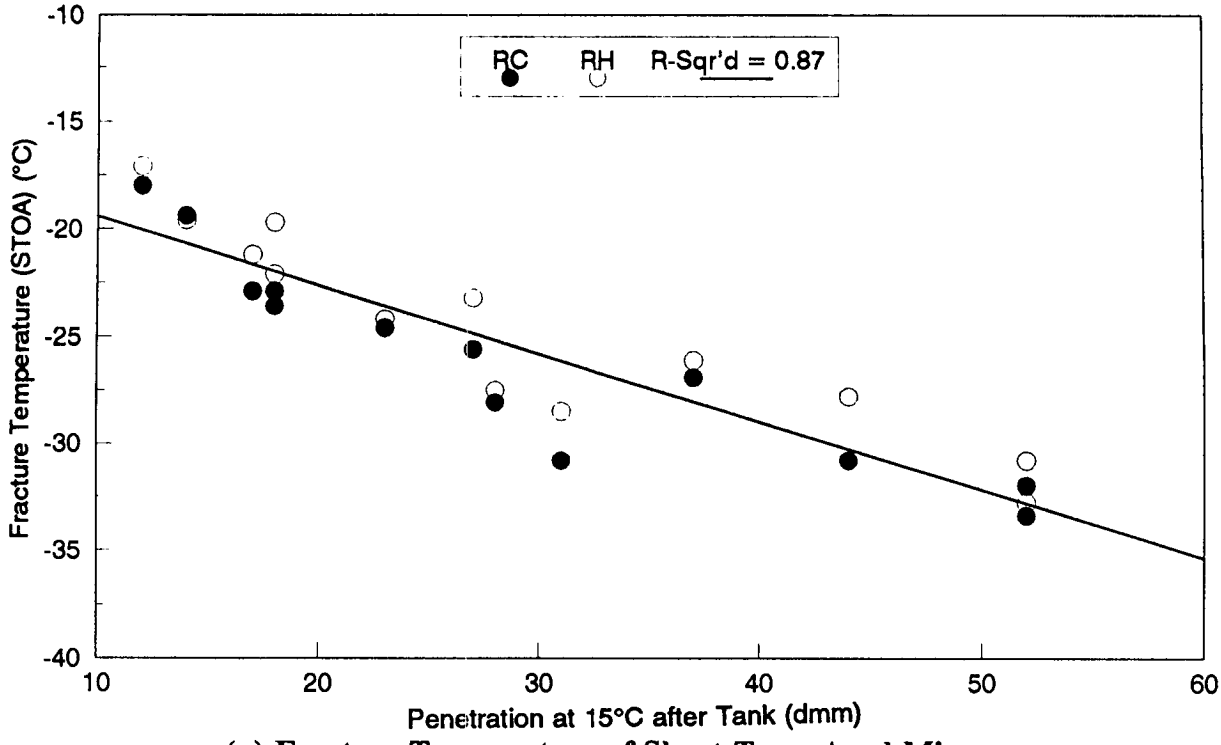

(a) Fracture Temperature of Short-Term Aged Mixes

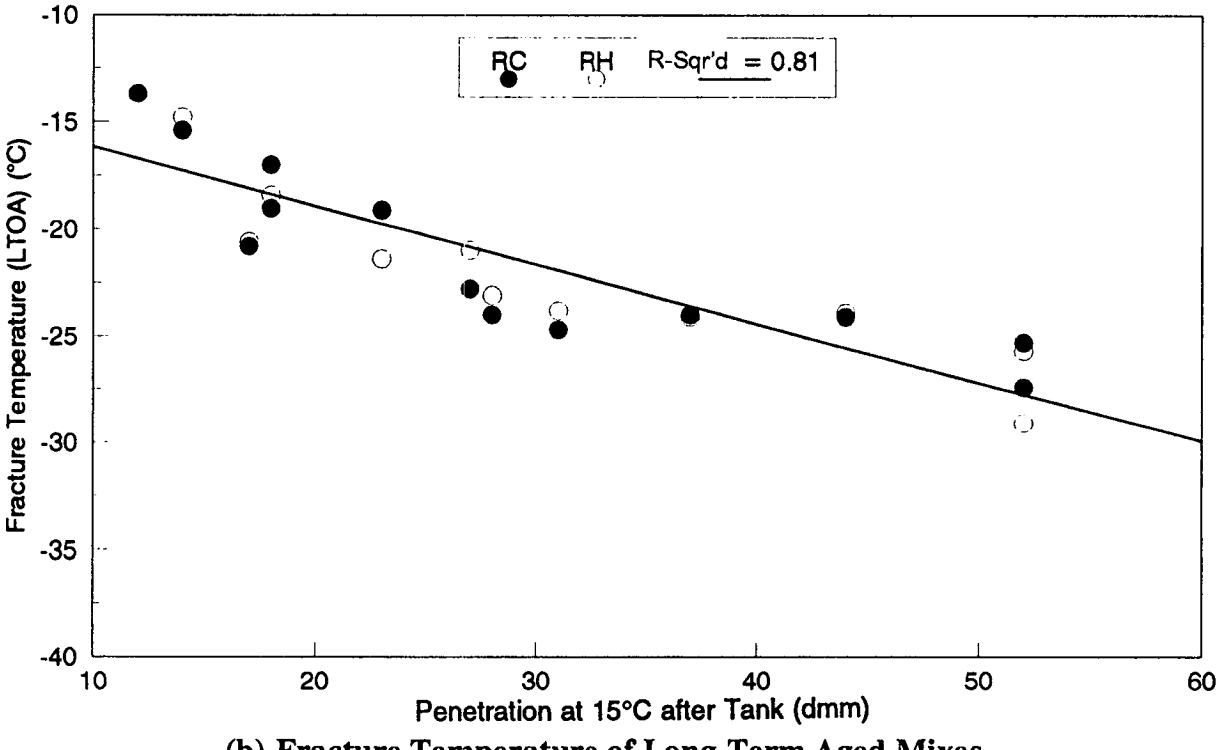

(b) Fracture Temperature of Long-Term Aged Mixes

Figure 6.10. Relationship between fracture temperature and penetration at 15°C after tank (unaged)

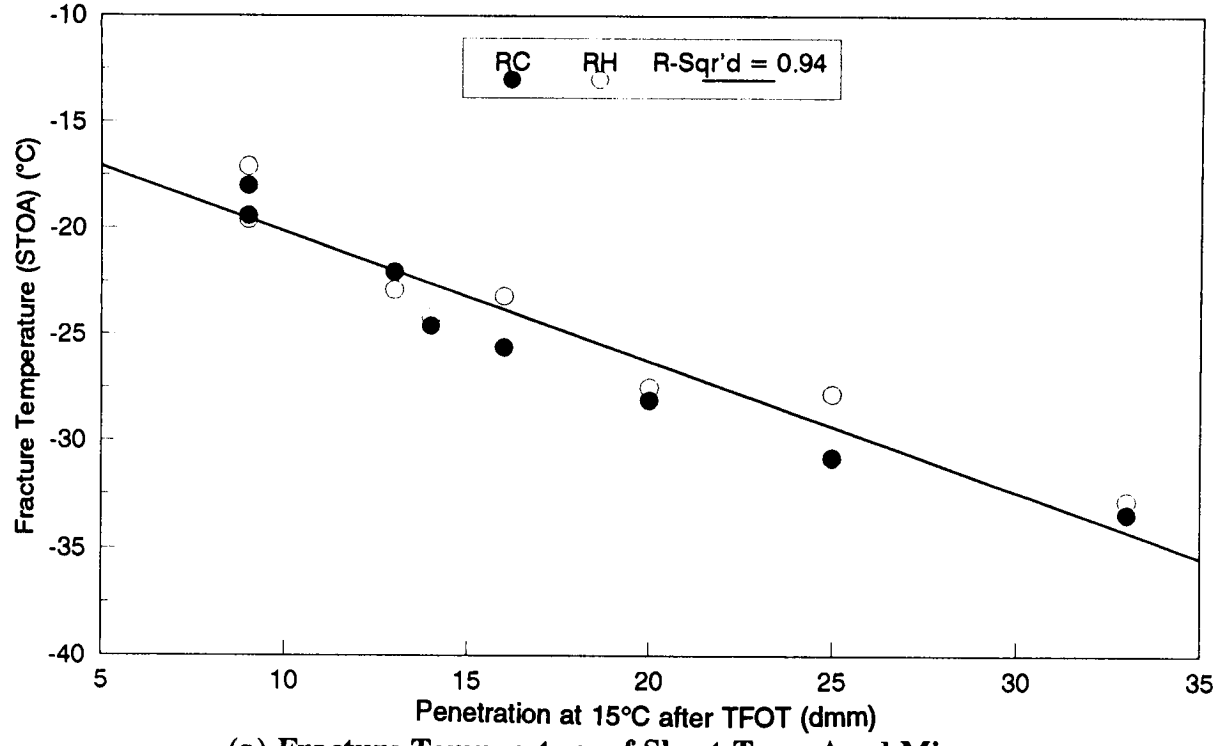

(a) Fracture Temperature of Short-Term Aged Mixes

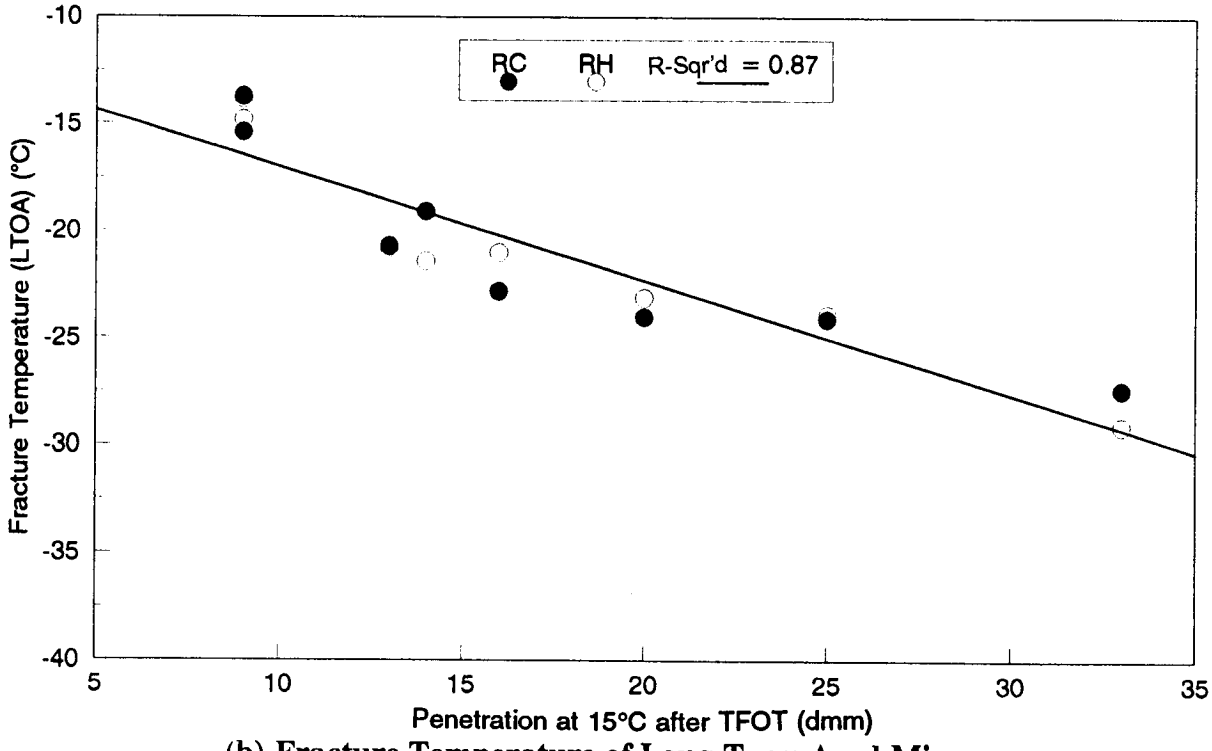

(b) Fracture Temperature of Long-Term Aged Mixes

Figure 6.11. Relationship between fracture temperature and penetration at 15°C after TFOT (aged)

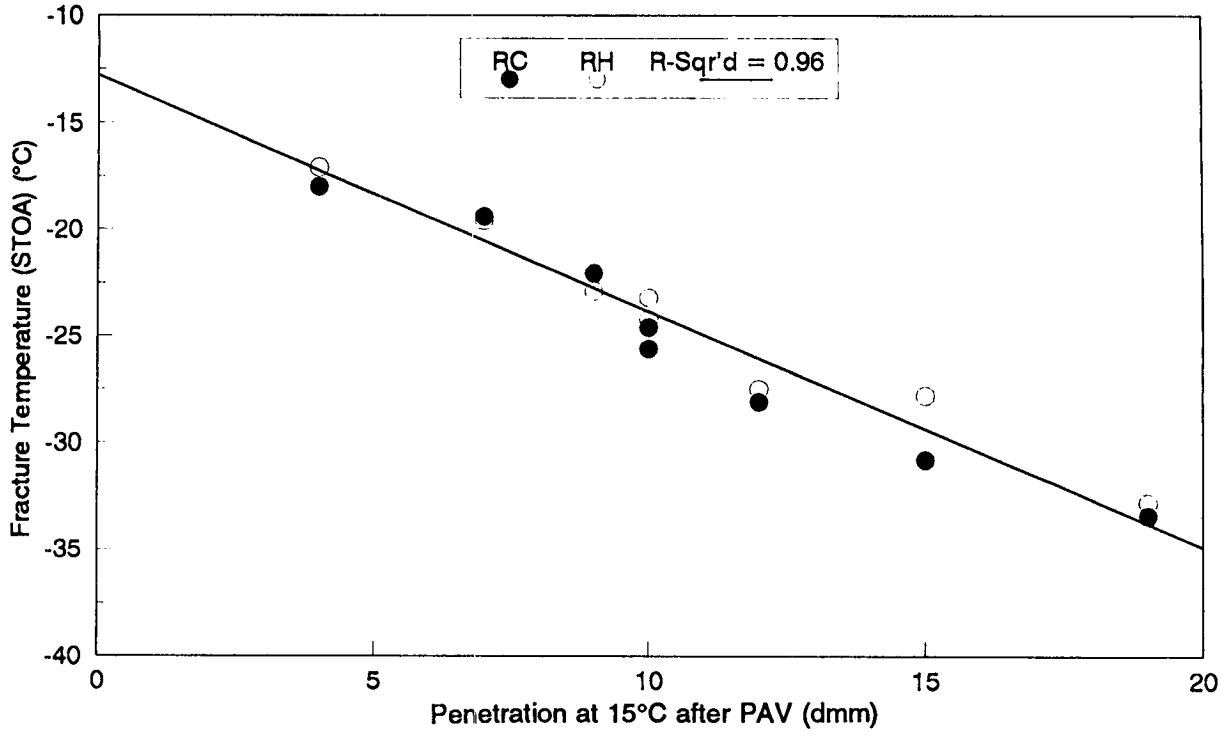

(a) Fracture Temperature of Short-Term Aged Mixes

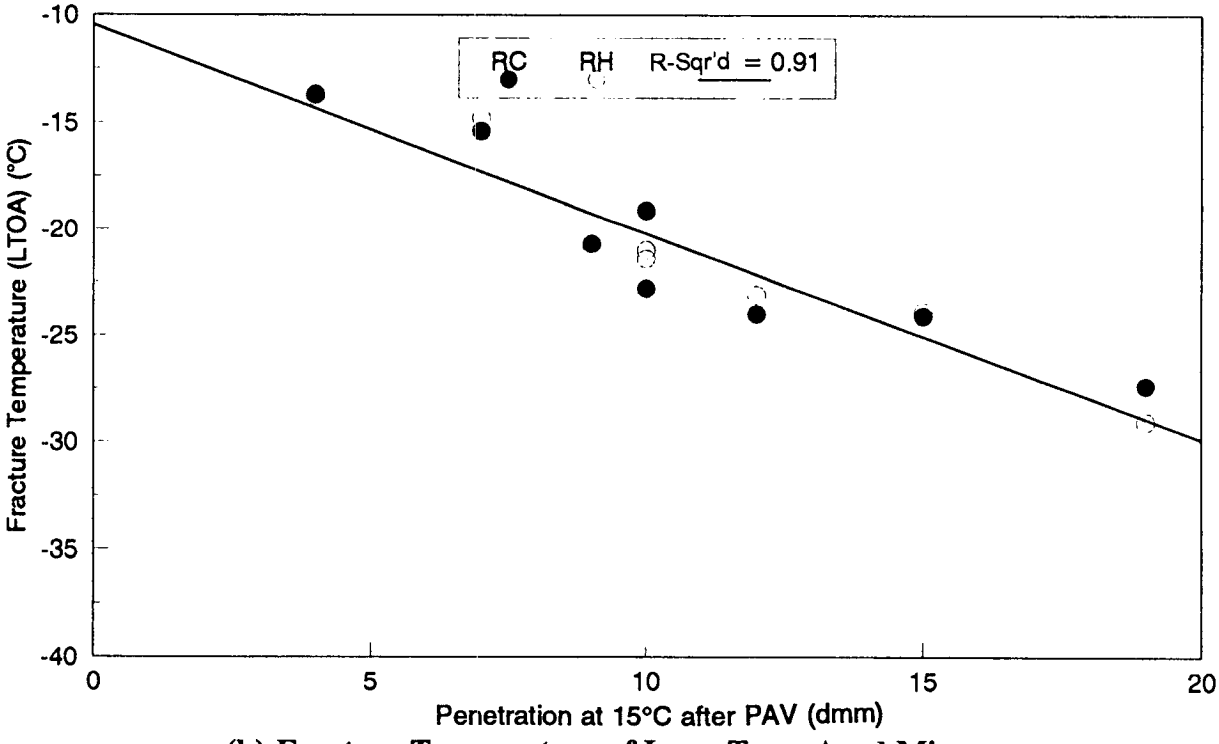

(b) Fracture Temperature of Long-Term Aged Mixes

Figure 6.12. Relationship between fracture temperature and penetration at 15°C after PAV (aged)

mixtures with SHRP's eight core asphalts were compared with the Fraass Brittle Point of unaged asphalt cement. Relationships between the fracture temperatures of short- and long-term aged mixtures (RC and RH aggregates) and the Fraass brittle point of unaged asphalt cement are presented in Figure 6.13. Fracture temperatures of both mixtures exhibit good correlation with the Fraass brittle point of unaged asphalt cement. The Fraass brittle point of unaged asphalt cement exhibits a better correlation with the fracture temperature of long-term aged mixtures. R-squared values are 0.94 for the fracture temperature of long-term aged mixtures and 0.82 for short-term aged mixtures.

Figures 6.14 and 6.15 compare the measured fracture temperatures of short- and long-term aged mixtures, respectively, to the predicted fracture temperature with the A-002A asphalt cement properties. For short-term aged mixtures, standard errors between the measured fracture temperature and the predicted value with the penetration of unaged and aged asphalt cements ranged from 0.35 to 1.0, depending on the asphalt type. For long-term aged mixtures, standard errors between the measured fracture temperature and the predicted value with the penetration of unaged and aged asphalt cement and the Fraass brittle point of unaged asphalt cement ranged from 0.43 to 1.50, depending on the asphalt type.

6.4 Significance of Results

The limiting stiffness temperatures of both unaged and aged (PAV) asphalt cements correlated well to the fracture temperatures of both short- and long-term aged mixtures. The limiting stiffness temperatures of both unaged and aged (PAV) asphalt cements showed better correlation with the fracture temperature of short-term aged mixtures. The limiting stiffness temperature of aged (PAV) asphalt cement does not exhibit a better correlation with the fracture temperature of long-term aged mixtures than it does with unaged asphalt cement.

The creep stiffness of aged (PAV) asphalt cement was well correlated to the fracture temperatures of both short- and long-term aged mixtures.

The m-value at 0°C and the ultimate strain at failure at -26°C of unaged asphalt cement were well correlated to the fracture temperature of short-term aged mixtures only. The m-value at -10°C and the ultimate strain at -10°C of aged asphalt cement did not exhibit good correlation with the fracture temperature of either short- and long-term aged mixtures.

The penetration of both unaged and aged (TFOT and PAV) asphalt cements at 15°C exhibited good correlation with the fracture temperatures of both short- and long-term aged mixtures. The penetration of aged (TFOT and PAV) asphalt cements exhibited better correlation with the fracture temperature of short-term aged mixtures than with long-term aged mixtures. Also, the penetration of aged asphalt cement after PAV exhibited slightly better correlation with the fracture temperatures of both short- and long-term aged mixtures than the penetration after TFOT.

The Fraass brittle point of unaged asphalt cement showed a better correlation with the fracture temperature of long-term aged mixes than with short-term aged mixtures.

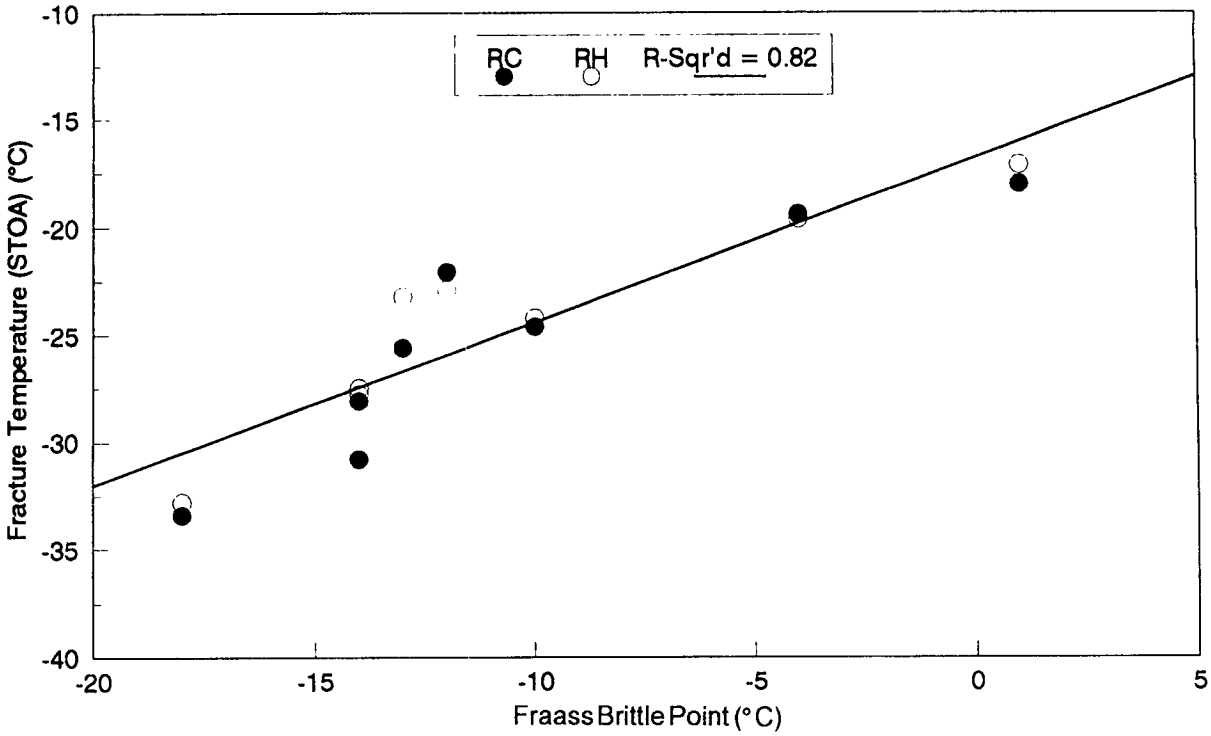

(a) Fracture Temperature of Short-Term Aged Mixes

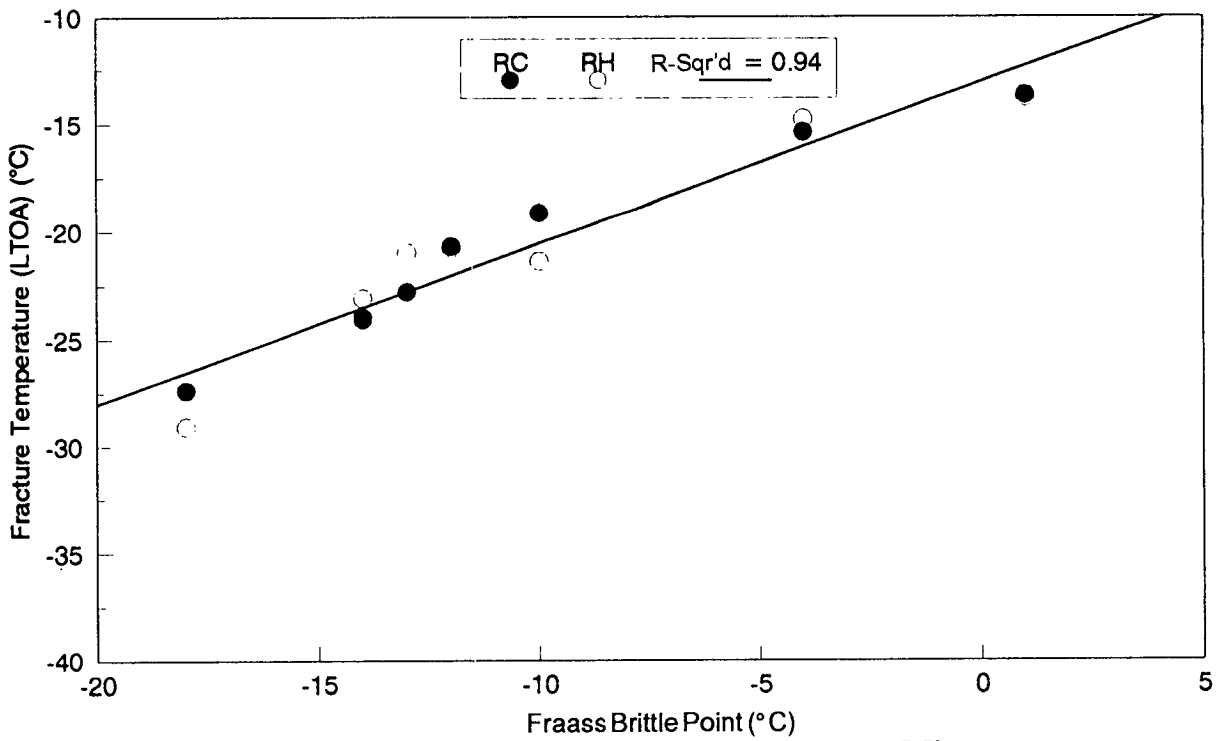

(b) Fracture Temperature of Long-Term Aged Mixes

Figure 6.13. Relationship between fracture temperature and Fraass brittle point after tank (unaged)

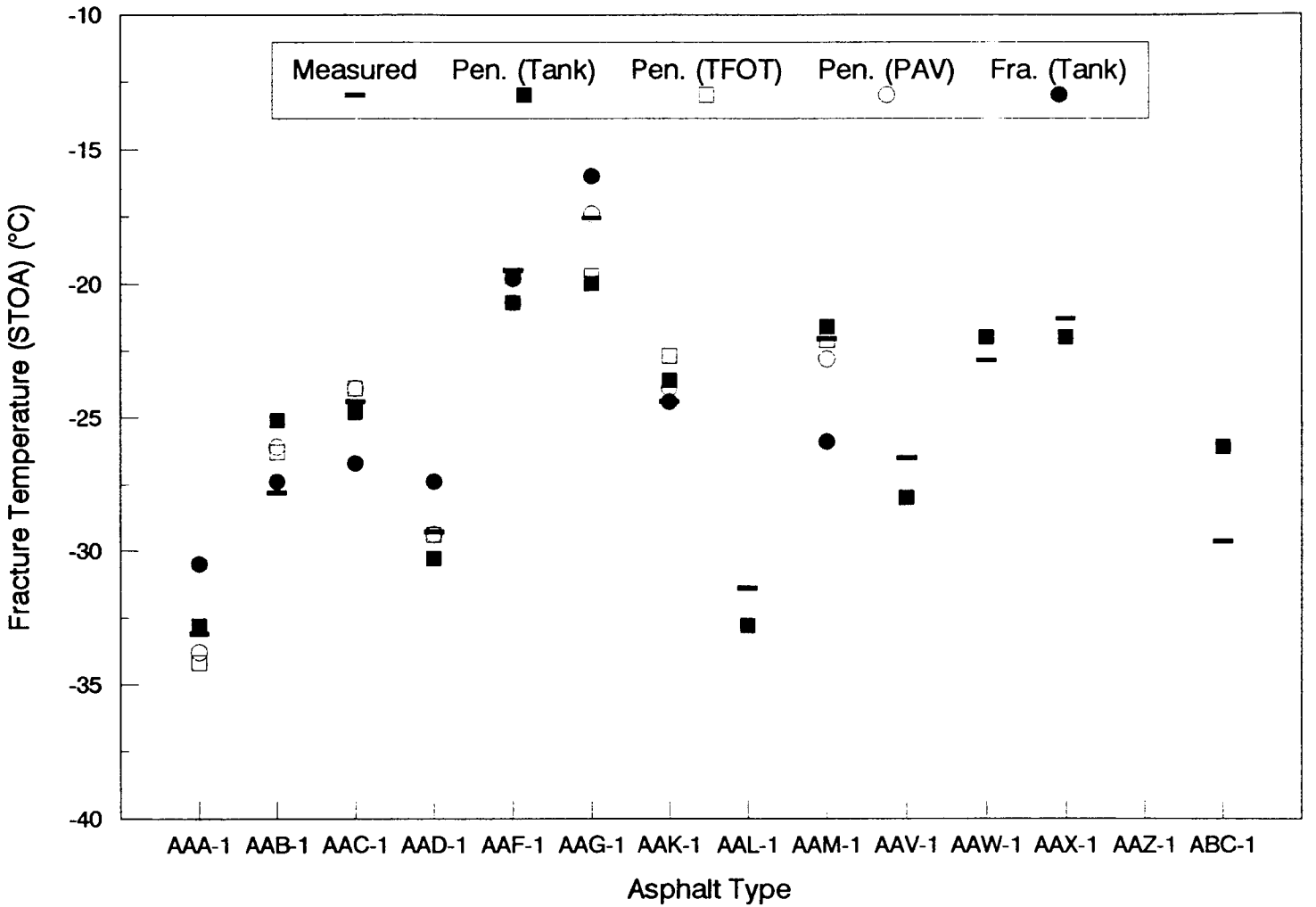

Figure 6.14. Comparison of fracture temperature (STOA) predicted with A-002A asphalt cement properties

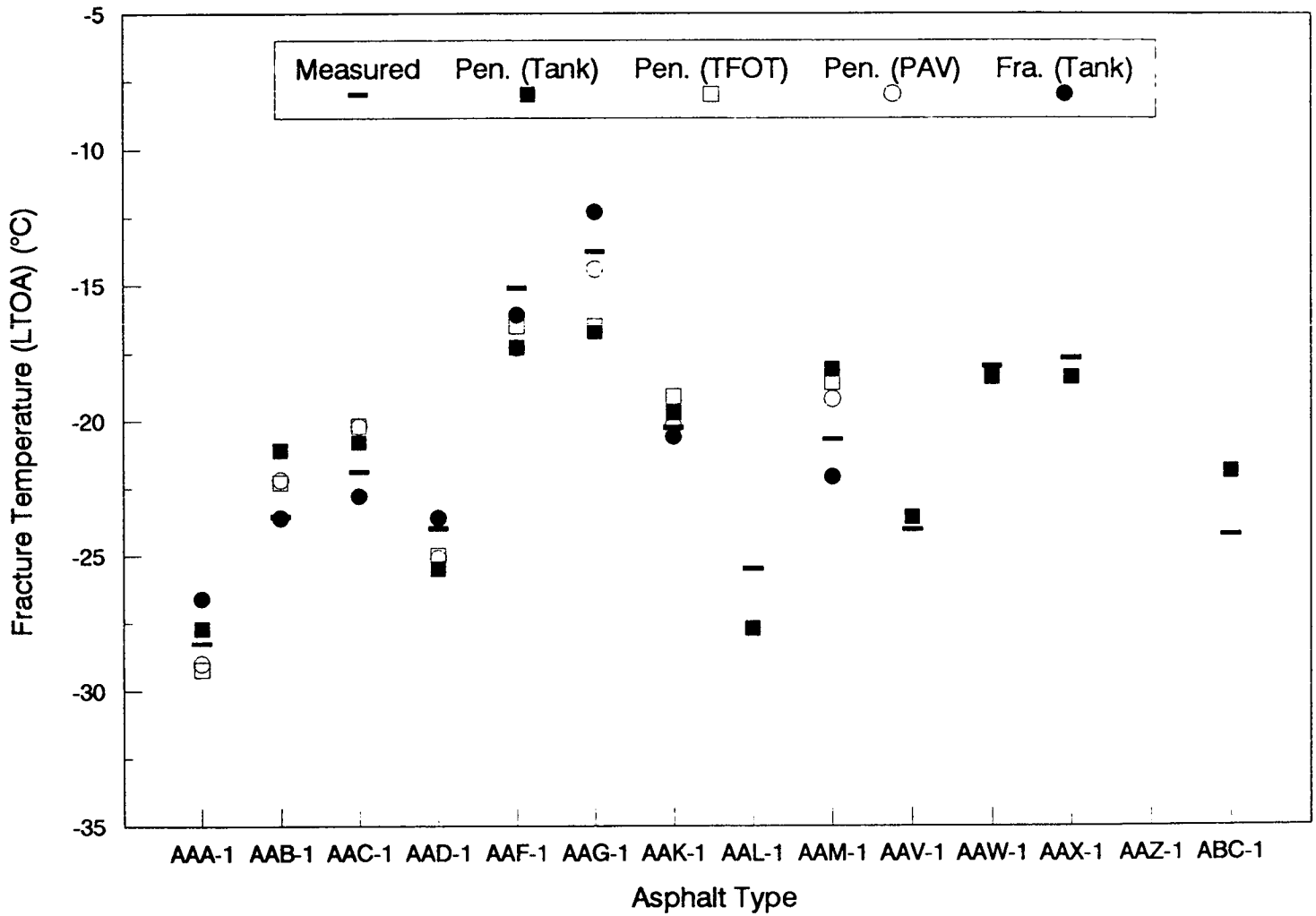

Figure 6.15. Comparison of fracture temperature (LTOA) predicted with A-002A asphalt cement properties

7

Conclusions and Recommendations

7.1 Conclusions

Based on the results presented herein, the following conclusions are appropriate.

1. The 95 percent repeatability limit of TSRST was less than 30 percent for fracture and transition temperatures. For fracture strength and slope, the 95 percent repeatability limit was less than 50 percent for most asphalts.

2. Degree of aging, asphalt type, air void content, and aggregate type are major factors that have a substantial effect on the low-temperature cracking resistance of asphalt concrete mixtures. Interactions between mixture properties (e.g., ASP*AGG, ASP*AGE, and AGG*AGE) have a minor effect.

3. Degree of aging, asphalt type, air void content, and the interaction between asphalt and degree of aging are significant factors for fracture temperature. Fracture temperature is most affected by degree of aging, followed by asphalt type, and is also affected by air void content and the interaction between asphalt type and degree of aging to a much lesser extent.

4. Air void content, aggregate type, the interaction between aggregate and degree of aging, and asphalt type are significant factors for the fracture strength. Fracture strength is highly influenced by air void content, followed by aggregate type. Fracture strength was greater for mixtures with lower air voids than for mixtures with higher air voids. Fracture strength was greater for mixtures with RH aggregate than for mixtures with RC aggregate. Asphalt type and the interaction between aggregate type and degree of aging have a minor influence on fracture strength. The effect of degree of aging on fracture strength is inconclusive.

5. Aggregate type, air void content, the interaction between aggregate type and degree of aging, and asphalt type are significant factors of slope (dS/dT). Slope is most affected by aggregate type, followed by air void content, and is also affected

by asphalt type and the interaction between aggregate type and degree of aging to a much lesser extent. Slope was greater for mixtures with lower air voids and also greater for mixtures with RH aggregate. The effect of degree of aging on slope is inconclusive.

6. Degree of aging, asphalt type, aggregate type, and the interaction between asphalt type and degree of aging are significant factors in transition temperature. Transition temperature is most affected by degree of aging, followed by asphalt type, and also affected by aggregate type and the interaction between asphalt type and degree of aging to a lesser extent.

7. A ranking of asphalt concrete mixtures based on fracture temperature compares favorably with a ranking based on fundamental properties of the asphalt cements given by A-002A.

8. Fracture temperature was highly correlated to A-002A low-temperature index test results — specifically, the limiting stiffness temperature, the m-value, the creep stiffness, and the ultimate strain at failure. The limiting stiffness temperature of both unaged and pressure aging vessel (PAV) aged asphalt cements, and the creep stiffness of PAV aged asphalt cement were well correlated to fracture temperatures of both short- and long-term aged mixes. The m-value at 0°C and the ultimate strain at failure at -26°C of unaged asphalt cements were well correlated to the fracture temperature of short-term aged mixes only. The m-value and the ultimate strain of PAV aged asphalt cement did not exhibit good correlation with the fracture temperatures of either short- or long-term aged mixes.

9. The penetration of asphalt cements at 15°C is a good indicator of the low-temperature cracking characteristics of asphalt concrete mixtures. The penetration of both unaged and aged (thin film oven test [TFOT] and PAV) asphalt cements at 15°C showed good correlation with fracture temperatures of both short- and long-term aged mixes. The penetration of aged (TFOT and PAV) asphalt cements exhibited better correlation with the fracture temperatures of short-term aged mixes than that of long-term aged mixes. Also, the penetration of aged asphalt cement after PAV showed slightly better correlations with the fracture temperature of both short- and long-term aged mixes than that after TFOT. The fracture temperature was colder for mixtures with softer asphalt cements.

10. The Fraass brittle point of asphalt cements also provided a good indication of the low-temperature characteristics of asphalt concrete mixtures. Fraass brittle point of unaged asphalt cement exhibited good correlations with the fracture temperature of both short- and long-term aged mixes. It exhibited a better correlation with the fracture temperature of long-term aged mixes than that of short-term aged mixes.

7.2 Recommendations

1. It is highly desirable to control low-temperature cracking of asphalt concrete mixtures based solely on a consideration of fundamental properties of the asphalt cement. Before this goal is achieved, however, it is recommended that correlations between TSRST fracture temperature and fundamental properties of the asphalt cement be developed for modified asphalt cements and for asphalt cements that exhibit a wide range of sulfur, wax, and asphaltene contents.

2. It is also recommended that the specification to control low-temperature cracking of asphalt concrete mixtures include a consideration of the aging characteristics.

8

References

Bahia, H. U., D. A. Anderson, and D.W. Christiansen (1992). The bending beam rheometer: a simple device for measuring low-temperature rheology of asphalt binders. Proceedings of the Association of Asphalt Paving Technologists, Vol. 61.

Branthover, J. G., J. C. Petersen, R. E. Robertson, J. J. Duvall, S. S. Kim, P. M. Harnsberger, T. Mill, E. K. Ensley, F. A. Barbour, and J. F. Schabron (1993). Binder Characterization and Evaluation, Volume 2: Chemistry. SHRP Report A-368. SHRP, National Research Council, Washington, DC.

Jung, D-H. and T. S. Vinson. *Low-Temperature Cracking — Test Selection.* Report No. SHRP-A-400. Strategic Highway Research Program, National Research Council, Washington DC: 1994. Forthcoming.

Materials Reference Library (1992). Asphalt properties. Personal communication from University of Texas in April, June, and October.

Peterson, J. C. et al. (December 1992). Binder characterization and evaluation. Draft final report, SHRP Contract A-002A.

Robertson, R. E., J. F. Branthaver, D. A. Anderson, and J. C. Petersen (June 1991). Binder characterization and evaluation. SHRP Quarterly Report, A-002A.

SAS Institute Inc. (1986). SAS system for regression. Cary, N.C.

SAS Institute Inc. (1991). SAS/STAT user's guide, release 6.03ed. Cary, N.C.

SAS Institute Inc. (1991). SAS language guide for personal computers, release 6.03ed. Cary, N.C.

Appendix A
Results of TSRST

Table A.1. Results of TSRST for short-term aged (STOA) mixtures with RC aggregate

Specimen ID	Asphalt Type	Air Void Content (%)	Fracture Temperature (°C)	Fracture Strength (psi)	Fracture Strength (MPa)	dS/dT (psi/°C)	Transition Temperature (°C)
CA1H01	AAA-1	6.1	-31.4	353	2.4357	20.2	-21.8
CA1H02		5.8	-30.7	411	2.8359	23.6	-22.3
CA1L02		8.6	-34.1	374	2.5806	20.9	-23.5
CB1L01	AAB-1	8.0	-28.0	323	2.2287	17.6	-16.5
CB1L02		8.1	-28.2	300	2.0700	17.0	-17.4
CB1L22		7.9	-27.9	300	2.0700	17.0	-17.1
CB1L23		5.7	-24.6	333	2.2977	18.8	-16.6
CC1L01	AAC-1	7.0	-24.3	312	2.1528	20.0	-16.9
CC1L02		9.0	-26.7	273	1.8837	15.4	-17.1
CC1L12		6.6	-22.3	315	2.1735	20.6	-15.9
CC1L22		6.4	-23.7	362	2.4978	22.7	-16.6
CD1H01	AAD-1	7.8	-30.4	382	2.6358	20.1	-20.3
CD1L01		6.6	-29.9	318	2.1942	19.7	-20.9
CD1L02		9.2	-31.6	276	1.9044	15.3	-20.7
CF1H01	AAF-1	7.0	-18.7	281	1.9389	20.3	-10.7
CF1L01		6.3	-17.9	291	2.0079	21.5	-11.5
CF1L02		8.6	-20.7	241	1.6629	15.5	-11.3
CF1L12		6.6	-17.1	279	1.9251	19.5	-10.3
CG1H01	AAG-1	9.7	-21.8	298	2.0562	18.9	-11.8
CG1H13		8.8	-19.9	314	2.1666	22.8	-10.6
CG1L02		8.2	-18.4	275	1.8975	21.3	-10.7
CG1L22		9.2	-20.4	300	2.0700	22.1	-10.5

Continued on page 100

Table A.1 (continued). Results of TSRST for short-term aged (STOA) mixtures with RC aggregate

Specimen ID	Asphalt Type	Air Void Content (%)	Fracture Temperature (°C)	Fracture Strength (psi)	Fracture Strength (MPa)	dS/dT (psi/°C)	Transition Temperature (°C)
CK1H01	AAK-1	10.2	-26.8	261	1.8009	15.6	-16.4
CK1H02		10.6	-26.4	248	1.7112	15.0	-16.3
CK1H12		9.1	-24.8	327	2.2563	19.9	-16.3
CK1H22		8.4	-23.0	280	1.9320	19.2	-16.0
CK1L22		6.3	-23.3	313	2.1597	19.1	-16.2
CL1L01	AAL-1	8.4	-32.2	338	2.3322	20.2	-22.3
CL1L32		6.8	-31.3	465	3.2085	24.0	-22.9
CM1L02	AAM-1	7.9	-22.9	394	2.7186	23.5	-15.3
CM1L12		5.6	-20.5	431	2.9739	28.4	-15.6
CM1L22		8.2	-23.4	397	2.7393	23.8	-15.7
CM1L32		3.8	-19.6	472	3.2568	32.0	-15.2
CV1H12	AAV-1	8.0	-26.4	286	1.9734	19.2	-18.2
CV1H22		8.2	-27.4	285	1.9665	19.3	-18.9
CV1L02		9.5	-28.6	245	1.6905	16.1	-18.3
CW1H22	AAW-1	7.2	-20.9	320	2.2080	21.8	-12.8
CW1L12		5.6	-21.8	384	2.6496	22.6	-12.7
CW1L22		6.4	-21.7	345	2.3805	20.6	-12.1
CX1H02	AAX-1	9.2	-22.3	276	1.9044	15.5	-13.8
CX1L01		9.2	-19.7	271	1.8699	19.6	-14.1
CX1L02		6.3	-21.5	362	2.4978	22.4	-13.6
CX1L22		5.8	-22.0	388	2.6772	22.7	-13.6
CX1L32		4.9	-21.4	426	2.9394	****	*****
CZ1H01	AAZ-1	6.1	-23.0	392	2.7048	24.8	-14.4
CZ1H02		6.9	-22.9	359	2.4771	25.7	-14.3
CZ1L01		4.4	-21.5	493	3.4017	32.6	-14.1
CZ1L02		4.8	-21.3	435	3.0015	28.4	-14.5
CBC1L02	ABC-1	7.1	-30.1	363	2.5047	18.6	-19.4
CBC1L42		5.4	-28.7	393	2.7117	22.7	-20.6

Table A.2. Results of TSRST for long-term aged (LTOA) mixtures with RC aggregate

Specimen ID	Asphalt Type	Air Void Content (%)	Fracture Temperature (°C)	Fracture Strength (psi)	Fracture Strength (MPa)	dS/dT (psi/°C)	Transition Temperature (°C)
LCA1H03	AAA-1	5.5	-28.0	500	3.4500	26.9	-19.7
LCA1L03		8.6	-27.7	387	2.6703	20.6	-19.1
LCA1L04		8.8	-28.9	379	2.6151	21.5	-20.1
LCB1H42	AAB-1	7.6	-24.4	354	2.4426	20.0	-15.1
LCB1L04		6.5	-23.7	370	2.5530	20.7	-15.0
LCB1L33		6.8	-23.9	357	2.4633	20.0	-15.0
LCB1L43		4.0	-23.0	463	3.1947	25.6	-15.1
LCC1L04	AAC-1	10.4	-24.1	324	2.2356	18.3	-14.6
LCC1L32		6.0	-22.1	473	3.2637	29.0	-14.1
LCC1L42		6.6	-22.5	465	3.2085	29.2	-15.0
LCD1L03	AAD-1	8.8	-25.3	400	2.7600	21.4	-14.0
LCD1L32		4.9	-21.6	383	2.6427	18.3	-9.7
LCD1L42		5.8	-23.0	440	3.0360	23.6	-14.4
LCF1L03	AAF-1	7.9	-17.6	414	2.8566	26.4	-8.8
LCF1L04		10.8	-17.9	324	2.2356	18.3	-8.3
LCF1L32		7.0	-14.0	297	2.0493	20.1	-7.5
LCF1L42		7.3	-13.5	265	1.8285	18.1	-7.4
LCG1L32	AAG-1	6.0	-15.8	445	3.0705	33.5	-7.2
LCK1H03	AAK-1	11.8	-20.1	310	2.1390	18.0	-10.5
LCK1H04		12.2	-18.2	254	1.7526	15.0	-10.0
LCK1L32		7.1	-21.4	425	2.9325	24.1	-11.0
LCK1L42		6.9	-19.3	389	2.6841	24.5	-10.0
LCL1L03	AAL-1	9.7	-26.3	380	2.6220	22.1	-17.4
LCL1L04		7.7	-24.4	424	2.9256	28.7	-17.0
LCM1H04	AAM-1	9.0	-22.7	346	2.3874	25.7	-15.0
LCM1L03		7.1	-20.1	443	3.0567	26.3	-14.1
LCM1L04		7.7	-20.3	423	2.9187	24.8	-14.0

Continued on page 102

Table A.2 (continued). Results of TSRST for long-term aged (LTOA) mixtures with RC aggregate

Specimen ID	Asphalt Type	Air Void Content (%)	Fracture Temperature (°C)	Fracture Strength (psi)	Fracture Strength (MPa)	dS/dT (psi/°C)	Transition Temperature (°C)
LCV1H32	AAV-1	8.6	-24.2	324	2.2356	23.0	-17.4
LCV1H42		8.9	-23.9	312	2.1528	21.3	-17.3
LCV1L32		5.7	-24.3	432	2.9808	25.6	-16.7
LCW1H32	AAW-1	8.8	-19.9	341	2.3529	20.6	-10.3
LCW1H42		8.0	-18.5	371	2.5599	21.8	-10.0
LCW1L03		7.6	-19.4	400	2.7600	22.2	-10.3
LCW1L04		8.9	-19.7	350	2.4150	19.6	-10.0
LCW1L42		5.0	-18.4	461	3.1809	27.2	-10.3
LCX1L03	AAX-1	6.6	-18.5	404	2.7876	24.7	-10.1
LCX1L04		7.0	-18.2	358	2.4702	23.1	-10.0
LCZ1H03	AAZ-1	8.2	-16.6	335	2.3115	23.7	-10.3
LCZ1H04		9.0	-19.0	264	1.8216	20.7	-10.6
LCZ1L04		7.5	-17.5	369	2.5461	25.3	-10.3
LCBC1L03	ABC-1	8.4	-25.4	361	2.4909	19.1	-17.5
LCBC1L04		7.6	-25.8	381	2.6289	20.3	-17.0

Table A.3. Results of TSRST for short-term aged (STOA) mixtures with RH aggregate

Specimen ID	Asphalt Type	Air Void Content (%)	Fracture Temperature (°C)	Fracture Strength (psi)	Fracture Strength (MPa)	dS/dT (psi/°C)	Transition Temperature (°C)
HA1L01	AAA-1	5.1	-31.9	513	3.5397	37.4	-25.4
HA1L02		6.2	-32.4	505	3.4845	36.7	-26.0
HB1H01	AAB-1	9.0	-27.9	364	2.5116	23.9	-18.8
HB1H02		6.4	-27.5	429	2.9601	29.0	-18.9
HB1L01		6.4	-26.9	383	2.6427	29.2	-18.4
HB1L12		4.2	-26.8	481	3.3189	30.0	-18.7
HB1L22		4.6	-26.5	458	3.1602	29.6	-18.5
HC1H01	AAC-1	8.7	-23.4	350	2.4150	27.9	-17.4
HC1H02		5.9	-21.6	369	2.5461	34.5	-16.5
HC1L01		8.0	-22.3	328	2.2632	28.1	-17.3
HC1L12		4.9	-21.8	381	2.6289	31.2	-17.7
HC1L22		3.9	-20.6	387	2.6703	34.7	-16.6
HD1H01	AAD-1	5.6	-28.1	461	3.1809	31.8	-21.2
HD1H04		6.1	-28.4	450	3.1050	28.5	-21.0
HD1H23		9.8	-28.7	337	2.3253	23.6	-21.5
HF1L02	AAF-1	5.3	-17.7	411	2.8359	34.0	-13.3
HF1H12		7.7	-18.6	360	2.4840	26.7	-13.6
HF1H22		8.3	-20.4	367	2.5323	26.2	-13.2
HG1H01	AAG-1	6.7	-15.0	407	2.8083	39.0	-10.3
HG1H02		7.0	-15.6	380	2.6220	38.6	-10.7
HG1L01		8.7	-17.9	354	2.4426	30.0	-10.7
HG1L22		7.3	-16.7	360	2.4840	33.3	-10.6
HK1H02	AAK-1	8.4	-24.7	432	2.9808	28.0	-17.7
HK1L02		8.8	-24.1	418	2.8842	26.0	-17.9
HK1L12		3.6	-23.0	491	3.3879	35.0	-17.0
HK1L32		3.8	-23.2	442	3.0498	33.1	-17.4

Continued on page 104

Table A.3 (continued). Results of TSRST for short-term aged (STOA) mixtures with RH aggregate

Specimen ID	Asphalt Type	Air Void Content (%)	Fracture Temperature (°C)	Fracture Strength (psi)	Fracture Strength (MPa)	dS/dT (psi/°C)	Transition Temperature (°C)
HL1H12	AAL-1	8.5	-31.3	380	2.6220	24.4	-22.7
HL1H42		8.8	-29.8	353	2.4357	25.3	-22.5
HL1L12		4.3	-30.2	456	3.1464	31.5	-22.5
HL1L22		5.4	-31.9	483	3.3327	30.0	-22.6
HM1H01	AAM-1	6.9	-21.0	444	3.0636	33.2	-15.6
HM1H02		6.7	-20.7	464	3.2016	34.8	-15.2
HM1L21		6.7	-20.6	463	3.1947	35.1	-15.4
HM1L13		7.5	-20.2	447	3.0843	34.7	-15.0
HM1L23		7.9	-21.8	442	3.0498	32.2	-16.0
HM1L14		6.2	-20.7	459	3.1671	35.2	-15.2
HV1H12	AAV-1	9.9	-25.7	295	2.0355	24.0	-19.8
HV1L02		7.6	-27.0	357	2.4633	28.3	-20.0
HV1L12		6.1	-25.7	417	2.8773	33.0	-20.4
HV1L22		4.1	-25.6	499	3.4431	38.0	-20.2
HW1H01	AAW-1	8.6	-21.7	323	2.2287	22.8	-15.0
HW1L02		6.3	-21.8	449	3.0981	28.9	-15.0
HW1L03		7.5	-22.3	379	2.6151	26.4	-15.1
HW1L12		5.0	-20.1	388	2.6772	32.1	-15.2
HW1L22		6.5	-22.1	448	3.0912	30.6	-15.0
HX1L01	AAX-1	6.6	-20.5	366	2.5254	30.2	-14.5
HX1L02		6.0	-20.6	379	2.6151	30.3	-14.6
HX1L12		3.7	-19.1	428	2.9532	33.2	-14.3
HX1L22		3.8	-19.8	433	2.9877	34.0	-14.1
HZ1H22	AAZ-1	9.2	-21.1	309	2.1321	26.9	-15.0
HZ1L12		5.8	-20.5	449	3.0981	37.0	-15.0
HZ1L22		6.2	-18.9	387	2.6703	35.2	-14.8
HZ1L32		8.9	-19.5	311	2.1459	27.7	-14.6
HBC1H02	ABC-1	7.7	-28.2	326	2.2494	21.2	-21.1
HBC1L01		5.8	-28.8	423	2.9187	26.1	-21.5

Table A.4. Results of TSRST for long-term aged (LTOA) mixtures with RH aggregate

Specimen ID	Asphalt Type	Air Void Content (%)	Fracture Temperature (°C)	Fracture Strength (psi)	Fracture Strength (MPa)	dS/dT (psi/°C)	Transition Temperature (°C)
LHA1H03	AAA-1	8.3	-29.2	498	3.4362	34.0	-22.1
LHA1H04		8.0	-28.9	501	3.4569	34.8	-22.7
LHA1L03		5.3	-27.0	504	3.4776	35.0	-21.5
LHA1L04		7.0	-28.3	497	3.4293	33.7	-21.4
LHB1L32	AAB-1	3.5	-22.1	449	3.0981	32.4	-15.3
LHB1L42		3.5	-22.0	408	2.8152	34.0	-15.0
LHC1H03	AAC-1	9.1	-21.9	350	2.4150	26.8	-15.0
LHC1H04		8.9	-22.1	414	2.8566	30.0	-16.0
LHC1L03		6.5	-21.3	443	3.0567	32.9	-16.0
LHC1L32		9.0	-21.1	365	2.5185	26.6	-15.0
LHC1L33		5.0	-19.6	406	2.8014	34.1	-15.0
LHC1L43		4.6	-20.0	426	2.9394	35.2	-15.0
LHD1H03	AAD-1	7.8	-23.6	402	2.7738	26.0	-16.6
LHD1H43		9.2	-25.5	365	2.5185	22.9	-16.4
LHD1L03		5.7	-23.1	446	3.0774	27.2	-15.6
LHD1L32		4.4	-23.0	474	3.2706	30.5	-16.1
LHD1L42		5.1	-23.1	409	2.8221	28.0	-16.4
LHF1H04	AAF-1	8.9	-15.8	373	2.5737	28.8	-10.3
LHG1H03	AAG-1	8.5	-14.5	393	2.7117	33.3	-8.6
LHG1H04		7.4	-14.0	415	2.8635	36.5	-9.0
LHG1L43		3.8	-12.6	309	2.1321	34.0	-8.1
LHG1L23		5.1	-13.1	309	2.1321	32.0	-8.9
LHK1H03	AAK-1	8.0	-21.2	430	2.9670	29.0	-13.6
LHK1L42		3.5	-20.8	480	3.3120	33.0	-13.5
LHL1H03	AAL-1	9.2	-26.9	352	2.4288	23.5	-18.6
LHL1H32		9.3	-26.9	367	2.5323	24.0	-19.1
LHL1L04		6.6	-25.5	421	2.9049	28.2	-18.2
LHL1L32		6.0	-25.0	422	2.9118	31.4	-19.0
LHL1L42		6.0	-24.6	402	2.7738	31.2	-18.8

Continued on page 106

Table A.4 (continued). Results of TSRST for long-term aged (LTOA) mixtures with RH aggregate

Specimen ID	Asphalt Type	Air Void Content (%)	Fracture Temperature (°C)	Fracture Strength (psi)	Fracture Strength (MPa)	dS/dT (psi/°C)	Transition Temperature (°C)
LHM1H04	AAM-1	6.7	-20.7	478	3.2982	34.2	-15.0
LHM1L03		6.7	-20.8	484	3.3396	32.5	-14.7
LHM1L41		6.2	-20.2	492	3.3948	34.0	-14.2
LHM1L34		3.6	-19.0	513	3.5397	38.8	-14.8
LHM1L44		6.2	-20.6	506	3.4914	34.8	-14.6
LHV1H42	AAV-1	8.8	-23.6	350	2.4150	27.0	-17.5
LHV1L32		3.3	-23.3	482	3.3258	38.2	-18.0
LHV1L42		4.0	-23.8	416	2.8704	33.0	-18.4
LHW1H03	AAW-1	9.7	-18.3	321	2.2149	21.5	-11.0
LHW1H04		9.1	-17.3	320	2.2080	22.7	-11.2
LHW1L32		5.0	-16.0	365	2.5185	****	*****
LHW1L42		7.2	-17.2	385	2.6565	28.2	-11.2
LHX1L03	AAX-1	7.5	-18.8	374	2.5806	26.9	-11.7
LHX1L04		6.4	-17.3	390	2.6910	28.4	-11.6
LHX1L42		4.8	-17.0	412	2.8428	33.0	-12.0
LHZ1H04	AAZ-1	8.3	-18.9	445	3.0705	30.0	-12.4
LHZ1L04		7.4	-18.3	438	3.0222	33.4	-12.3
LHZ1L32		3.8	-17.4	418	2.8842	30.0	-12.0
LHZ1L42		4.8	-18.0	426	2.9394	35.0	-12.0
LHBC1H04	ABC-1	7.9	-24.6	377	2.6013	24.0	-16.0
LHBC1L04		6.4	-23.1	348	2.4012	23.8	-15.5